UNIVERSIDADE ESTADUAL DE CAMPINAS

INSTITUTO DE BIOLOGIA

Patricia Pereira Coltri

Estudo funcional e estrutural de Nip7p, uma proteína conservada envolvida na síntese de ribossomos

Tese apresentada ao Instituto de Biologia para obtenção do Título de Doutor em Genética e Biologia Molecular, na área de Genética Animal e Evolução.

Orientador: Prof. Dr. Nilson Ivo Tonin Zanchin

Campinas, 2007

FICHA CATALOGRÁFICA ELABORADA PELA
BIBLIOTECA DO INSTITUTO DE BIOLOGIA – UNICAMP

C722e

Coltri, Patrícia Pereira
Estudo funcional e estrutural de Nip7p, uma proteína conservada envolvida na síntese de ribossomos / Patrícia Pereira Coltri. – Campinas, SP: [s.n.], 2007.

Orientador: Nilson Ivo Tonin Zanchin.
Tese (doutorado) – Universidade Estadual de Campinas, Instituto de Biologia.

1. Ribossomos. 2. RNA ribossômico. 3. Proteínas – Síntese. 4. Proteínas - Estrutura. 5. Sistema duplo-híbrido de leveduras. I. Zanchin, Nilson Ivo Tonin. II. Universidade Estadual de Campinas. Instituto de Biologia. III. Título.

(rcdt/ib)

Título em inglês: Functional and structural analysis of Nip7p, a conserved protein involved in ribosome biogenesis.
Palavras-chave em inglês: Ribosomes; RNA Ribosomal; Protein – Synthesis; Protein – Structure; Yeast two-hybrid system.
Área de concentração: Genética Animal e Evolução.
Titulação: Doutora em Genética e Biologia Molecular.
Banca examinadora: Nilson Ivo Tonin Zanchin, Jörg Kobarg, Marcelo Menossi Teixeira, Beatriz Amaral de Castilho, Gustavo Henrique Goldman.
Data da defesa: 10/12/2007.
Programa de Pós-Graduação: Genética e Biologia Molecular.

Campinas, 10 de dezembro de 2007.

BANCA EXAMINADORA

Prof. Dr. Nilson Ivo Tonin Zanchin (Orientador)

Assinatura

Prof. Dr. Jörg Kobarg

Assinatura

Prof. Dr. Marcelo Menossi Teixeira

Assinatura

Profa. Dra. Beatriz Amaral de Castilho

Assinatura

Prof. Dr. Gustavo Henrique Goldman

Assinatura

Prof. Dr. Michel Georges Albert Vincentz

Assinatura

Prof. Dr. Luis Eduardo Soares Netto

Assinatura

Profa. Dra. Aparecida Sadae Tanaka

Assinatura

AGRADECIMENTOS

À Fundação de Amparo à Pesquisa do Estado de São Paulo, FAPESP, pela concessão do auxílio a este e a outros projetos do laboratório.

Ao Laboratório Nacional de Luz Síncrotron, LNLS, por proporcionar a excelente infra-estrutura para a pesquisa nas diferentes áreas.

Ao Programa de Pós Graduação em Genética e Biologia Molecular da UNICAMP.

Ao Nilson Zanchin, pela orientação e ensinamentos nestes anos de doutorado e por ter me oferecido a oportunidade de trabalhar neste projeto.

À Carla C. Oliveira, por ter me recebido em seu laboratório, pelos ensinamentos e pelo apoio em vários momentos.

À Beatriz G. Guimarães, pelo que aprendi na área de cristalografia de proteínas durante esses anos e pela disposição em colaborar neste trabalho.

Aos Profs. Dra. Maria Isabel Cano e Dr. Jörg Kobarg, pela disponibilidade, sugestões e críticas na avaliação prévia deste trabalho.

Às Profas. Dra. Beatriz Amaral de Castilho e Dra. Aparecida Sadae Tanaka e aos Profs. Dr. Gustavo H. Goldman, Dr. Marcelo Menossi Teixeira, Dr. Prof. Jörg Kobarg, Dr. Luis Eduardo Soares Netto e Dr. Michel Vincentz pela participação na banca de avaliação deste trabalho.

Aos pesquisadores, funcionários e alunos do CeBiME pela intensa troca de experiências e pelas sugestões.

Às amigas do laboratório, Sandra, Thais, Bia, Ju, Dani e Flávia pela nossa alegre convivência.

Aos colegas Thiago, Cédric, Liliane, Larissa, Marco Antônio, Carlos, Diane, Melissa, Gustavo, Daniel Trindade, Daniel Lanza, Alexandre, Rosi, Andrés, Marina, Juliana Oliveira, Tininha e Júlio por estarem sempre dispostos a ajudar.

Aos colegas Daniela Granato, Juliana Luz, Fernando Gonzales e Celso Ramos pela colaboração nos diferentes trabalhos e por terem me recebido no laboratório em São Paulo.

À Tereza Lima, Elaine Teixeira e Adriana Alves pela excelente contribuição neste trabalho em diversos momentos.

À Zildene Correia, responsável pelo sequenciamento de DNA e a Givanil Garrido, funcionária da esterilização de materiais, por estarem sempre dispostas a ajudar.

Às técnicas Andréia Meza, Veruska Soares e M. Eugênia Camargo pela ajuda.

À secretária Lourdes Fagundes, da CPG-Genética, por todo apoio.

Aos meus queridos amigos biólogos Celisa, Gisele, Cíntia, Renato, Aluana, Yu Jie e Rodrigo, por terem sempre me incentivado e pela nossa amizade.

Aos amigos Laísa, Fábio, Mauro e Thales pelo apoio e carinho durante esses anos.

À Yoko Bomura Rosato, que me iniciou na pesquisa, por todo apoio.

À Vera, Paulo e Michelle, por todo apoio e pela ótima convivência.

Ao Paulo Guimarães Jr., pelo carinho e compreensão em tantos momentos e por me ensinar que a beleza da vida está no aprendizado. Obrigada pelo incentivo e por sempre ter me encorajado a crescer.

A todos os meus familiares e em especial à minha irmã querida, Priscila, pelo apoio em todos os momentos e por ter sempre sido um exemplo para mim.

Aos meus pais, Maria Inês e Claudio, meus maiores incentivadores, por todo seu amor e esforço em proporcionar as melhores condições para minha educação. Obrigada por sempre acreditarem nos meus sonhos e no meu futuro profissional.

ÍNDICE

LISTA DE FIGURAS

LISTA DE ABREVIAÇÕES

3'ETS	Espaçador externo 3' (*external transcribed spacer 3'*)
3-AT	3-aminotriazol
5'ETS	Espaçador externo 5' (*external transcribed spacer 5'*)
ArcTGT	Archaeosina transglicosilase (*archaeosine transglycosilase*)
BCIP	*5-bromo-4-chloro-3-indolylphosphate*
CAPS	Ácido N-Ciclohexil-3-aminopropanesulfônico
CMCT	1-Ciclohexil-3-[2-morpholinoethil] carbodiicarbonato
DAPI	4'-6'-Diamidino-2-phenilindol
DTT	Ditiotreitol
EDTA	Ácido etilenodiaminotetracético
EGFP	Proteína de fluorescência verde intensa (*enhanced green fluorescent protein*)
EMSA	Ensaio de interação proteína-RNA (*electrophoretic mobility shift assay*)
FTSJ3	Proteína hipotética com domínio FtsJ de rRNA metil-transferase
GFP	Proteína fluorescente verde (*green fluorescent protein*)
GST	Glutationa S-transferase
hnRNP	Ribonucleoproteína nuclear heterogênea (*heterogeneous nuclear ribonucleoprotein*)
HsNip7	Ortóloga humana da proteína Nip7p
IPI	Complexo envolvido no processamento da região ITS2 (*involved in processing of ITS2*)
IPTG	Isopropil- β-D-galactopiranosídeo
IRES	Sítio interno para início da tradução (*internal ribosome entry site*)
ITS1	Espaçador interno 1 (*internal spacer 1*)

ITS2	Espaçador interno 2 (*internal spacer 2*)
LB	Meio de cultura de bactérias “Luria Bertani”
Lsm	Proteína envolvida no processamento de mRNA semelhante ao complexo “Sm” (*like-Sm proteins*)
MEM	Meio essencial mínimo para cultura de células de mamíferos (*Minimum essential medium*)
mRFP	Proteína de fluorescência vermelha monomérica (*monomeric red fluorescent protein*)
mRNA	RNA mensageiro
NBT	*Nitroblue tetrazolium*
Nip7p	Proteína de importação nuclear 7 de *Saccharomyces cerevisiae* (*nuclear import protein* 7)
Nop8p	Proteína nucleolar 8 de *S. cerevisiae* (*nucleolar protein* 8)
Nop53p	Proteína nucleolar 53 de *S. cerevisiae* (*nucleolar protein* 53)
OD_{600}	Densidade óptica a 600 nanômetros
PBS	Tampão fosfato (*phosphate buffer saline*)
PCR	Reação de polimerase em cadeia (*polymerase chain reaction*)
PDB	Banco de dados de estrutura de proteínas (*protein data bank*)
PMSF	*Phenylmethylsulfonyl fluoride*
PNPase	Fosforilase de RNA (*polynucleotide phosphorylase*)
PUA	Domínio encontrado em pseudo-uridina sintases e archaeosina transglicosilases (*pseudouridine synthases and archaeosine tranglycosilases*)
rRNA	RNA ribossomal
RNase	Ribonuclease
RRM	Domínio de reconhecimento ao RNA (*RNA recognition motif*)

Rrp43p	Proteína de processamento do RNA ribosomal 43 (*S. cerevisiae ribosomal RNA processing protein* 43)
SBDS	Proteína associada a síndrome de *Shwachman-Bodian-Diamond* (*Shwachman-Bodian-Diamond syndrome*)
SDS-PAGE	Eletroforese em gel de poliacrilamida na presença de duodecil-sulfato de sódio (*sodium duodecyl-sulphate polyacrilamide gel eletrophoresis*)
SIRAS	Substituição isomórfica com espalhamento anômalo (*single isomorphous replacement with anomalous scattering*)
snoRNA	Pequeno RNA nucleolar (*small nucleolar RNA*)
snoRNP	Pequena partícula ribonucleoprotéica nucleolar (*small nucleolar ribonucleoprotein*)
snRNA	Pequeno RNA nuclear (*small nuclear RNA*)
SSU processomo	Complexo de processamento da subunidade ribossomal menor (*small subunit processome*)
SUMO-2	Pequeno modificador similar a ubiquitina 2 (*small ubiquitin-like modifier* 2)
TAP	Purificação por afinidade em sequência (*tandem affinity purification*)
TBE	Tampão Tris-borato-EDTA (*Tris-borate-EDTA buffer*)
tRNA	RNA transportador
Utp	Proteína do complexo U3 (*U-three-protein*)
X-gal	5-bromo-4-cloro-β-D-galactopiranosídeo

RESUMO

A síntese de ribossomos é um processo conservado em eucariotos e se inicia com a transcrição dos rRNAs no nucléolo. Mais de 170 fatores atuam de forma transitória no processamento dos precursores para gerar os rRNAs maduros que formarão as subunidades ribossomais no citoplasma. Entre as proteínas envolvidas na síntese de ribossomos está a Nip7p, uma proteína nucleolar de 21 kDa associada ao complexo pré-60S em *Saccharomyces cerevisiae*. Nip7p é conservada e possui ortólogas em eucariotos e em Archaea. A análise da seqüência primária revela a presença de um domínio conservado na região C-terminal, denominado PUA, encontrado em diversas proteínas associadas a modificações no RNA. Neste trabalho, foram realizadas análises estruturais e funcionais com o objetivo de investigar a função molecular da proteína Nip7 no processamento e modificação do rRNA. A estrutura tri-dimensional de PaNip7, ortóloga de Nip7p em *Pyrococcus abyssi* foi resolvida por difração de raios-X até 1,8Å de resolução, utilizando o método SIRAS. Comparação estrutural seguida por ensaios *in vitro* confirmaram o envolvimento do domínio PUA na interação com RNA. Além disso, tanto Nip7p como suas ortólogas PaNip7 e HsNip7 interagem com seqüências ricas em uridina, indicando que atuam de forma semelhante no processamento do rRNA. Essa preferência por uridina pode ainda explicar a afinidade da proteína Nip7p de *S. cerevisiae* pelo RNA da região ITS2, conforme observado em ensaios de interação utilizando *UV-crosslinking*. De fato, uma análise funcional realizada por *primer extension* comprovou que ocorre um bloqueio no processamento da região espaçadora ITS2 na ausência de Nip7p. Nip7p interage com várias proteínas do complexo pré-60S, entre as quais Nop8p e Nop53p, ambas associadas ao processamento do pré-27S. Embora os ensaios de co-purificação tenham confirmado a interação com as proteínas do complexo *H/ACA box*, deficiência em Nip7p não afeta a pseudo-uridinilação do rRNA. O duplo-híbrido realizado com a ortóloga humana de Nip7p, HsNip7, revelou interações com FTSJ3 e com a proteína SUMO-2. A interação direta de HsNip7 com estas proteínas foi confirmada por ensaios *in vitro*. HsNip7 e FTSJ3 colocalizaram na região nucleolar de células HEK293. FTSJ3 é uma proteína não caracterizada que possui o domínio FtsJ, descrito inicialmente para rRNA metil-transferases de procariotos. Além disso, FTSJ3 apresenta similaridade de sequência à proteína Spb1p de levedura, cuja função na metilação do rRNA 25S na posição Gm_{2922} já

foi estabelecida. Embora a Nip7p não interaja com a Spb1p, estes dados indicam que FTSJ3 deve ser a ortóloga humana da Spb1p. As proteínas SUMO estão envolvidas na modificação pós-traducional (*sumoylation*) que regula a localização subcelular de proteínas. Em levedura, a provável ortóloga de SUMO, Smt3p, foi descrita na partícula pré-60S, portanto a interação HsNip7-SUMO-2 pode ser específica. Estes dados sugerem que as proteínas atuem no mesmo complexo da formação da subunidade 60S também em células humanas.

ABSTRACT

Ribosome biogenesis is conserved throughout eukaryotes and takes place in the nucleolus, a specialized nuclear compartment where the rRNA precursors are transcribed. More than 170 trans-acting factors coordinately interact to generate the mature rRNAs. Among the proteins identified in the pre-60S particle in *Saccharomyces cerevisiae* is Nip7p. Highly conserved Nip7p orthologues are found in all eukaryotes and Archaea. The analysis of Nip7p sequence reveals a conserved C-terminal domain named PUA, also found in a number of RNA-interacting proteins. In this work, we performed structural and functional analysis to investigate Nip7p molecular role on rRNA processing and modification. The structure of *Pyrococcus abyssi* Nip7p ortholog, PaNip7, was solved using X-ray diffraction data to 1,8Å resolution. Structural analysis followed by *in vitro* assays confirmed the involvement of PUA domain in RNA interaction. *S. cerevisiae* Nip7p and its archaeal and human counterparts show preference for binding uridine-rich sequences, indicating conserved functional features among the orthologues. The preference for uridine can explain the higher affinity of *S. cerevisiae* Nip7p for ITS2 sequence, as observed by UV-crosslinking assays. Consistently, functional analysis revealed pre-rRNA processing in the ITS2 region is seriously impaired. Yeast two-hybrid analysis confirmed by pull down assays revealed Nip7p interacts with Nop8p and Nop53p, two nucleolar proteins involved in pre-27S processing and components of pre-60S particle. Although yeast two-hybrid and pull down assays indicated that Nip7p interacts with H/ACA box core proteins, pseudouridylation is not affected under conditions of Nip7p depletion. In addition, yeast two-hybrid analysis confirmed by GST-pull down revealed HsNip7 interaction with FTSJ3 and SUMO-2. Both HsNip7 and FTSJ3 showed nucleolar subcellular localization in HEK293 cells. FTSJ3 is an uncharacterized protein containing the FtsJ domain, initially described in prokaryotic rRNA methyl-transferases. FTSJ3 shows sequence similarity to yeast Spb1p, an rRNA methyl-transferase involved in methylation of Gm_{2922}, indicating that FTSJ3 may be the human orthologue of Spb1p. Sumoylation is a post-transcriptional covalent modification involved in regulation of protein subcellular localization. Putative yeast orthologues of SUMO, such as Smt3p, have been described in the pre-60S ribosomal particle, suggesting that SUMO-2 might play a specific role in 60S subunit biogenesis.

1. INTRODUÇÃO

1.1. Síntese de ribossomos em eucariotos

Em eucariotos, transcrição e tradução são eventos separados, temporal e espacialmente. Os RNAs mensageiros (mRNAs) são transcritos e processados no núcleo e posteriormente transportados para o citoplasma, onde ocorre sua associação com as partículas ribossomais, responsáveis pelo processo de síntese protéica. Os ribossomos são compostos por quatro moléculas de RNAs ribossomais (rRNAs) distintas e cerca de 80 proteínas. A síntese dos RNAs ribossomais se inicia em um compartimento especializado do núcleo, o nucléolo, e termina com o transporte das subunidades ribossomais para o citoplasma, onde o ribossomo atua (Tollervey & Kiss, 1997; Kressler *et al.*, 1999; Venema & Tollervey, 1995, 1999; Nissan *et al.*, 2002).

A maquinaria de síntese ribossomal é conservada entre os eucariotos e está mais bem caracterizada em *Saccharomyces cerevisiae*. Os rRNAs são transcritos no nucléolo pela RNA polimerase I a partir de uma sequência repetitiva de 9,1 kb gerando um longo transcrito primário, denominado pré-35S em leveduras, e pré-47S em mamíferos. Este transcrito possui a seqüência para os rRNAs maduros 18S, 5,8S e 25/28S intercalados pelos espaçadores internos (ITS1 e ITS2) e pelos externos, nas extremidades 5'e 3' (5'ETS e 3'ETS). Estes espaçadores são removidos por sucessivas clivagens em sítios específicos, com o auxílio de mais de 170 fatores que se associam de forma transitória ao pré-rRNA (Figura 1.1). Entre estes fatores estão endo- e exoribonucleases, RNA-helicases dependentes de ATP e diversas outras proteínas não ribossomais, como a Nip7p. Um quarto rRNA, 5S, é transcrito separadamente pela RNA polimerase III em sentido oposto, e o transcrito primário sofre maturação independente. A extremidade 3' é rapidamente clivada por exoribonucleases para gerar o rRNA maduro 5S, que será reunido ao pré-60S ainda no nucléolo (Kressler *et al.*, 1999; Fromont-Racine *et al.*, 2003).

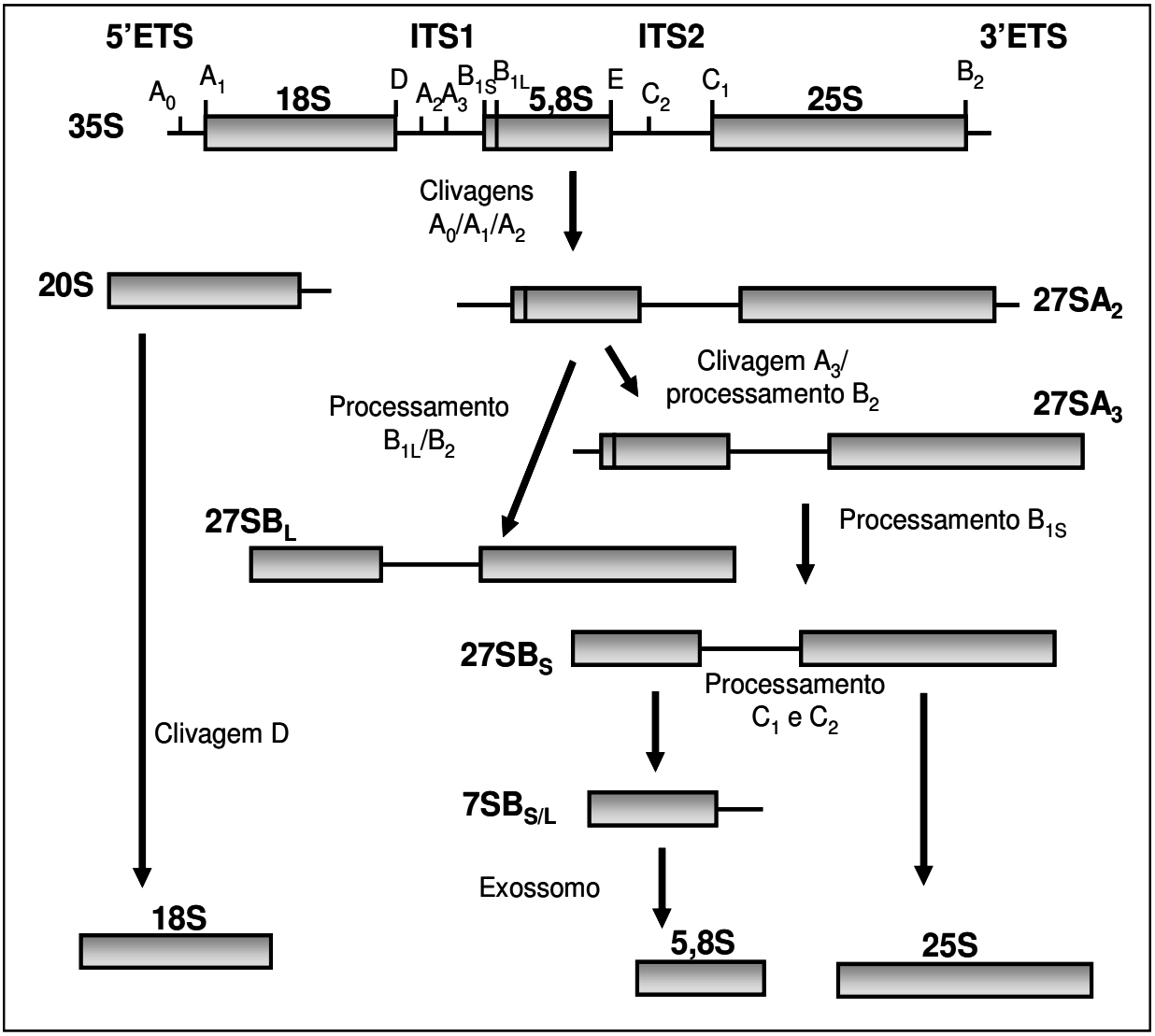

Figura 1.1. Esquema do processamento do rRNA 35S em *S. cerevisiae*. O longo transcrito primário 35S de *S. cerevisiae* possui a seqüência para os rRNAs maduros 18S, 5,8S e 25S intercalados pelos espaçadores internos (ITS1 e ITS2) e pelos externos, nas extremidades 5' e 3' (5'ETS e 3'ETS). O processamento se inicia com uma clivagem no sítio A_0, gerando o pré-rRNA 33S. Este precursor sofre clivagem no sítio A_1 por uma exonuclease, gerando o pré-rRNA 32S, que será clivado no sítio A_2, separando o precursor em duas moléculas: 20S e $27SA_2$. O precursor 20S será processado na extremidade 3' por uma endonuclease gerando o rRNA maduro 18S. O segundo produto da clivagem, o precursor $27SA_2$ compõe a partícula pré-60S e é processado por duas vias alternativas. Cerca de 85% das moléculas são clivadas no sítio A_3 pelo complexo de endonucleases RNase MRP gerando o precursor $27SA_3$. Em seguida, a sequência entre A_3 e B_{1S} é processada pela exonuclease 5'-3' Rat1p, gerando o precursor $27SB_S$. Aproximadamente 15% de $27SA_2$ será diretamente processado no sítio B_{1L} formando o precursor $27SB_L$. Estas vias alternativas de processamento geram duas formas de rRNAs 5,8S, um mais curto ($5,8S_S$), produto da via mais comum, e outro, cerca de 8 nucleotídeos mais longo ($5,8S_L$). O sítio B_2 é processado ao mesmo tempo em que a extremidade 5' do rRNA 25S é formada, pelo processamento no sítio C_1 e clivagens endonucleolíticas em C_2. As clivagens nos sítios C_1 e C_2 liberam o rRNA 25S e os pre-rRNAs $7S_S$ e $7S_L$. A extremidade 3' do pré-7S é finalmente processada pelo exossomo, gerando a extremidade 3' madura do rRNA 5,8S.

Em *S. cerevisiae*, o precursor 35S associado à partícula ribonucleoprotéica U3 e a diversas proteínas que atuam no processamento da subunidade 40S, formam a partícula pré-ribossomal 90S (Grandi *et al.*, 2002). Entre as proteínas associadas ao complexo U3 estão as Utp (*U-three-protein*), além de Sof1p, Mpp10p, Imp3p, Imp4p, Lcp5p, Rrp9p e Rrp5p (Lee & Baserga, 1997; Dragon *et al.*, 2002; Bernstein *et al.*, 2004). O complexo, denominado "processomo SSU" (*small subunit processome*), atua diretamente na maturação do pré-18S, embora as endonucleases específicas responsáveis pelas clivagens neste precursor ainda não tenham sido identificadas (Fromont-Racine *et al.*, 2003). Após as clivagens iniciais, o pré-90S é rapidamente convertido nas partículas precursoras das subunidades 40S e 60S (Figura 1.2). Enquanto o pré-40S é transportado para o citoplasma para finalizar a maturação do rRNA 18S, o pré-60S segue no nucléolo, onde mais de 70 proteínas, incluindo diversas endo- e exonucleases e proteínas não ribossomais, promovem a maturação dos rRNAs 5,8S e 25S (Grandi *et al.*, 2002; Nissan *et al.*, 2002). As proteínas associadas ao processamento do pré-60S não foram identificadas na molécula pré-90S, indicando que sua associação ocorre após a separação das partículas pré-ribossomais (Baβler *et al.*, 2001; Nissan *et al.*, 2002). O modelo dinâmico do processamento da partícula pré-60S pressupõe que a associação e dissociação dos fatores ocorra de maneira coordenada com o processamento dos precursores 27S e 7S, gerando os RNAs maduros 25S e 5,8S (Venema & Tollervey, 1999; Fatica & Tollervey, 2002; Fatica *et al.*, 2002).

Muitos fatores que atuam no processamento do rRNA em mamíferos são conservados (Andersen *et al.*, 2002). O complexo nucleolar PeBoW composto pelas proteínas Pes1, Bop1 e WDR12, atua no processamento do precursor 32S, interferindo na maturação dos rRNAs 5,8S e 28S (Strezoska *et al.*, 2000; Lapik *et al.*, 2004; Hölzel *et al.*, 2005; Grimm *et al.*, 2006; Rohrmoser *et al.*, 2007). Em levedura, as ortólogas Nop7p, Erb1p e Ytm1p também estão associadas à maturação da subunidade 60S. Além disso, este complexo pode atuar na regulação dos níveis da proteína p53, relacionando o processo de síntese de ribossomos ao controle do ciclo celular em mamíferos (Grimm *et al.*, 2006).

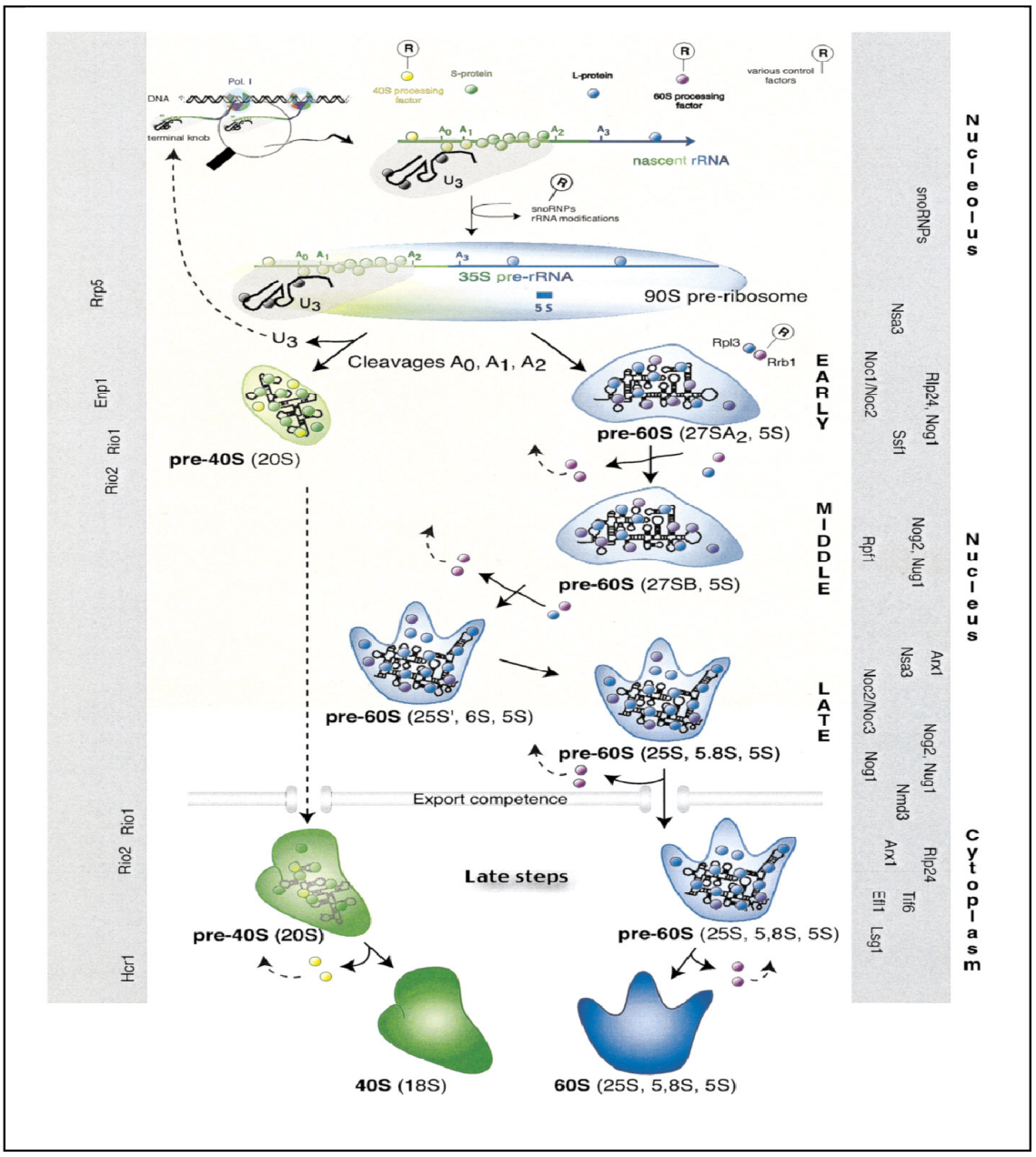

Figura 1.2. Representação esquemática da síntese das subunidades ribossomais em eucariotos, do nucléolo até o citoplasma. Em *S. cerevisiae*, o longo precursor de rRNA é transcrito a partir de uma sequência repetitiva de 9,1 kb no nucléolo pela RNA polimerase I. A partícula pré-ribossomal 90S é formada pelo precursor de rRNA 35S associado a partícula ribonucleoprotéica U3 e a diversas proteínas relacionadas ao processamento da subunidade 40S. Após as clivagens em A_0, A_1 e A_2, o pré-90S é convertido nas partículas precursoras das subunidades 40S e 60S. Enquanto o pré-40S (em verde) é transportado para o citoplasma para finalizar a maturação do rRNA 18S, o pré-60S (em azul) segue no nucléolo, onde diversas endo- e exonucleases e proteínas não ribossomais se associam de maneira transitória para promover o processamento do precursor até gerar os rRNAs maduros 5,8S e 25S. Um quarto rRNA, 5S, é transcrito separadamente pela RNA polimerase III em sentido oposto, e será reunido ao complexo pré-60S. As subunidades são exportadas para o citoplasma. Figura extraída de Fromont-Racine *et al.*, 2003.

Após o longo processamento e modificação dos rRNAs, as subunidades são transportadas para o citoplasma. A subunidade ribossomal 40S é composta pelo rRNA 18S associado a 32 proteínas ao passo que a subunidade 60S é formada pelos rRNAs 5S, 5,8S e 25S associados a 46 proteínas ribossomais (Kressler *et al.*, 1999). Embora sintetizadas separadamente, as subunidades ribossomais mantêm uma razão estequiométrica precisa, regulada principalmente pela transcrição coordenada dos genes que codificam as proteínas ribossomais e pela degradação rápida das proteínas produzidas em excesso (Warner, 1989).

1.1.1. Fatores envolvidos nas clivagens do pré-rRNA

As clivagens endo- e exonucleolíticas dependem da associação de complexos ribonucleoprotéicos ao pré-rRNA em etapas específicas. Nas primeiras etapas do processamento, o precursor 35S sofre as clivagens nos sítios A_0, A_1 e A_2. O snoRNA U14 atua nas clivagens em A_1 e A_2 e na metilação 2' OH das riboses do rRNA 18S (Liang & Fournier, 1995). A molécula ribonucleoprotéica U3, formada pelo snoRNA U3 associado ao complexo SSU, composto por mais de 40 proteínas, realiza o processamento nos sítios A_0, A_1 e A_2 (Dragon *et al.*, 2002).

O complexo RNase MRP, responsável pelas clivagens endonucleolíticas no sítio A_3, é formado pela molécula de snoRNA MRP e nove componentes protéicos (Pop1p, Pop3p a Pop8p, Rpp1p e Snm1p). Através do processamento no sítio A_3, o complexo MRP interfere diretamente na maturação da extremidade 5' do rRNA 5,8S (Lygerou *et al.*, 1994; Kressler *et al.*, 1999; Venema & Tollervey, 1999). A endonuclease Rnt1p atua na remoção do espaçador 3'ETS do precursor 35S (Geerlings *et al.*, 2000). As exonucleases 5'→3' Rat1p e Xrn1p são enzimas funcionalmente similares e participam de processos essenciais no núcleo e no citoplasma, respectivamente (Johnson, 1997). Além de auxiliar no processamento no sítio A_3, Rat1p atua, junto com Rnt1p e o exossomo, no processamento de snoRNAs poli-cistrônicos ou provenientes de *introns*. Xrn1p, por sua vez, atua na última etapa da degradação de mRNAs no citoplasma, após a deadenilação e a retirada do *cap* da extremidade 5' (Johnson, 1997; Venema & Tollervey, 1999).

O exossomo é um complexo com atividade de exonuclease 3'→ 5' responsável pela maturação e degradação de RNAs no núcleo e citoplasma (Mitchell *et al.*, 1997; Allmang *et*

al., 2000). A análise das sequências das subunidades protéicas do complexo revela alta similaridade com domínios PH de RNases de *Escherichia coli* e com domínios do tipo S1 de ligação ao RNA. Em *E. coli*, o homotrímero PNPase possui domínios de ligação ao RNA e domínios PH responsáveis pela atividade exonucleolítica (Houseley *et al.*, 2006). Em *S. cerevisiae*, o exossomo nuclear é composto por 11 proteínas, sendo que Rrp44p (também denominada Dis3p) possui atividade exonucleolítica *in vivo* (Dziembowski *et al.*, 2007). As subunidades Rrp41p/Rrp45p, Rrp46p/Rrp43p e Rrp42p/Mtr3p formam o anel PH, ao qual se associam as proteínas Csl4p, Rrp4p, Rrp40p, Rrp6p e Rrp44p (Burkard & Butler, 2000; Hernández *et al.*, 2006; Liu *et al.*, 2006; Luz *et al.*, 2007). Trabalhos recentes mostraram a alta similaridade estrutural entre os exossomos de Archaea e de eucariotos (Lorentzen *et al.*, 2005; Ramos *et al.*, 2006). Em Archaea, duas proteínas com domínio PH formam um anel composto por três heterodímeros idênticos de aRrp41 e aRrp42. Uma das faces do anel se associa a aRrp4, que possui o domínio S1 de ligação ao RNA, e a outra se liga a aCsl4 (Lorentzen *et al.*, 2005; Houseley *et al.*, 2006).

O exossomo nuclear tem grande importância na maturação e processamento de diversas espécies de RNAs. Em levedura, o processamento correto da extremidade 3' do rRNA 5,8S depende da formação do complexo nuclear completo. A degradação de espaçadores do pré-rRNA, como o 5'ETS, e de precursores aberrantes de mRNA, tRNA e rRNA também é dependente do exossomo nuclear, possivelmente através de um mecanismo que controla a qualidade destes RNAs. Além disso, o complexo atua diretamente na maturação de rRNAs, mRNAs, snRNAs e snoRNAs (Houseley *et al.*, 2006). No citoplasma, o exossomo exerce um papel importante na degradação de pré-mRNAs não processados e dos que possuem códon de terminação prematuro (Houseley *et al.*, 2006).

1.1.2. Modificações covalentes

A modificação de bases ocorre na molécula de pré-rRNA no complexo 90S, ainda nas primeiras etapas do processamento (Lee & Baserga, 1997; Dez *et al.*, 2002). Os rRNAs sofrem metilações de bases e riboses e pseudo-uridinilação em sítios específicos, mediadas pelos pequenos RNAs nucleolares (*small nucleolar RNAs*, snoRNAs) associados a proteínas em complexos ribonucleoprotéicos (*small nucleolar ribonucleoprotein*, snoRNP)

(Kressler *et al.*, 1999; Venema & Tollervey, 1999; Fatica & Tollervey, 2002; Fromont-Racine *et al.*, 2003). Os sítios específicos de modificação no rRNA são determinados por complementaridade e pareamento de bases do rRNA com a seqüência do snoRNA (Balakin *et al.*, 1996; Cavaille *et al.*, 1996; Kiss-László *et al.*, 1996). Embora a função exata das modificações de bases ainda seja desconhecida, há hipóteses de que elas promovam alterações estruturais capazes de facilitar a estabilização e conformação do rRNA e o ajuste da atividade ribossomal durante a tradução (Fromont-Racine *et al.*, 2003; King *et al.*, 2003; Torchet *et al.*, 2005). A natureza hidrofóbica das bases metiladas e a capacidade intrínseca de ligação a hidrogênio por pseudo-uridinas podem ser fatores importantes na conformação correta do rRNA maduro, facilitando as interações entre RNAs ou destes com proteínas (Ganot *et al.*, 1997; Kressler *et al.*, 1999). Na verdade, muitas modificações estão próximas aos sítios ativos do ribossomo, importantes para a tradução e para interação entre as subunidades ribossomais e quase nenhuma modificação é observada em sítios onde ocorre interação com proteínas ribossomais (Decatur & Fournier, 2002; King *et al.*, 2003).

Em *S. cerevisiae* são cerca de 10 bases metiladas, 55 riboses metiladas na posição 2'OH e 45 nucleotídeos que sofrem isomerização da uridina em pseudo-uridina (ψ) por rotação de bases (Kressler *et al.*, 1999; Torchet *et al.*, 2005). Os 150 snoRNAs distintos encontrados no nucléolo de *S. cerevisiae* são resultantes de diferentes estratégias de expressão. Eles podem ser transcritos a partir de promotores próprios pelas RNA polimerases II e III. Podem ser poli-cistrônicos, passando por um processamento que separa as unidades de snoRNAs. A maior parte, entretanto, provém de *introns* encontrados entre *exons* que irão codificar proteínas funcionais na síntese de ribossomos, o que sugere um mecanismo de co-regulação da expressão de snoRNAs e das proteínas que participam da biogênese de ribossomos (Lafontaine & Tollervey, 1995). Os snoRNAs são divididos em três classes, com base em homologias de seqüências conservadas, os *C/D box*; os *H/ACA box* e *MRP*. Cada classe de snoRNA possui proteínas específicas associadas, formando os complexos ribonucleoprotéicos que atuam na modificação e processamento do pré-rRNA.

Os snoRNAs *C/D box* são caracterizados por duas seqüências conservadas, o *box C* (5' PuUGAUGA 3', sendo Pu uma purina), na extremidade 5' e o *box D* (5'CUGA 3'), na extremidade 3'. Entre os *C/D box*, estão snoRNAs essenciais como U14 e U3, responsáveis pelo processamento inicial da molécula precursora 35S (Dragon *et al.*, 2002). A maior parte

dos *C/D box* se associa ao grupo de proteínas Nop1p, Nop56p, Nop58p e Snu13p, e promove a metilação de riboses na posição 2'OH. Nop1p e sua ortóloga em mamíferos, a proteína fibrilarina, apresentam atividade RNA metil-transferase (Ni *et al.*, 1997; Ganot *et al.*, 1997; Galardi *et al.*, 2002). A especificidade é determinada por uma seqüência de 10-21 nucleotídeos, localizada na região anterior ao *box D*, complementar ao sítio de metilação no rRNA. A metilação ocorre a 5 nucleotídeos de distância do *box D* (Ganot *et al.*, 1997).

Os snoRNAs *H/ACA box* são formados por 2 *hairpin* intercalados por uma região espaçadora ("*hinge*"). O *box H* (ANANNA, sendo N qualquer um dos nucleotídeos) fica na região espaçadora ("*hinge*") e o *box ACA* representa o trinucleotídeo encontrado a 3 nucleotídeos da extremidade 3' do snoRNA. A pseudo-uridinilação é uma reação de isomerização da uridina em pseudo-uridina e ocorre por rotação de bases. Esta modificação é realizada pelos snoRNAs *H/ACA box* associados ao complexo de proteínas Cbf5p, Gar1p, Nop10p e Nhp2p. Cbf5p é a enzima responsável pela conversão de uridinas em pseudo-uridinas (Lafontaine *et al.*, 1998; Henras *et al.*, 2004). Seqüências específicas do *hairpin* flanqueiam o substrato uridina, e o sítio de pseudo-uridinilação fica a uma distância de 14-16 nucleotídeos dos *box H* ou *ACA*. A ausência de Cbf5p, Nop10p ou Nhp2p leva a diminuição de todos os snoRNAs *H/ACA box*, indicando que este complexo de proteínas tem atividade importante na estabilização dos snoRNAs (Kressler *et al.*, 1999). Além destes componentes, a montagem correta do complexo depende de Naf1p, uma proteína que auxilia no acúmulo e estabilização dos snoRNAs *H/ACA box* (Dez *et al.*, 2002; Fatica *et al.*, 2002). Naf1p possui homologia a Gar1p e interage diretamente com Cbf5p durante a montagem do complexo (Leulliot *et al.*, 2007). Na ausência de Cbf5p são observados defeitos no processamento do precursor 27S, levando a diminuição nos níveis de rRNAs 25S e 5,8S maduros (Cadwell *et al.*, 1997). Estes dados indicam que Cbf5p pode atuar no processamento do rRNA através de interações com outros fatores, como ocorre com a proteína ortóloga em mamíferos, dyskerina (Mochizuki *et al.*, 2004). Gar1p possui as regiões N- e C-terminal ricas em glicina e arginina (*glycine and arginine domain*), possivelmente responsáveis pela interação da proteína com o pré-rRNA. Além de atuar no complexo *H/ACA box*, esta proteína interfere no processamento dos sítios A_1 e A_2 (Henras *et al.*, 1998; Torchet *et al.*, 2005), passos importantes na maturação do rRNA 18S (Vanrobays *et al.*, 2001). Nop10p e Nhp2p interagem especificamente com todos os *H/ACA*

box snoRNAs, e na ausência destas proteínas o processamento do rRNA fica comprometido (Henras *et al.*, 2001). Nhp2p possui uma região de 53 resíduos relacionada à ligação ao RNA, o que permite sua ligação aos snoRNAs e limita a degradação destes RNAs por exonucleases (Henras *et al.*, 2001). A reconstituição do complexo ribonucleoprotéico *H/ACA box* a partir de proteínas de Archaea mostrou que sua estrutura é bastante conservada (Hamma *et al.*, 2005). Em Archaea, Nop10p e Gar1p interagem diretamente, mas independentemente, com Cbf5p e a reconstituição do complexo ativo, capaz de realizar a isomerização da uridina, depende da associação de Cbf5p e Nop10p (Manival *et al.*, 2006).

Em *S. cerevisiae*, dentre os mais de 170 fatores que atuam de forma transitória durante o processamento do rRNA, está a proteína Nip7p (Baβler *et al.*, 2001; Gavin *et al.*, 2006). Horsey *et al.* (2004) identificaram, pelo método de purificação por afinidade da fusão TAP-Rrp1p seguido de espectrometria de massas, 28 proteínas envolvidas na biogênese da subunidade 60S. Em sua maioria, as proteínas identificadas são conservadas e nucleolares, assim como a Nip7p, também identificada neste estudo.

1.2. A proteína Nip7p

O alelo termo-sensível *nip7-1* foi isolado em uma seleção genética para mutantes que apresentavam defeito na importação nuclear de proteínas em *S. cerevisiae* (*nuclear import protein*) (Gu *et al.*, 1992). O gene *NIP7* foi clonado a partir de uma biblioteca genômica de *S. cerevisiae* por complementação do defeito termo sensível da cepa *nip7-1* (Zanchin *et al.*, 1997). Nip7p é uma proteína essencial de 21 kDa (181 aminoácidos), identificada entre as proteínas do complexo pré-60S (Zanchin *et al.*, 1997; Baβler *et al.*, 2001). Nip7p possui ortólogos em todos eucariotos e em Archaea, sugerindo um papel importante e conservado na maturação ribossomal. Em *S. cerevisiae*, a deficiência em Nip7p resulta no acúmulo do precursor 27SB e na redução dos rRNAs maduros 25S e 5,8S, levando a um desequilíbrio das subunidades ribossomais com diminuição significativa na quantidade de subunidades 60S (Zanchin *et al.*, 1997). Esse desequilíbrio leva a uma redução na taxa de síntese protéica. Efeitos secundários também são observados, como o acúmulo de precursor 35S e o bloqueio da primeira clivagem no sítio A_0, já que células

deficientes em Nip7p acumulam um pré-rRNA aberrante de 23S, similar ao encontrado em cepas com defeito na clivagem neste sítio (Zanchin *et al.*, 1997).

Além dos defeitos observados em células deficientes em Nip7p, sua interação direta com outros fatores que participam do complexo pré-60S, como as proteínas Nop8p e Nop53p, é mais uma evidência de sua participação na maturação ribossomal. Células deficientes em Nop8p apresentam defeitos similares aos encontrados na ausência de Nip7p, com acentuada redução no nível de subunidades 60S. Entretanto, análises com mutantes condicionais revelaram que enquanto a ausência de Nip7p leva ao processamento retardado do precursor 27SB, a deficiência em Nop8p leva a rápida degradação deste precursor (Zanchin & Goldfarb, 1999a). Nop53p, por sua vez, também é uma proteína nucleolar e interage diretamente com o rRNA da região 5,8S. O acúmulo do precursor 7S leva a diminuição na quantidade de rRNA 5,8S, similar ao encontrado na ausência de Nip7p (Granato *et al.*, 2005; Thomson & Tollervey, 2005).

Estudos anteriores envolvendo análises de duplo-híbrido, confirmadas por experimentos de co-purificação, revelaram que Nip7p também se associa *in vivo* com Rrp43p, uma componente do exossomo (Zanchin & Goldfarb, 1999a,b; Oliveira *et al.*, 2002). Como parte do exossomo, Rrp43p participa do processamento da extremidade 3' do rRNA 5,8S (Mitchell *et al.*, 1997), entretanto sua deficiência afeta principalmente a biogênese da subunidade 40S (Zanchin & Goldfarb, 1999b).

Ensaios de localização utilizando fusões com a proteína GFP (*green fluorescent protein*) mostraram maior concentração das proteínas Nip7 no nucléolo, tanto em células de *S. cerevisiae* como em células de mamíferos (Zanchin *et al.*, 1997; Sekiguchi *et al.*, 2004). A ortóloga humana de Nip7p interage com a porção C-terminal da proteína Nop132, ortóloga da proteína Nop8p em mamíferos, também encontrada no nucléolo (Sekiguchi *et al.*, 2004). A interação da proteína Nip7 humana com a proteína SBDS, cuja alteração leva ao desenvolvimento da síndrome de *Swachmann-Bodian-Diamond*, foi recentemente relatada (Hesling *et al.*, 2007). Os ensaios de imunoprecipitação utilizando extratos de células HEK293 e a proteína GST-SBDS confirmaram que HsNip7 e SBDS fazem parte do mesmo complexo, revelando que Nip7p pode estar associada à biogênese da subunidade 60S também em mamíferos (Hesling *et al.*, 2007). Em levedura, a proteína Sdo1p, ortóloga de SBDS, foi associada à biogênese de ribossomos. Sdo1p atua na reciclagem de Tif6p, um

fator nucleolar envolvido com a exportação da subunidade ao citoplasma e com a iniciação da tradução. A participação de Sdo1p nas etapas finais da maturação da subunidade 60S sugere que a interação com Nip7 possa ser conservada em eucariotos (Menne *et al.*, 2007).

1.2.1. O domínio PUA

A análise da seqüência de Nip7p e suas ortólogas revela alta similaridade entre as proteínas de eucariotos. O alinhamento estrutural entre as ortólogas humana (Liu *et al.*, 2004; PDB 1SQW), de *Pyrococcus abyssi* (PaNip7; PDB 2P38), e do modelo gerado para a proteína de *S. cerevisiae* neste trabalho, mostra alta similaridade estrutural entre as proteínas Nip7. A análise da seqüência revela a presença de um domínio conservado na sua região C-terminal, denominado "PUA". Embora não apresente alta identidade na comparação de seqüências primárias, a estrutura do domínio PUA é relativamente conservada, sendo geralmente composta por 2 α-hélices e 6 folhas-β (Pérez-Arelano *et al.*, 2007). A principal diferença estrutural observada entre as proteínas Nip7 está na α-hélice 7, que compreende os resíduos 149 a 156 das proteínas eucarióticas, ausente na proteína de *P. abyssi*.

O domínio PUA possui entre 66 e 94 aminoácidos, e foi inicialmente identificado em pseudo-uridina sintases e archaeosina transglicosilases, duas enzimas envolvidas com a modificação do RNA em Archaea (Aravind & Koonin, 1999; Pérez-Arelano *et al.*, 2007). PUA é um domínio encontrado em cerca de 600 proteínas de diferentes famílias, incluindo pseudo-uridina sintases da família TruB, transglicosilases, uma metil-transferase de *E. coli* (YebU), a glutamato 5-kinase de *E. coli* (G5K) e o oncogene MCT-1 (Aravind & Koonin, 1999; Ishitani *et al.*, 2002; Hallberg *et al.*, 2006; Reinert *et al.*, 2006; Marco-Marín *et al.*, 2007; Pérez-Arelano *et al.*, 2007). De acordo com dados de reconstituição do complexo *H/ACA box*, o domínio PUA da pseudo-uridina sintase Cbf5p tem grande importância na ligação ao RNA (Charpentier *et al.*, 2005; Manival *et al.*, 2006; Rashid *et al.*, 2006; Li & Ye, 2006), preferencialmente a trinucleotídeos NCA (Hoang & Ferre D'Amare, 2001). Mutações na região do domínio PUA do gene *DKC1*, que codifica a proteína dyskerina, ortóloga de Cbf5p em mamíferos, levam ao desenvolvimento da disqueratose congênita. Esta doença se caracteriza por envelhecimento precoce acompanhado por insuficiência da

medula óssea, anormalidade na epiderme e por maior suscetibilidade ao câncer. A análise realizada com células de camundongo com mutações no gene *DKC1* revelou diminuição na tradução de mRNAs do supressor tumoral p27 e de outros fatores anti-apoptose como Bcl-xL e XIAP, indicando um defeito no mecanismo de tradução dependente de IRES (*internal ribosome entry site*). Estes resultados relacionam a proteína com a atividade ribossomal e a progressão tumoral (Yoon *et al.*, 2006; Manival *et al.*, 2006). O domínio PUA encontrado no oncogene humano MCT-1 medeia a interação da proteína com o complexo de fatores de tradução que se associam ao 7-metil-GTP da extremidade 5' do mRNA, indicando que MCT-1 pode ter um papel no controle da iniciação da tradução (Reinert *et al.*, 2006).

No caso da proteína ArcTGT de *P. horikoshii*, o domínio PUA está diretamente envolvido na ligação ao tRNA (Ishitani *et al.*, 2002; 2003). Resíduos de lisina e arginina promovem a ligação eletrostática de ArcTGT às bases do tRNA (Ishitani *et al.*, 2003). É interessante observar que esses resíduos são conservados no domínio PUA da ortóloga de Nip7p em Archaea, indicando que a interação com RNA pode ocorrer de forma semelhante nestas proteínas. Embora importante para a ligação ao tRNA, o domínio PUA da enzima ArcTGT não atua diretamente na seleção do sítio ou na modificação da guanina em *P. furiosus* (Sabina & Söll, 2006).

Archaea são organismos procariotos cujos componentes celulares básicos tem alta semelhança aos de eucariotos. Proteínas ortólogas a Nop1p e Nop56p/Nop58p foram identificadas em todos genomas de Archaea já seqüenciados (Omer *et al.*, 2000). Além disso, ortólogos dos pequenos RNAs nucleolares eucarióticos também foram identificados (Dennis *et al.*, 2001; Omer *et al.*, 2003). A formação de complexos ribonucleoprotéicos é bastante conservada, como o complexo de proteínas ortólogas a Lsm, envolvidas com os mecanismos de *splicing* e processamento de mRNA (Collins *et al.*, 2001). Da mesma forma, a estrutura e o mecanismo de interação e processamento do RNA no complexo exossomo apresentam alta conservação em Archaea (Lorentzen *et al.*, 2005; Ramos *et al.*, 2006).

1.3. Estudo funcional e estrutural das proteínas Nip7

O objetivo central deste trabalho foi a investigação da função molecular da proteína Nip7. Para isso, foram realizadas análises funcionais e estruturais, visando compreender melhor as interações com proteínas e com RNA e também o papel do domínio PUA.

No Capítulo 1 estão detalhados os resultados da expressão, purificação e cristalização da proteína PaNip7, ortóloga de Nip7p em *P. abyssi*. A cristalização de PaNip7 foi realizada na condição de 4,1 M NaCl e 100 mM HEPES pH 7,2 pelo método de difusão de vapor por gota pendente. A estrutura de PaNip7, resolvida utilizando o método de substituição isomórfica (SIRAS) e a análise do mecanismo de interação com RNA estão descritos no Capítulo 2. O alinhamento estrutural com as proteínas ortólogas de eucariotos mostrou alta conservação entre as proteínas Nip7. A comparação estrutural seguida por ensaios *in vitro* utilizando proteínas com mutações sítio-dirigidas demonstrou o envolvimento do domínio PUA na interação com RNA. Além disso, tanto a PaNip7 como a Nip7 de eucariotos possuem maior afinidade por seqüências ricas em uridina, indicando que atuam de forma semelhante no processamento do rRNA.

Os dados da análise funcional de Nip7p e sua interação com outras proteínas estão descritos no Capítulo 3. As análises de interação pelo método de duplo-híbrido, confirmadas por experimentos de co-purificação a partir de células de *S. cerevisiae*, mostraram que Nip7p interage com todas as proteínas do complexo *H/ACA box*, envolvido na pseudo-uridinilação do rRNA. Experimentos funcionais de *primer extension* mostraram, no entanto, que a ausência de Nip7p não interfere diretamente na pseudo-uridinilação do rRNA. Um efeito mais pronunciado foi observado nas reações de clivagem do pré-rRNA, especialmente no sítio C_2. Na ausência de Nip7p o processamento da região ITS2 não ocorre corretamente, o que pode explicar o acúmulo do precursor 27S em cepas deficientes de Nip7p (Zanchin *et al.*, 1997). Além disso, foram demonstradas as interações de Nip7p com as proteínas Rrp15p e Nop53p, ambas envolvidas na biogênese da subunidade 60S. Em conjunto, os resultados apresentados fortalecem a hipótese de que a Nip7p faz parte de um grande complexo de proteínas que atua no processamento do pré-rRNA de 27S.

No Capítulo 4, está relatada a análise das interações de HsNip7, a ortóloga humana de Nip7. HsNip7 interage diretamente com a proteína FTSJ3, uma provável

metiltransferase do rRNA 25/28S, e com SUMO-2, relacionada à modificação pós-traducional de proteínas. Ensaios de localização subcelular revelaram que HsNip7 e FTSJ3 são nucleolares. Estes resultados fortalecem a hipótese de que ambas as proteínas possam atuar em um grande complexo de proteínas durante a síntese da subunidade ribossomal 60S em mamíferos.

1.4. Referências Bibliográficas

Allmang, C., Mitchell, P., Petfalski, E. and Tollervey, D. (2000) Degradation of ribosomal RNA precursors by the exosome. *Nucleic Acids Res.*, 28, 1684-1691.

Andersen, J. S., Lyon, C. E., Fox, A. H., Leung, A. K., Lam, Y. W., Steen, H., Mann, M. and Lamond, A. I. (2002) Directed proteomic analysis of the human nucleolus. *Curr. Biol.*, 12, 1-11.

Aravind, L. and Koonin, E. (1999) Novel predicted RNA-binding Domains Associated with the Translation Machinery. *J. Mol. Evol.*, 48, 291-302.

Balakin, A. G., Smith, L. and Fournier, M. J. (1996) The RNA world of the nucleolus: two major families of small RNAs defined by different box elements with related functions. *Cell*, 86, 823-834.

Baßler, J., Grandi, P., Gadal, O., Leßmann, T., Petfalski, E., Tollervey, D., Lechner, J. and Hurt, E. (2001) Identification of a 60S preribosomal particle that is closely linked to nuclear export. *Mol. Cell*, 8, 517-529.

Bernstein, K.A., Gallagher, J.E., Mitchell, B.M., Granneman, S. and Baserga, S.J. (2004) The small-subunit processome is a ribosome assembly intermediate. *Eukaryot. Cell*, 3, 1619-1626.

Burkard, K.T.D. and Butler, J.S. (2000) A nuclear 3'-5' exonuclease involved in mRNA degradation interacts with poly(A) polymerase and the hnRNA protein Npl3p. *Mol. Cell. Biol.*, 20, 604-616.

Cadwell, C., Yoon, H.J., Zebarjadian, Y. and Carbon, J. (1997) The yeast nucleolar protein Cbf5p is involved in rRNA biosynthesis and interacts genetically with the RNA polymerase I transcription factor RRN3. *Mol. Cell. Biol.*, 17, 6175-6183.

Cavaille, J., Nicoloso, M. and Bachellerie, J. P. (1996) Targeted ribose methylation of RNA *in vivo* directed by tailored antisense RNA guides. *Nature*, 383, 732-735

Charpentier, B., Muller, S. and Branlant, C. (2005) Reconstitution of archaeal H/ACA small ribonucleoprotein complexes active in pseudouridylation. *Nucleic Acids Res.*, 33, 3133-3144.

Collins, B.M., Harrop, S.J., Kornfeld, G.D., Dawes, I.W., Curmi, P.M. and Mabbutt, B.C. (2001) Crystal structure of a heptameric Sm-like protein complex from archaea: implications for the structure and evolution of snRNPs. *J. Mol. Biol*., 309, 915-923.

Decatur, W.A. and Fournier, M.J. (2002) rRNA modifications and ribosome function. *Trends Biochem. Sci*., 27, 344-351.

Dennis, P.P., Omer, A. and Lowe, T. (2001) A guided tour: small RNA function in Archaea. *Mol. Microbiol.*, 40, 509-519.

Dez, C., Noaillac-Depeyre, J., Caizergues-Ferrer, M. and Henry, Y. (2002) Naf1p, an essential nucleoplasmic factor specifically required for accumulation of box H/ACA small nucleolar RNPs. *Mol. Cell. Biol*, 22, 7053-7065.

Dragon, F., Gallagher, J.E., Compagnone-Post, P.A., Mitchell, B.M., Porwancher, K.A., Wehner, K.A., Wormsley, S., Settlage, R.E., Shabanowitz, J., Osheim, Y., Beyer, A.L., Hunt, D.F. and Baserga, S.J. (2002) A large nucleolar U3 ribonucleoprotein required for 18S ribosomal RNA biogenesis. *Nature*, 417, 967-970.

Dziembowski, A., Lorentzen, E., Conti, E. and Séraphin, B. (2007) A single subunit, Dis3, is essentially responsible for yeast exosome core activity. *Nat. Struct. Mol. Biol.*, 14, 15-22.

Fatica, A. and Tollervey, D. (2002) Making ribosomes. *Curr. Opin. Cell Biol.*, 14, 313-318.

Fatica, A., Cronshaw, A. D., Dlakiæ, M. and Tollervey, D. (2002) Ssf1p prevents premature processing of an early pre-60S ribosomal particle. *Mol. Cell*, 9, 341–351.

Fromont-Racine, M., Senger, B., Saveanu, C. and Fasiolo, F. (2003) Ribosome assembly in eukaryotes. *Gene*, 313, 17-42.

Galardi, S., Fatica, A., Bachi, A., Scaloni, A., Presutti, C. and Bozzoni, I. (2002) Purified box C/D snoRNPs are able to reproduce site-specific 2'-O-methylation of target RNA *in vitro*. *Mol. Cell Biol*., 22, 6663-6668.

Ganot, P., Bortolin, M.L. and Kiss, T. (1997) Site-specific pseudouridine formation in preribosomal RNA is guided by small nucleolar RNAs. *Cell*, 89, 799-809.

Gavin, A.C., Aloy, P., Grandi, P., Krause, R., Boesche, M., Marzioch, M., Rau, C., Jensen, L.J., Bastuck, S., Dümpelfeld, B., Edelmann, A., Heurtier, M.A., Hoffman, V., Hoefert, C., Klein, K., Hudak, M., Michon, A.M., Schelder, M., Schirle, M., Remor, M., Rudi, T., Hooper, S., Bauer, A., Bouwmeester, T., Casari, G., Drewes, G., Neubauer, G., Rick, J.M., Kuster, B., Bork, P., Russell, R.B. and Superti-Furga, G. (2006) Proteome survey reveals modularity of the yeast cell machinery. *Nature*, 440, 631-636.

Geerlings, T.H., Vos, J.C. and Raué, H.A. (2000) The final step in the formation of 25S rRNA in *Saccharomyces cerevisiae* is performed by 5'→3' exonucleases. *RNA*, 6, 1698-1703.

Granato, D.C., Gonzales, F.A., Luz, J.S., Cassiola, F., Machado-Santelli, G.M. and Oliveira, C.C. (2005) Nop53p, an essential nucleolar protein that interacts with Nop17p and Nip7p, is required for pre-rRNA processing in *Saccharomyces cerevisiae*. *FEBS J*., 272, 4450-4463.

Grandi, P., Rybin, V., Bassler, J., Petfalski, E., Strauss, D., Marzioch, M., Schäfer, T., Kuster, B., Tschochner, H., Tollervey, D., Gavin, A.C. and Hurt, E. (2002) 90S pre-

ribosomes include the 35S pre-rRNA, the U3 snoRNP, and 40S subunit processing factors but predominantly lack 60S synthesis factors. *Mol. Cell*, 10, 105-115.

Grimm, T., Hölzel, M., Rohrmoser, M., Harasim, T., Malamoussi, A., Gruber-Eber, A., Kremmer, E. and Eick, D. (2006) Dominant-negative Pes1 mutants inhibit ribosomal RNA processing and cell proliferation via incorporation into the PeBoW-complex. *Nucleic Acids Res.*, 31, 3030-3043.

Gu, Z., Moerschell, R. P., Sherman, F. and Goldfarb, D. S. (1992) *NIP1*, a gene required for nuclear transport in yeast. *Proc. Natl. Acad. Sci. USA*, 89, 10355-10359.

Hallberg, B.M., Ericsson, U.B., Johnson, K.A., Andersen, N.M., Douthwaite, S., Nordlund, P., Beuscher, A.E. 4th and Erlandsen, H. (2006) The structure of the RNA m5C methyltransferase YebU from *Escherichia coli* reveals a C-terminal RNA-recruiting PUA domain. *J. Mol. Biol.*, 360, 774-787.

Hamma, T., Reichow, S.L., Varani, G. and Ferre-D'Amare, A.R. (2005) The Cbf5-Nop10 complex is a molecular bracket that organizes box H/ACA RNPs. *Nat. Struct. Mol. Biol.*, 12, 1101-1107.

Henras, A., Henry, Y., Bousquet-Antonelli, C., Noaillac-Depeyre, J., Gélugne, J.P. and Caizergues-Ferrer, M. (1998) Nhp2p and Nop10p are essential for the function of H/ACA snoRNPs. *EMBO J.*, 17, 7078-7090.

Henras, A., Capeyrou, R., Henry, Y. and Caizergues-Ferrer, M. (2004) Cbf5p, the putative pseudouridine synthase of H/ACA-type snoRNPs, can form a complex with Gar1p and Nop10p in absence of Nhp2p and box H/ACA snoRNAs. *RNA*, 10, 1704-1712.

Henras, A., Dez, C., Noaillac-Depeyre, J., Henry, Y. and Caizergues-Ferrer, M. (2001) Accumulation of H/ACA snoRNPs depends on the integrity of the conserved central domain of the RNA-binding protein Nhp2p. *Nucleic Acids Res.*, 29, 2733-2746.

Hernández, H., Dziembowski, A., Taverner, T., Séraphin, B. and Robinson, C. V. (2006) Subunit architecture of multimeric complexes isolated directly from cells, *EMBO Rep.*, 7, 605-610.

Hesling, C., Oliveira, C. C., Castilho, B. A., and Zanchin, N. I. T. (2007) The Shwachman-Bodian-Diamond syndrome associated protein interacts with HsNip7 and its down-regulation affects gene expression at the transcriptional and translational levels. *Exp. Cell Res.*, 313, 4180-4195.

Hoang, C. and Ferre-D'Amare, A.R. (2001) Cocrystal structure of a tRNA Psi55 pseudouridine synthase: nucleotide flipping by an RNA-modifying enzyme. *Cell*, 107, 929-939.

Hölzel, M., Rohrmoser, M., Schlee, M., Grimm, T., Harasim, T., Malamoussi, A., Gruber-Eber, A., Kremmer, E., Hiddemann, W., Bornkamm, G.W., Eick, D. (2005) Mammalian

WDR12 is a novel member of the Pes1-Bop1 complex and is required for ribosome biogenesis and cell proliferation. *J. Cell Biol.*, 170, 367-378.

Horsey, E.W., Jakovljevic, J., Miles, T.D., Harnpicharnchai, P. and Woolford, Jr, J.L. (2004) Role of the yeast Rrp1p protein in the dynamics of pre-ribosome maturation. *RNA*, 10, 813-827.

Houseley, J., LaCava, J. and Tollervey, D. (2006) RNA-quality control by the exosome. *Nat. Rev. Mol. Cell. Biol*., 7, 529-539.

Ishitani, R., Nureki, O., Fukai, S., Kijimoto, T., Nameki, N., Watanabe, M., Kondo, H., Sekine, M., Okada, N., Nishimura, S. and Yokoyama, S. (2002) Crystal Structure of Archaeosine tRNA-guanine Transglycosylase. *J. Mol. Biol.,* 318, 665-677.

Ishitani, R., Nureki, O., Nameki, N., Okada, N., Nishimura, S. and Yokoyama, S. (2003) Alternative tertiary structure of tRNA for recognition by a posttranscriptional modification enzyme. *Cell*, 113, 383-394.

Johnson, A.W. (1997) Rat1p and Xrn1p are functionally interchangeable exoribonucleases that are restricted to and required in the nucleus and cytoplasm, respectively. *Mol. Cell. Biol.*, 17, 6122-6130.

Kiss-László, Z., Henry, Y., Bachellerie, J.P., Caizergues-Ferrer, M. and Kiss, T. (1996) Site-specific ribose methylation of preribosomal RNA: a novel function for small nucleolar RNAs. *Cell*, 85, 1077-1088.

King, T.H., Liu, B., McCully, R.R. and Fournier, M.J. (2003) Ribosome structure and activity are altered in cells lacking snoRNPs that form pseudouridines in the peptidyl transferase center. *Mol. Cell*, 11, 425-435.

Kressler, D., Linder, P. and de la Cruz, J. (1999) Protein trans-acting factors involved in ribosome biogenesis in *Saccharomyces cerevisiae*. *Mol. Cell. Biol.*, 19, 7897-7912.

Lafontaine, D. and Tollervey, D. (1995) Trans-acting factors in yeast pre-rRNA and pre-snoRNA processing. *Biochem. Cell Biol.*, 73, 803-812.

Lafontaine, D.L., Bousquet-Antonelli, C., Henry, Y., Caizergues-Ferrer, M. and Tollervey, D. (1998) The box H+ACA snoRNAs carry Cbf5p, the putative rRNA pseudouridine synthase. *Genes Dev*., 15, 527-537.

Lapik, Y.R., Fernandes, C.J., Lau, L.F. and Pestov, D.G. (2004) Physical and functional interaction between Pes1 and Bop1 in mammalian ribosome biogenesis. *Mol. Cell*, 15, 17-29.

Lee, S.J. and Baserga, S.J. (1997) Functional separation of pre-rRNA processing steps revealed by truncation of the U3 small nucleolar ribonucleoprotein component, Mpp10. *Proc. Natl. Acad. Sci. USA*, 94, 13536-13541.

Leulliot, N., Godin, K.S., Hoareau-Aveilla, C., Quevillon-Cheruel, S., Varani, G., Henry, Y. and Van Tilbeurgh, H. (2007) The box H/ACA RNP assembly factor Naf1p contains a domain homologous to Gar1p mediating its interaction with Cbf5p. *J. Mol. Biol.*, 371, 1338-1353.

Li, L., and Ye, K. (2006) Crystal structure of an *H/ACA box* ribonucleoprotein particle, *Nature*, 443, 302-307.

Liang, W.Q. and Fournier, M.J. (1995) U14 base-pairs with 18S rRNA: a novel snoRNA interaction required for rRNA processing. *Genes Dev*., 9, 2433-2443.

Liu, J. F., Wang, X. Q., Wang, Z. X., Chen, J. R., Jiang, T., An, X. M., Chang, W. R. and Liang, D. C. (2004) Crystal structure of KD93, a novel protein expressed in human hematopoietic stem/progenitor cells. *J. Struct. Biol.*, 148, 370-374.

Liu, Q., Greimann, J.C. and Lima, C.D. (2006) Reconstitution, activities, and structure of the eukaryotic RNA exosome. *Cell*, 127, 1223-1237.

Lorentzen, E., Walter, P., Fribourg, S., Evguenieva-Hackenberg, E., Klug, G. and Conti, E. (2005) The archaeal exosome core is a hexameric ring structure with three catalytic subunits. *Nat. Struct. Mol. Biol*.,12, 575-581.

Luz, J. S., Tavares, J.R., Gonzales, F. A., Santos, M.C.T. and Oliveira, C. C. (2007) Analysis of the *Saccharomyces cerevisiae* exosome architecture and of the RNA binding activity of Rrp40p. *Biochimie*, 89, 686-691.

Lygerou, Z., Mitchell, P., Petfalski, E., Séraphin, B. and Tollervey, D. (1994) The POP1 gene encodes a protein component common to the RNase MRP and RNase P ribonucleoproteins. *Genes Dev*., 8, 1423-1433.

Manival, X., Charron, C., Fourmann, J.B., Godard, F., Charpentier, B. and Branlant, C. (2006) Crystal structure determination and site-directed mutagenesis of the *Pyrococcus abyssi* aCBF5-aNOP10 complex reveal crucial roles of the C-terminal domains of both proteins in H/ACA sRNP activity. *Nucleic Acids Res.*, 34, 826-839.

Marco-Marín, C., Gil-Ortiz, F., Pérez-Arellano, I., Cervera, J., Fita, I., and Rubio, V. (2007) A novel two-domain architecture within the amino acid kinase enzyme family revealed by the crystal structure of *Escherichia coli* glutamate 5-kinase, *J. Mol. Biol.,* 367, 1431-1446.

Menne, T.F., Goyenechea, B., Sánchez-Puig, N., Wong, C.C., Tonkin, L.M., Ancliff, P.J., Brost, R.L., Costanzo, M., Boone, C. and Warren, A.J. (2007) The Shwachman-Bodian-Diamond syndrome protein mediates translational activation of ribosomes in yeast. *Nat. Genet*., 39, 486-495.

Mitchell, P., Petfalski, E., Shevchenko, A., Mann, M. and Tollervey, D. (1997) The exosome: A conserved eukaryotic RNA processing complex containing multiple 3'→5' exoribonucleases. *Cell*, 91, 457-466.

Mochizuki, Y., He, J., Kulkarni, S., Bessler, M. and Mason, P.J. (2004) Mouse dyskerin mutations affect accumulation of telomerase RNA and small nucleolar RNA, telomerase activity, and ribosomal RNA processing. *Proc. Natl. Acad. Sci. USA*, 101, 10756-10761.

Ni, J.W., Tien, A.L. and Fournier, M.J. (1997) Small nucleolar RNAs direct site-specific synthesis of pseudouridine in ribosomal RNA. *Cell*, 89, 565-573.

Nissan, T.A., Bassler, J., Petfalski, E., Tollervey, D. and Hurt, E. (2002) 60S pre-ribosome formation viewed from assembly in the nucleolus until export to the cytoplasm. *EMBO J.*, 21, 5539-5547.

Oliveira, C.C., Gonzales, F.A. and Zanchin, N.I.T. (2002) Temperature-sensitive mutants of the exosome subunit Rrp43p show a deficiency in mRNA degradation and no longer interact with the exosome. *Nucleic Acids Res.*, 30, 4186-4198.

Omer, A.D., Lowe, T.M., Russell, A.G., Ebhardt, H., Eddy, S.R. and Dennis, P.P. (2000) Homologs of small nucleolar RNAs in Archaea. *Science,* 288, 517-522.

Omer, A.D., Ziesche, S., Decatur, W.A., Fournier, M.J. and Dennis, P.P. (2003) RNA-modifying machines in archaea. *Mol. Microbiol.*, 48, 617-629.

Pérez-Arellano, I., Gallego, J., and Cervera, J. (2007) The PUA domain - a structural and functional overview, *FEBS J.*, 274, 4972-4984.

Ramos, C.R., Oliveira, C.L., Torriani, I.L. and Oliveira, C.C. (2006) The *Pyrococcus* exosome complex: structural and functional characterization. *J. Biol. Chem.*, 281, 6751-6759.

Rashid, R.; Liang, B., Baker, D.L., Youssef, O.A., He,Y., Phipps, K., Terns, R.M., Terns, M.P. and Li, H. (2006) Crystal structure of a Cbf5-Nop10-Gar1 complex and implications in RNA-guided pseudouridylation and dyskeratosis congenita. *Mol. Cell*, 21,249-260.

Reinert, L.S., Shi, B., Nandi, S., Mazan-Mamczarz, K., Vitolo, M., Bachman, K.E., He, H., and Gartenhaus, R.B. (2006) MCT-1 protein interacts with the cap complex and modulates messenger RNA translational profiles. *Cancer Res.*, 66, 8994- 9001.

Rohrmoser, M., Hölzel, M., Grimm, T., Malamoussi, A., Harasim, T., Orban, M., Pfisterer, I., Gruber-Eber, A., Kremmer, E. and Eick, D. (2007) Interdependence of Pes1, Bop1, and WDR12 controls nucleolar localization and assembly of the PeBoW complex required for maturation of the 60S ribosomal subunit. *Mol. Cell. Biol.*, 27, 3682-3694.

Sabina, J. and Söll, D. (2006) The RNA-binding PUA domain of archaeal tRNA-guanine transglycosylase is not required for archaeosine formation. *J. Biol. Chem.*, 281, 6993-7001.

Sekiguchi, T., Todaka, Y., Wang, Y., Hirose, E., Nakashima, N. and Nishimoto, T. (2004) A novel human nucleolar protein, Nop132, binds to the G proteins, RRAG A/C/D. *J. Biol. Chem.*, 279, 8343-8350.

Strezoska, Z., Pestov, D. G., Lau, L. F. (2000) Bop1 is a mouse WD40 repeat nucleolar protein involved in 28S and 5.8S rRNA processing and 60S ribosome biogenesis. *Mol. Cell. Biol.*, 20, 5516-5528.

Thomsom, E. and Tollervey, D. (2005) Nop53p is required for late 60S ribosome subunit maturation and nuclear export in yeast. *RNA*, 11, 1215-1224.

Tollervey, D. and Kiss, T. (1997) Function and synthesis of small nucleolar RNAs. *Curr. Opin. Cell Biol.*, 9, 337-342.

Torchet, C., Badis, G., Devaux, F., Costanzo, G., Werner, M. and Jacquier, A. (2005) The complete set of H/ACA snoRNAs that guide rRNA pseudouridylations in *Saccharomyces cerevisiae*. *RNA*, 11, 928-938.

Vanrobays, E., Gleizes, P.E., Bousquet-Antonelli, C., Noaillac-Depeyre, J., Caizergues-Ferrer, M. and Gélugne, J.P. (2001) Processing of 20S pre-rRNA to 18S ribosomal RNA in yeast requires Rrp10p, an essential non-ribosomal cytoplasmic protein. *EMBO J.*, 20, 4204-4213.

Venema, J. and Tollervey, D. (1995) Processing of pre-ribosomal RNA in *Saccharomyces cerevisiae*. *Yeast*, 11, 1629-1650.

Venema, J. and Tollervey, D. (1999) Ribosome synthesis in *Saccharomyces cerevisiae*. *Annu. Rev. Genet.*, 33, 261-311.

Warner, J.R. (1989) Synthesis of ribosomes in *Saccharomyces cerevisiae*. *Microbiol. Rev.*, 53, 256-271.

Yoon, A., Peng, G., Brandenburg, Y., Zollo, O., Xu, W., Rego, E. and Ruggero, D. (2006) Impaired Control of IRES-Mediated Translation in X-Linked Dyskeratosis Congenita. *Science*, 312, 902-906.

Zanchin, N.I.T. and Goldfarb, D.S. (1999a) Nip7p interacts with Nop8p, an essential nucleolar protein required for 60S ribosome biogenesis, and the exosome subunit Rrp43p. *Mol. Cell. Biol.*, 19, 1518-1525.

Zanchin, N.I.T. and Goldfarb, D.S. (1999b) The exosome subunit Rrp43p is required for the efficient maturation of 5.8S, 18S and 25S rRNA. *Nucleic Acids Res.*, 27, 1283-1288.

Zanchin, N.I.T., Roberts, P., DeSilva, A., Sherman, F. and Goldfarb, D.S. (1997) *Saccharomyces cerevisiae* Nip7p is required for efficient 60S ribosome subunit biogenesis. *Mol. Cell. Biol*, 17, 5001-5015.

2. OBJETIVOS

Os objetivos específicos do presente trabalho são os seguintes:

1. Resolver a estrutura tri-dimensional da ortóloga de Nip7p em *P. abyssi*, PaNip7.

2. Investigar o mecanismo de interação da proteína Nip7p com RNA.

3. Analisar o papel da proteína Nip7p de *S. cerevisiae* na modificação do rRNA e na interação com outras proteínas.

4. Caracterizar as interações da ortóloga humana de Nip7 com outras proteínas.

3.1. Capítulo 1

Expression, crystallization and preliminary X-ray analysis of the *Pyrococcus abyssi* protein homologue of *Saccharomyces cerevisiae* Nip7p

Patrícia P. Coltri, Beatriz G. Guimarães, Carla C. Oliveira and Nilson I. T. Zanchin

Acta Crystallographica D Biological Crystallography, **60**, 1925-1928 (2004).

Acta Crystallographica Section D
Biological Crystallography
ISSN 0907-4449

Expression, crystallization and preliminary X-ray analysis of the *Pyrococcus abyssi* protein homologue of *Saccharomyces cerevisiae* Nip7p

Patrícia Pereira Coltri,[a] Beatriz Gomes Guimarães,[a] Carla Columbano Oliveira[b] and Nilson Ivo Tonin Zanchin[a]*

[a]Center for Structural Molecular Biology, Brazilian Synchrotron Light Laboratory, LNLS CP 6192, CEP 13084-971, Campinas SP, Brazil, and [b]Department of Biochemistry, Chemistry Institute, University of São Paulo, Av. Prof. Lineu Prestes 748, São Paulo, SP 05508-000, Brazil

Correspondence e-mail: zanchin@lnls.br

Received 15 June 2004
Accepted 13 August 2004

Saccharomyces cerevisiae Nip7p is a nucleolar protein required for accurate processing of the 27S precursor of the 25S and 5.8S ribosomal RNAs. Nip7p homologues are found in eukaryotes and archaea. The *Pyrococcus abyssi* homologue of Nip7p (PaNip7) was cloned, expressed in *Escherichia coli* and purified for crystallization. X-ray diffraction data were collected from native crystals and an iodide derivative using synchrotron radiation. PaNip7 native crystals diffract to 1.8 Å and belong to space group *C*2, with unit-cell parameters $a = 88.49$, $b = 90.28$, $c = 63.35$ Å, $\beta = 134.29^\circ$. The PaNip7 structure was solved using the SIRAS method.

1. Introduction

Ribosome biogenesis requires a fine balance between synthesis of the ribosomal proteins and transcription, processing and modification of the rRNA precursors (pre-rRNA). In eukaryotes, pre-rRNA processing and modification take place simultaneously with assembly of the ribosomal proteins (r-proteins) onto the rRNA, forming large ribonucleoprotein particles in the nucleolus. Over 170 *trans*-acting factors involved in rRNA biosynthesis have already been identified and include endo- and exonucleases, putative ATP-dependent RNA helicases, rRNA-modifying enzymes and an increasing number of small nucleolar ribonucleoprotein (snoRNP) complexes (Kressler *et al.*, 1999; Venema & Tollervey, 1999; Fromont-Racine *et al.*, 2003).

The yeast *Saccharomyces cerevisiae* has been an important model organism for the study of eukaryotic ribosome biogenesis. The *nip7* gene was isolated by complementation of the *S. cerevisiae* temperature-sensitive strain *nip7-1* (Zanchin *et al.*, 1997). The *nip7*-encoded protein Nip7p is essential for cell viability and 60S subunit formation. Its depletion causes a series of pre-rRNA processing defects that include accumulation of the 35S pre-rRNA transcript, presence of a 23S aberrant precursor, decreased 20S pre-rRNA levels and accumulation of 27S pre-rRNA. Delayed processing of 27S pre-rRNA is the cause of reduced synthesis of 25S and 5.8S rRNAs relative to 18S rRNA in cells deficient in Nip7p (Zanchin *et al.*, 1997). Nip7p interacts physically with the proteins Rrp43p and Nop8p (Zanchin & Goldfarb, 1999*a*,*b*). Rrp43p is a subunit of the exosome complex and was initially reported to be necessary for accurate 5.8S rRNA 3′-end formation (Mitchell *et al.*, 1997), but its deficiency mainly affects 40S subunit biosynthesis (Zanchin & Goldfarb, 1999*a*); it is also required for 18S rRNA biosynthesis and for degradation of the excised 5′ external transcribed sequence. Yeast cells depleted of Nop8p show an imbalance in ribosomal subunits with reduced levels of 60S subunits. However, whereas deficiency of Nip7p results in slower processing of the 27S pre-rRNA, deficiency of Nop8p leads to rapid degradation of this pre-rRNA, indicating that Nip7p and Nop8p are required for different 27S pre-rRNA processing steps. The molecular function of both proteins, however, still remains to be determined. Human homologues of both Nop8p (named Nop132) and Nip7p have been isolated and their physical interaction has also been demonstrated (Zanchin *et al.*, 1997; Sekiguchi *et al.*, 2004), further confirming that the mechanism of ribosome biosynthesis is highly conserved in eukaryotes.

Archaea are prokaryotic organisms in regard to the absence of a nucleus, but certain cellular processes show a resemblance to those of eukaryotes. Homologues of the eukaryotic nucleolar proteins Nop1p and Nop56p/Nop58p have been identified in all archaeal genomes sequenced (Amiri, 1994; Omer *et al.*, 2000). These proteins are found in box C/D snoRNPs that are responsible for ribose methylation on the rRNA (Decatur & Fournier, 2003). Small RNA homologues of the eukaryotic small nucleolar RNAs, which function as guides to the methylation sites of snoRNP, are also found in archaea (Dennis *et al.*, 2001; Omer *et al.*, 2003). A protein showing sequence similarity to Nip7p was identified in archaea and *Archaeoglobus fulgidus* contains the most similar archaeal Nip7p homologue, showing 25% and 45% amino-acid identity and similarity, respectively, to the yeast protein. The *Pyrococcus abyssi* Nip7 homologue shares 17.5% amino-acid identity and 38% similarity

DOI: 10.1107/S0907444904020219

with the yeast Nip7p. Comparative sequence analysis identified a putative RNA-binding domain at the C-terminal region of Nip7p (Aravind & Koonin, 1999). This domain is found in a number of RNA-modifying enzymes and was named PUA after pseudouridine synthases and archaeosine-specific transglycosylases. The PUA domain comprises approximately 78–83 amino acids, showing a predicted β-strand-rich structure (Aravind & Koonin, 1999). These observations indicate that Nip7p shows a conserved RNA-binding activity and led us to investigate the three-dimensional structure of *P. abyssi* Nip7 by X-ray crystallography.

Table 1
Data-collection statistics.

Values in parentheses are for the outer resolution shell.

	Native crystal	Iodide derivative
Beamline	LNLS D03B-CPR	LNLS D03B-CPR
Wavelength (Å)	1.4270	1.4270
Space group	*C*2	*C*2
Unit-cell parameters (Å, °)	a = 88.49, b = 90.28, c = 63.35, β = 134.29	a = 87.33, b = 88.99, c = 63.59, β = 133.36
Resolution limits (Å)	31.6–1.80 (1.90–1.80)	32.1–1.90 (2.00–1.90)
Total observations	235642	458129
Unique reflections	33002	27392
Completeness (%)	99.9 (100.0)	98.5 (96.9)
Multiplicity	7.1 (7.0)	16.7 (16.6)
R_{sym} (%)	4.9 (30.1)	6.2 (26.7)
Mean $I/\sigma(I)$	8.6 (1.7)	6.4 (2.4)
Anomalous completeness (%)		98.4 (97.1)
Anomalous R factor (%)		7.3 (13.0)
Isomorphous R factor (%)		38.3 (43.6)

2. Methods

2.1. Cloning of the *P. abyssi* Nip7 homologue

DNA cloning and analysis were performed according to previously described standard procedures (Sambrook *et al.*, 1989) using *Escherichia coli* strain DH5α, which was maintained in LB medium containing 50 µg ml^{-1} ampicillin. The *P. abyssi* Nip7 homologue is a 166-amino-acid protein with a molecular weight of 19 291.38 Da and was identified by database searches for proteins showing sequence similarity to the *S. cerevisiae* Nip7p protein. A 502 base-pair DNA fragment comprising the coding sequence of the *P. abyssi* Nip7 homologue (PAB0176; PaNip7) was amplified by polymerase chain reaction (PCR) from genomic DNA using oligonucleotides containing *NdeI* and *Bam*HI restriction sites (forward, 5′-AGGAAGCATATGAGTGGTGAGCTGAGG-3′; reverse, 5′-CCGGATCCAGTTAGGCAAGAAAACAAG-3′). The PCR product was cloned using the pGEM-T system (Promega) and subsequently subcloned into the pCYTEXP3 (Schneppe *et al.*, 1994) expression vector, producing vector pCYTEX-PaNip7. The nucleotide sequence of the PCR product was verified by DNA sequencing analysis using an Applied Biosystems ABI Prism 377 DNA-sequence analyzer.

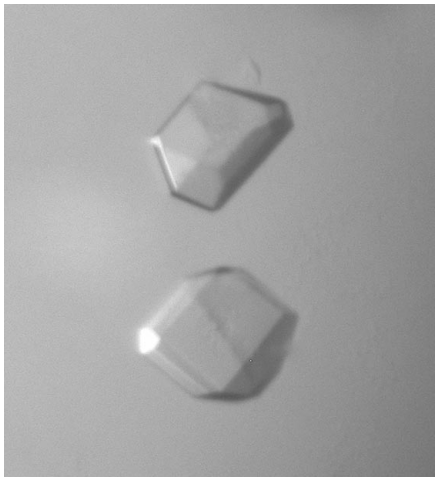

Figure 1
Crystals of *P. abyssi* Nip7 obtained by vapour-diffusion equilibration against a reservoir solution consisting of 4.1 *M* NaCl and 100 m*M* HEPES pH 7.2. Maximum crystal dimensions were 150 × 150 × 75 µm.

2.2. Expression and purification of PaNip7

E. coli DH5α harbouring plasmid pCYTEX-PaNip7 was incubated overnight at 303 K in LB medium containing ampicillin (50 µg ml^{-1}). This pre-culture was used to inoculate 4 l of fresh LB–ampicillin medium and incubated at 303 K until an optical density at 600 nm (OD_{600}) of approximately 0.8–0.9 was reached. PaNip7 expression was induced by transferring the culture to 315 K for 4 h. Cells were harvested by centrifugation, resuspended in buffer *A* [10 m*M* Tris–HCl pH 7.0, 50 m*M* NaCl, 1 m*M* EDTA, 0.5 m*M* phenylmethylsulfonyl fluoride (PMSF)] and treated with lysozyme (50 µg ml^{-1}) for 30 min on ice. Subsequently, cells were disrupted by sonication using a Branson sonifier (Branson Ultrasonics Co). The cell extract was initially incubated at 338 K for 1 h for thermal denaturation of *E. coli* proteins. The suspension was submitted to centrifugation at 20 000*g* for 30 min at 277 K and the soluble fraction was applied onto a heparin-Sepharose column (Amersham-Pharmacia) equilibrated with buffer *A*. The column was eluted with a linear 50 m*M* to 1 *M* NaCl gradient. The purified protein was dialyzed against a buffer containing 10 m*M* Tris–HCl pH 7.0 and 5 m*M* β-mercaptoethanol for 48 h at 277 K and concentrated using an Ultrafree 4 concentrator (Millipore). This expression system yielded approximately 2 mg of protein per litre of culture.

2.3. Crystallization assays

PaNip7 was crystallized by the hanging-drop vapour-diffusion method at a concentration of 12 mg ml^{-1} in 10 m*M* Tris–HCl pH 7.0 and 5 m*M* β-mercaptoethanol at 293 K. Initial crystallization trials were performed using Crystal Screen, Crystal Screen II (Hampton Research), Wizard I and Wizard II (Decode Genetics). 24-well plates were used and 300 µl reservoir solution was used in each well. Equal volumes (2 µl) of protein sample and reservoir solution were mixed for crystallization. Small needle-shaped crystals were observed in most wells 24 h after the assay was begun. Monocrystals were only observed in a Crystal Screen II well containing 4.3 *M* NaCl and 100 m*M* HEPES pH 7.5 after 2 d. This crystallization condition was refined by changing the NaCl concentration and the pH of the HEPES buffer. Crystals were observed in wells containing reservoir solutions with NaCl concentration in the range 3.9–4.3 *M* and pH in the range 7.2–8.2. Larger crystals were obtained using 4.1 *M* NaCl and 100 m*M* HEPES pH 7.2 after 2 d at 293 K. The crystals grew to dimensions of 150 × 150 × 75 µm (Fig. 1).

2.4. Data collection and processing

X-ray diffraction data were collected at the protein crystallography beamline D03B-CPR of the Brazilian Synchrotron Light Laboratory, LNLS, Campinas, Brazil. Native crystals were cryoprotected with 20% glycerol prior to flash-cooling in a 100 K nitrogen-gas stream. Iodide-derivative (I^-) crystals were obtained by the rapid cryo-soaking technique (Dauter *et al.*, 2000; Nagem *et al.*, 2001). The soaking solution

consisted of 20% glycerol, 100 m*M* HEPES pH 7.2, 3.1 *M* NaCl and 1.0 *M* NaI (1.0 *M* NaCl of the mother liquor was replaced by NaI in order to facilitate iodide-anion incorporation). Crystals were incubated in the soaking solution for 2 min prior to flash-cooling. Complete data sets were collected from native and derivative crystals using a MAR CCD detector. The beamline wavelength was set to 1.427 Å. In order to obtain highly redundant data from the derivative crystal, 700 oscillation images ($\Delta\varphi = 1^\circ$) were taken. Data processing and scaling was performed using the programs *MOSFLM* (Leslie, 1992) and *SCALA* (Kabsch, 1988; Blessing, 1995) from the *CCP*4 package (Collaborative Computational Project 4, Number 4, 1994).

3. Results and discussion

PaNip7 native crystals diffract to 1.8 Å resolution and belong to space group *C*2. I^--derivative crystals diffract to 1.9 Å resolution and belong to the same space group with similar unit-cell parameters. Table 1 summarizes the data-collection statistics. According to Matthews (1968), a solvent content of 48% corresponds to V_M = 2.4 Å^3 Da^{-1}, indicating the presence of two monomers in the asymmetric unit.

The structure of PaNip7 was determined using the SIRAS method. LNLS D03B is a monochromatic beamline and with the experimental setup used (wavelength = 1.427 Å) the theoretical f'' value of iodide is 6.0243. Seven I^- sites with occupancies greater than 0.7 were found with the program *SHELXD* (Sheldrick & Schneider, 2001) using only anomalous data from the derivative crystal. Derivative-to-native data scaling was performed using the program *SCALEIT* (Howell & Smith, 1992) from the *CCP*4 package (Collaborative Computational Project 4, Number 4, 1994). Anomalous and isomorphous data statistics are presented in Table 1. The high value of the isomorphous *R* factor also indicated the incorporation of a large number of iodide ions. Fig. 2 shows a comparison between the anomalous and isomorphous Patterson maps obtained from experimental data and the predicted Patterson map generated using the iodide coordinates found by *SHELXD*. According to the Matthews coefficient calculation, the asymmetric unit should contain two molecules (332 residues in total); therefore, *SHELXD* results indicate the presence of at least one anomalous scatterer per approximately 47 residues. Refinement of heavy-atom parameters and calculation of phases were carried out with *SHARP* (de La Fortelle & Bricogne, 1997) using data from native and derivative crystals. An improved electron-density map was obtained by solvent flattening with *SOLOMON* (Abrahams & Leslie, 1996). Model building and refinement are currently in progress.

In conclusion, we have crystallized the first homologue of *S. cerevisiae* Nip7p and expect that the three-dimensional structure of *P. abyssi* Nip7 will provide essential information about the molecular function of this group of proteins. Together with RNA-binding assays, the PaNip7 structural analysis is expected to confirm whether the PUA domain found in these proteins is a functional RNA-binding domain.

This work was supported by grant 00/02788-4 and the SMolBNet program (00/10266-8) from the Foundation for Research Support of the State of São Paulo (FAPESP). PPC is a recipient of a FAPESP

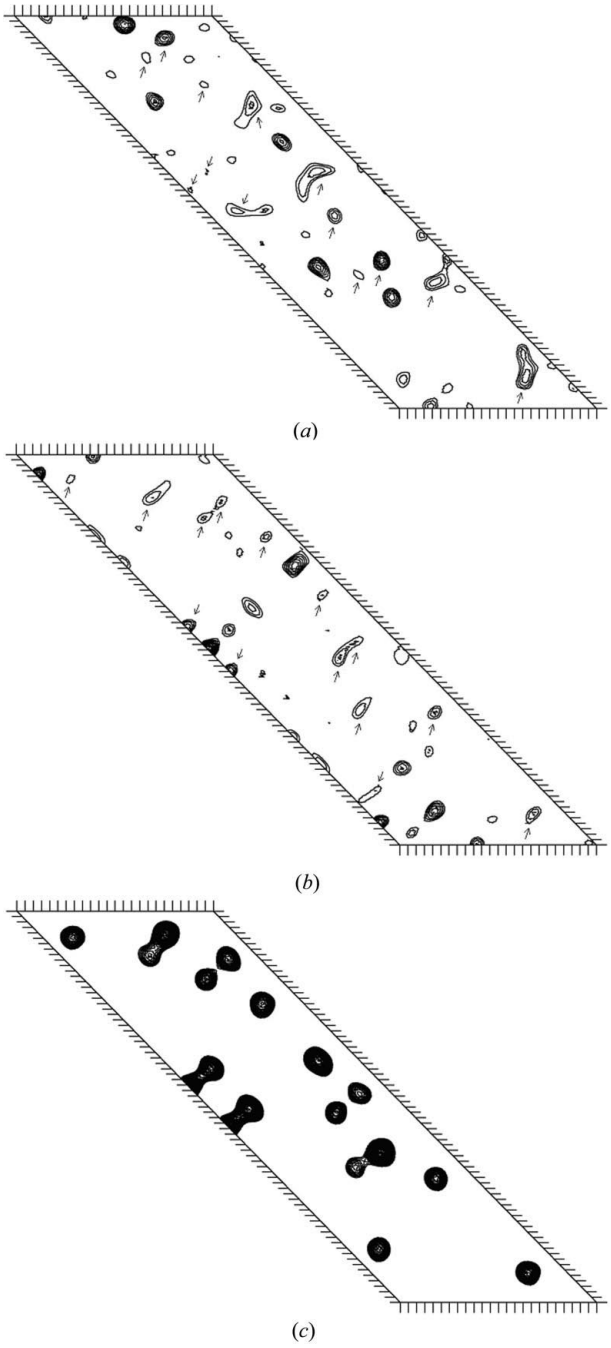

Figure 2
Harker sections of the anomalous (*a*) and isomorphous (*b*) Patterson maps (minimum contour level = 2.0σ). The peaks indicated by arrows are also found in the predicted Harker section (*c*) generated using the heavy-atom coordinates.

pre-doctoral fellowship (03/06299-6). The authors are also grateful to Adriana C. Alves for helping with protein purification and crystallization, Luciana R. Camillo for DNA-sequencing analysis and Tereza C. Lima Silva for technical support.

References

Abrahams, J. P. & Leslie, A. G. W. (1996). *Acta Cryst.* D**52**, 30–42.

Amiri, K. A. (1994). *J. Bacteriol.* **176**, 2124–2127.

Aravind, L. & Koonin, E. V. (1999). *J. Mol. Evol.* **48**, 291–302.

Blessing, R. H. (1995). *Acta Cryst.* A**51**, 33–38.

Collaborative Computational Project, Number 4 (1994). *Acta Cryst.* D**50**, 760–763.

Dauter, Z., Dauter, M. & Rajashankar, K. R. (2000). *Acta Cryst.* D**56**, 232–237.

Decatur, W. A. & Fournier, M. J. (2003). *J. Biol. Chem.* **278**, 695–698.

Dennis, P. P., Omer, A. & Lowe, T. (2001). *Mol. Microbiol.* **40**, 509–519.

Fromont-Racine, M., Senger, B., Saveanu, C. & Fasiolo, F. (2003). *Gene*, **313**, 17–42.

Howell, P. L. & Smith, G. D. (1992). *J. Appl. Cryst.* **25**, 81–86.

Kabsch, W. (1988). *J. Appl. Cryst.* **21**, 916–924.

Kressler, D., Linder, P. & Cruz, J. (1999). *Mol. Cell. Biol.* **19**, 7897–7912.

La Fortelle, E. de & Bricogne, G. (1997). *Methods Enzymol.* **276**, 472–494.

Leslie, A. G. W. (1992). *Jnt CCP4/ESF–EACBM Newsl. Protein Crystallogr.* **26**.

Matthews, B. W. (1968). *J. Mol. Biol.* **33**, 491–497.

Mitchell, P., Petfalski, E., Shevchenko, A., Mann, M. & Tollervey, D. (1997). *Cell*, **91**, 457–466.

Nagem, R. A. P., Dauter, Z. & Polikarpov, I. (2001). *Acta Cryst.* D**57**, 996–1002.

Omer, A. D., Lowe, T. M., Russell, A. G., Ebhardt, H., Eddy, S. R. & Dennis, P. P. (2000). *Science*, **288**, 517–522.

Omer, A. D., Ziesche, S., Decatur, W. A., Fournier, M. J. & Dennis, P. P. (2003). *Mol. Microbiol.* **48**, 617–629.

Sambrook, J., Fritsch, E. F. & Maniatis, T. (1989). *Molecular Cloning, a Laboratory Manual*, 2nd ed. Cold Spring Harbor, NY, USA: Cold Spring Harbor Laboratory Press.

Schneppe, B., Eichner, W. & McCarthy, J. E. (1994). *Gene*, **143**, 201–209.

Sekiguchi, T., Todaka, Y., Wang, Y., Hirose, E., Nakashima, N. & Nishimoto, T. (2004). *J. Biol. Chem.* **279**, 8343–8350.

Sheldrick, G. M. & Schneider, T. R. (2001). *Methods in Macromolecular Crystallography*, edited by D. Turk & L. Johnson, pp. 72–81. Amsterdam: IOS Press.

Venema, J. & Tollervey, D. (1999). *Annu. Rev. Genet.* **33**, 261–311.

Zanchin, N. I. T. & Goldfarb, D. S. (1999*a*). *Nucleic Acids Res.* **27**, 1283–1288.

Zanchin, N. I. T. & Goldfarb, D. S. (1999*b*). *Mol. Cell. Biol.* **19**, 1518–1525.

Zanchin, N. I. T., Roberts, P., DeSilva, A., Sherman, F. & Goldfarb, D. S. (1997). *Mol. Cell. Biol.* **17**, 5001–5015.

3.2. Capítulo 2

Structural Insights into the Interaction of the Nip7 PUA Domain with Polyuridine RNA

Patrícia P. Coltri, Beatriz G. Guimarães, Daniela Granato, Juliana Luz, Elaine Teixeira, Carla C. Oliveira and Nilson I. T. Zanchin

Biochemistry, **46**, 14177-14187 (2007)

Structural Insights into the Interaction of the Nip7 PUA Domain with Polyuridine RNA[†,‡]

Patrícia P. Coltri,[§,#] Beatriz G. Guimarães,[§,#] Daniela C. Granato,[||] Juliana S. Luz,[||] Elaine C. Teixeira,[§] Carla C. Oliveira,[||] and Nilson I. T. Zanchin*[,§]

Center for Structural Molecular Biology, Brazilian Synchrotron Light Laboratory, LNLS, Rua Giuseppe Maximo Scolfaro 10000, P.O. Box 6192, CEP13083-970, Campinas SP, Brazil, and Department of Biochemistry, Institute of Chemistry, University of São Paulo, Av. Prof. Lineu Prestes, 748, São Paulo, SP, 05508-900, Brazil

Received August 7, 2007; Revised Manuscript Received October 4, 2007

ABSTRACT: The conserved protein Nip7 is involved in ribosome biogenesis, being required for proper 27S pre-rRNA processing and 60S ribosome subunit assembly in *Saccharomyces cerevisiae*. Yeast Nip7p interacts with nucleolar proteins and with the exosome subunit Rrp43p, but its molecular function remains to be determined. Solution of the *Pyrococcus abyssi* Nip7 (PaNip7) crystal structure revealed a monomeric protein composed by two alpha-beta domains. The N-terminal domain is formed by a five-stranded antiparallel β-sheet surrounded by three α-helices and a 3_{10} helix while the C-terminal, a mixed β-sheet domain composed by strands β8 to β12, one α-helix, and a 3_{10} helix, corresponds to the conserved PUA domain (after *P*seudo-*U*ridine synthases and *A*rchaeosine-specific transglycosylases). By combining structural analyses and RNA interaction assays, we assessed the ability of both yeast and archaeal Nip7 orthologues to interact with RNA. Structural alignment of the PaNip7 PUA domain with the RNA-interacting surface of the ArcTGT (archaeosine tRNA-guanine transglycosylase) PUA domain indicated that in the archaeal PUA domain positively charged residues (R151, R152, K155, and K158) are involved in RNA interaction. However, equivalent positions are occupied by mostly hydrophobic residues (A/G160, I161, F164, and A167) in eukaryotic Nip7 orthologues. Both proteins can bind specifically to polyuridine, and RNA interaction requires specific residues of the PUA domain as determined by site-directed mutagenesis. This work provides experimental verification that the PUA domain mediates Nip7 interaction with RNA and reveals that the preference for interaction with polyuridine sequences is conserved in *Archaea* and eukaryotic Nip7 proteins.

Eukaryotic ribosome biogenesis takes place mainly in the nucleolus where a large pre-rRNA, containing the sequences of the mature 18S, 5.8S, and 25S/28S rRNAs separated by external and internal spacer sequences, is transcribed by RNA polymerase I, and the 5S rRNA is transcribed by RNA polymerase III. The pre-rRNA is assembled with processing factors concomitantly with transcription, undergoing subsequently extensive endo- and exonucleolytic cleavage and covalent modification to generate the mature rRNAs (*1*, *2*). Major pre-rRNA processing and ribosome assembly steps have already been described and a large number of factors identified especially in the yeast model system. The large *Saccharomyces cerevisiae* 35S pre-rRNA is assembled into a 90S particle, which is rapidly converted into the pre-40S and the pre-60S preribosomal particles. While the pre-40S particles are further processed in the cytoplasm, pre-60S pre-rRNAs undergo several endo- and exonucleolytic digestions before export to the cytoplasm, where ribosome assembly terminates (*1*, *3*). Important progress has recently been made regarding the identification of the components of the preribosomal complexes. The 90S preribosome contains the 35S pre-rRNA, the U3 snoRNP, 40S subunit processing factors and a large number of 40S subunit ribosomal proteins, along with a small number of 60S ribosomal proteins (*3*). Characterization of the U3 snoRNP led to the identification of the small subunit processing complex, termed SSU processome, which contains 28 proteins required for maturation of the 18S rRNA and 40S subunit biosynthesis (*4*). Absence of 27S pre-rRNA processing factors in the 90S preribosome indicates that the 60S subunit biogenesis factors and structural proteins join the complex later in the process (*4*−*6*).

Nip7p[1] is a conserved protein component of yeast pre-60S complexes (*5*) that is essential for cell viability and for biosynthesis of 60S ribosome subunits. It was initially identified in yeast as required for processing of the 27S pre-rRNA to form the mature 25S and 5.8S rRNAs (*7*). Accumulation of unprocessed 27S pre-rRNA in Nip7p-depleted cells implicates Nip7p in the processing of the internal transcribed spacer 2 (ITS2) (*7*). It localizes to the

[†] This work was supported by FAPESP grants CEPID/CBME-98/14138-2, SMolBNet-00/10266-8, and 06/02083-7 to N.Z. and B.G.G., and 03/06031-3 to C.C.O.

[‡] Coordinates and structure factors for the PaNip7 crystal structure were deposited at RCSB Data Bank with accession number 2P38.

* Corresponding author. Tel: 55 19 3512 1113, fax: 55 19 3512 1004, e-mail: zanchin@lnls.br.

[§] Brazilian Synchrotron Light Laboratory.

[||] University of São Paulo.

[#] These authors contributed equally to this work.

10.1021/bi7015876 CCC: $37.00
Published on Web 11/15/2007

Table 1: Plasmids Used in This Study

plasmid	relevant features	reference
pCYTEX-PaNip7	*P. abyssi* Nip7, Amp^R	(*21*)
pET-PaNip7$^{R151A/R152A}$	*P. abyssi* His-PaNip7-R151A/R152A, Kan^R	this study
pET-PaNip7$^{K155A/K158A}$	*P. abyssi* His-PaNip7-K155A/K158A, Kan^R	this study
pET28-Nip7	*S. cerevisiae* His-Nip7, Kan^R	this study
pET-Nip7$^{I161A/F164A}$	*S. cerevisiae* His-Nip7-I161A/F164A, Kan^R	this study
pGEM-5.8S	*S. cerevisiae* 5.8S rRNA, Amp^R	(*10*)
pGEM-5ETS	*S. cerevisiae* 5-ETS, Amp^R	this study
pGEM-ITS2	*S. cerevisiae* ITS2, Amp^R	this study

nucleolus but was also found to sediment in the region of free 60S subunits in sucrose density gradients (*7*) which is consistent with its presence in pre-60S complexes (*5*). Neither Nip7p nor its nucleolar interacting partners, Nop8p and Nop53p, whose molecular function also remains to be described, seem to possess intrinsic catalytic activity (*8*−*10*). Yeast Nip7p interacts also with the exosome subunit Rrp43p (*9*). Although an intact exosome is required for maturation of the 3′-end of the 5.8S rRNA following cleavage of the 27S pre-rRNA in ITS2 (*11*, *12*), our analyses of Nip7p-deficient yeast strains failed to provide a functional link connecting Nip7p to the exosome function. The interaction between the yeast proteins Nip7p-Nop8p is conserved by their human orthologues (*13*), and recently we have shown that the human Nip7 can be pulled-down from HEK293 cell extracts by the GST-tagged Shwachman−Bodian−Diamond syndrome associated protein (*14*), indicating that both proteins are part of the same complex, a finding that implicates Nip7p in 60S ribosome biogenesis also in humans.

Nip7 orthologues share a highly similar two-domain architecture with the C-terminal region corresponding to the conserved PUA domain. This domain, named after pseudouridine synthases and archaeosine-specific transglycosylases (*15*), was initially described in tRNA modifying enzymes and in pseudo-uridine synthases from *Archaea* and eukaryotes (*16*−*18*) and has been proposed to mediate protein−RNA interactions. However, the PUA domain was also found in the human candidate oncogene MCT1, which was reported to interact with the mRNA cap translation factor complex via its PUA domain and to modulate translation of a subset of mRNAs (*19*). Interestingly, one of the domains of the *Escherichia coli* glutamate 5-kinase, an enzyme with function not related to RNA metabolism, also contains a PUA domain (*20*).

Despite the information obtained from yeast conditional mutant strains and from protein interaction analyses (*7*, *10*), the molecular function of Nip7p remains elusive, and the scope of this work was to investigate the role played by Nip7 and particularly by its conserved C-terminal PUA domain in regard to RNA interaction. Following solution of the crystal structure of the archaeal Nip7 orthologue from *Pyrococcus abyssi* (PaNip7), comparative structural analyses revealed that the residues involved in RNA contacts are conserved in archaeal PUA domains, but equivalent residues are replaced by mostly hydrophobic residues in the PUA domain of eukaryotic Nip7. The initial working hypothesis involved the possible interaction of Nip7p with pre-rRNA sequences. Since yeast Nip7p showed low binding affinity for several regions of the pre-rRNA, additional RNA binding studies were conducted which revealed that both the yeast Nip7p and PaNip7 orthologues can bind directly to polyuridine sequences, indicating conserved functional features among the orthologues. The results presented in this work also include mutational analyses of the PUA domain residues predicted to mediate yeast Nip7p and PaNip7 interaction with RNA and have established a role for the PUA domain of Nip7 proteins in binding of uridine-rich RNAs.

EXPERIMENTAL PROCEDURES

Plasmids and Bacterial Strains. Plasmids used in this study are listed in Table 1, and cloning procedures are summarized below. Plasmid pET28-Nip7p for expression of histidine-tagged yeast Nip7p was generated by transferring the 546 bp Nip7p coding sequence from pCYTEX-Nip7 (*7*) to pET28a using the NdeI/BamHI restriction sites. Plasmid pCYTEX-PaNip7 has been described previously (*21*). The PaNip7 PaNip7$^{R151A/R152A}$ and PaNip7$^{K155A/K158A}$ mutant variants were constructed by PCR amplification of the PaNip7 coding sequence using plasmid pCYTEX-PaNip7 as DNA template, oligonucleotide ONZ184 as forward primer (5′AGG AAG CAT ATG AGT GGT GAG CTG AGG 3′) and either oligonucleotide ONZ519 (5′ GGA TCC CTA ACG CCT TAA AAA CTC CCC AAC ATC CTT TAA ATT TTT TAT AAA TGC TGC ATC GCT CTT CGG 3′) or ONZ520 (5′GGA TCC CTA ACG CCT TAA AAA CTC CCC AAC ATC CGC TAA ATT TGC TAT AAA TCT TCT ATC GC 3′) as reverse primers, containing the base substitutions to replace either R151 and R152 or K155 and K158 by alanine residues. The resulting PCR products were subsequently inserted into the pETTEV plasmid (*22*) using the NdeI/BamHI restriction sites, generating plasmids pET-PaNip7$^{R151A/R152A}$ and pET-PaNip7$^{K155A/K158A}$. These plasmids express histidine-tagged proteins to allow purification by metal chelating affinity chromatography. Construction of the yeast Nip7p$^{I161A/F164A}$ mutant was performed by two sequential PCR steps. Initially, an 80 bp fragment of the Nip7p C-terminal region was PCR-amplified using oligonucleotide ONZ522 as forward primer (5′ GGT GCA GTT GCT GCC AGA CAA GCA GAT ATT GG 3′), containing base substitutions to replace I161 and F164 by alanine, and oligonucleotide ONZ283 as reverse primer (5′ GCA GGT CGA CCT AAG TAA ACA AGG TGT C 3′). The resulting PCR product was used as reverse primer in combination with

[1] Abbreviations: Nip7p, *Saccharomyces cerevisiae* nuclear import protein 7; PaNip7, *Pyrococcus abyssi* Nip7p orthologue; HsNip7, *Homo sapiens* Nip7p orthologue; PUA domain, *P*seudo-*U*ridine synthases and *A*rchaeosine-specific transglycosylases-containing domain; ArcTGT, *P. horikoshii* archaeosine tRNA-guanine transglycosylase; Rrp43p, *S. cerevisiae* ribosomal RNA processing protein 43; Nop8p, *S. cerevisiae* nucleolar protein 8; Nop53p, *S. cerevisiae* nucleolar protein 53; EMSA, electrophoretic mobility shift assay; ITS1, internal transcribed spacer sequence 1; ITS2, internal transcribed spacer sequence 2; 5′ ETS, 5′ external transcribed spacer sequence; RNase A, ribonuclease A.

oligonucleotide ONZ521 (5′ CGG CAT ATG AGA CAG CTA ACA GAA GAA GAG 3′) for PCR-amplification of the complete Nip7p coding sequence containing the I161A/F164A mutations, which was subsequently subcloned into the pETTEV plasmid (*22*) using the NdeI/SalI restriction sites, generating plasmid pET-Nip7$^{I161A/F164A}$. The pre-rRNA coding sequence from the 5′-ETS up to cleavage site A_0 and the ITS2 sequence were PCR-amplified using *S. cerevisiae* genomic DNA and cloned into the plasmid pGEM-T (Promega), generating pGEM-5′ETS and pGEM-ITS2. Construction of plasmid pGEM-5.8S has been described previously (*10*).

All plasmid constructs were verified by DNA sequencing analysis. *E. coli* strains DH5α and BL21(DE3), used for DNA amplification and protein expression, respectively, were manipulated according to standard techniques (*23*).

Recombinant Proteins Expression and Purification. Expression and purification of PaNip7 has been described previously (*21*). Expression of proteins from pET28a-derivative plasmids was performed in *E. coli* BL21(DE3) cells incubated in LB medium containing kanamycin (50 μg mL^{-1}) at 30 °C. At an OD_{600} of ∼0.8, the cultures were induced by adding 0.5 mM IPTG and incubating at 30 °C for further 4−6 h. Cells were harvested by centrifugation, suspended in buffer containing 50 mM sodium phosphate pH 7.2, 100 mM NaCl, 10% glycerol, and 0.5 mM phenylmethylsulfonyl fluoride (PMSF), and treated with lysozyme (50 μg mL^{-1}) for 30 min on ice. Subsequently, cells were disrupted by sonication, and the his-tagged proteins were initially purified by metal-chelating affinity chromatography on Ni-NTA columns (Qiagen), using 20−200 mM imidazole gradients for elution. Nip7p was further purified by chromatography on a heparin-sepharose column (GE Healthcare) using the same buffer as above for binding and a 50 mM to 1 M KCl gradient for elution. PaNip7$^{R151A/R152A}$ and PaNip7$^{K155A/K158A}$ were purified further by ion exchange chromatography on a mono-Q column (GE Healthcare) using buffer containing 10 mM Tris-HCl pH 7.0, 1 mM EDTA, 50 mM NaCl, and 5 mM β-mercaptoethanol for binding and a 50 mM to 1 M NaCl gradient for elution. The Nip7p$^{I161A/F164A}$ protein was refolded from inclusion bodies as described previously for the wild-type Nip7p (*7*). Following refolding, Nip7p$^{I161A/F164A}$ was purified by metal-chelating affinity chromatography on a Ni-NTA column (Qiagen) using the procedure described above.

UV Cross-Linking Assays. For analysis of the interaction of yeast Nip7p with sequences of the yeast pre-rRNA, the RNA fragments corresponding to the 5.8S rRNA, the 5′ spacer (5′-ETS), the ITS2 spacer sequences, and an unrelated control RNA were transcribed *in vitro* with T7 or SP6 RNA polymerases using linearized plasmids in the presence of 10 μCi of [α-^{32}P]-UTP (*10*). *In vitro* transcription of linearized plasmids pGEM-5′ETS, pGEM-ITS2, and pGEM-5.8S using T7 RNA polymerase generate RNAs of 550, 220, and 180 nucleotides, respectively. The unrelated RNA was transcribed *in vitro* from linearized pBlueScript, generating a 65-nucleotide RNA. One picomole of radiolabeled RNA was incubated with different amounts of purified His-Nip7p in buffer A containing 20 mM Tris-Cl pH 8.0, 5 mM magnesium acetate, 150 mM potassium acetate, 0.2% v/v Triton X-100, 1 mM DTT, and 1 mM PMSF with 0.8 U RNAse OUT (Invitrogen) for 30 min at 37 °C. A 5−20 pmol amount of cold RNAs generated by parallel *in vitro* transcription of the plasmids cited above were used in the competition assays. UV cross-linking was performed by placing RNA−protein complexes on ice and irradiating for 5 min at 260 nm using a Fotodyne transilluminator (Stratagene). Subsequently, samples were treated with 10 μg of RNase A for 30 min at 37 °C. Complexes were resolved on 6% denaturing polyacrylamide gels using 20 mM CAPS pH 11.0 (*N*-cyclohexyl-3-aminopropanesulfonic acid) as buffer and visualized on a Phosphorimager. Relative band intensities were quantified by volume integration using the Image Quant software v. 5.0 (Molecular Dynamics).

Electrophoretic Mobility Shift Assays (EMSA). For EMSA under native conditions, 20 pmol of the RNA oligoribonucleotides poly-$G_{(18)}$, poly-$A_{(25)}$, poly-$U_{(25)}$, and poly-$C_{(25)}$ were [^{32}P]-labeled using 1 U T4 PNK (Fermentas) and 20 μCi [γ^{32}P]-ATP. A 0.4 pmol amount of each [^{32}P]-labeled oligoribonucleotide was incubated with different amounts of the indicated proteins in buffer A for 30 min at 37 °C. Complexes were resolved on 8% polyacrylamide gels using TBE buffer pH 8.0 for electrophoresis and visualized on a Phosphorimager. Relative band intensities were quantified by volume integration using the Image Quant software v. 5.0 (Molecular Dynamics).

Crystallization and Data Collection of the Pyrococcus abyssi Nip7p Orthologue. PaNip7 was crystallized as described previously using the vapor diffusion method (*21*). The best crystals were obtained using 100 mM HEPES buffer pH 7.2 and 4.1 M NaCl as precipitant. Data collection was performed at 100 K at the D03B-MX1 beam line of the Brazilian Synchrotron Light Laboratory using 1.427 Å radiation and recorded on a marCCD165 detector. Data from native crystals were processed to 1.8 Å resolution. Iodide derivative crystals were obtained by the quick cryosoaking technique (*24*, *25*) and diffracted to 1.9 Å resolution (*21*). Statistics from native and derivative data collection have been described previously by Coltri and co-workers (*21*).

Structure Solution and Refinement. The structure of PaNip7 was solved using the SIRAS method. At the time PaNip7 crystals were obtained, no structure from homologous proteins was available in the PDB. Seven I^- sites with occupancies greater than 0.7 were found with the program SHELXD (*26*) using only anomalous data from the derivative crystal. According to the Matthews coefficient calculation, the asymmetric unit should contain 332 residues (two monomers); therefore, SHELXD results indicated the presence of at least one anomalous scatterer per approximately 47 residues. Refinement of heavy atoms parameters and calculation of phases were carried out with SHARP (*27*) using data from native and derivative crystals. An improved electron density map (Supporting Information Figure 1) was obtained by solvent flattening with SOLOMON (*28*). The starting model was built using the program ARP/wARP (*29*). Fifty cycles of autobuilding resulted in seven polypeptide chain fragments containing a total of 289 residues (out of 332). The model was manually completed using the program O (*30*), and structure refinement was carried out with REFMAC (*31*) from the CCP4 package (*32*). Refinement cycles were alternated with visual inspection of the electron density maps and model rebuilding with the program O (*30*). During the final cycles, water molecules were added using the program ARP/wARP (*29*). The final model has an R_{factor}

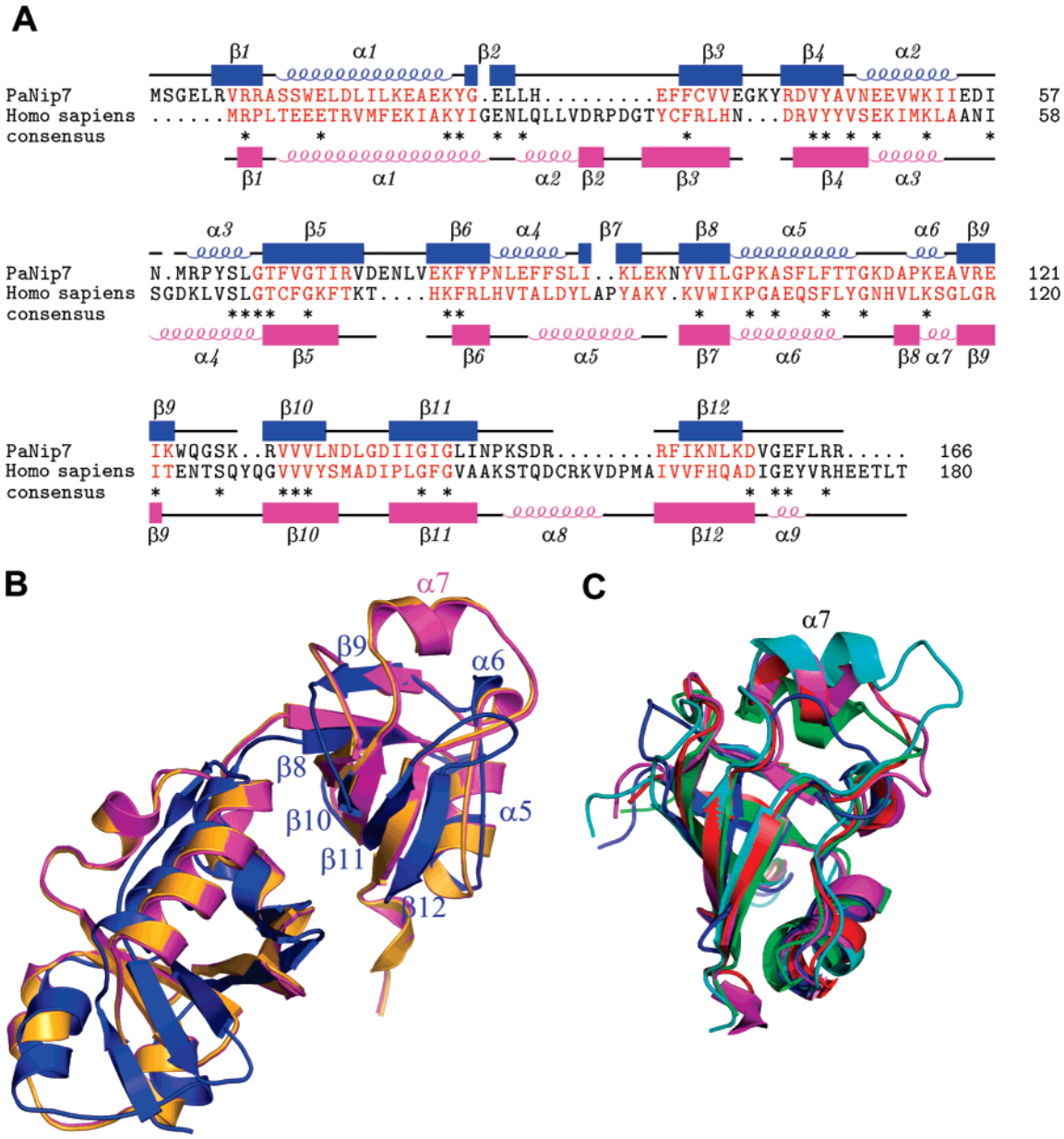

FIGURE 1: Structural comparison of Nip7 proteins. (A) Structure-based sequence alignment of human and *P. abyssi* Nip7 showing the insertion/deletion regions. Secondary structures are assigned on the top (PaNip7) and on the bottom (human Nip7). Structurally aligned residues are represented in red. (B) Superposition of PaNip7 (blue) and human Nip7 (magenta) crystallographic structures and *S. cerevisiae* Nip7p homology model (orange). Secondary structure elements of PaNip7 PUA domain and helix α7 in human and yeast Nip7 are indicated. (C) Superposition of PUA domains showing overall structural conservation and local differences: PaNip7 (blue), human Nip7 (PDB code 1SQW, magenta), *P. horikoshii* tRNA-guanine transglycosylase (PDB code 1J2B,green), *T. maritima* tRNA pseudouridine synthase (PDB code 1ZE1,cyan), *P. abyssi* Cbf5 (PDB code 2AUS,red). The region corresponding to helix α7, not found in PaNip7, is indicated.

of 20.7% (R_{free} = 25.7%) to 1.8 Å resolution with good overall stereochemistry. As defined by the program PROCHECK (*33*) all non-glycine and non-proline residues fall in the most favored or additionally allowed regions of the Ramachandran plot. Further details of refinement are presented in Table 2.

Molecular Modeling of Saccharomyces cerevisae Nip7p. The Nip7p homology model was generated using the SWISS-MODEL homology-modeling server (*34*). Atomic coordinates of human Nip7 homologue (PDB code 1SQW) were used as template. Pairwise alignment resulted in sequence identity of 56.8% between template and target with no gaps. High sequence identity allowed modeling of a continuous chain containing residues 1 to 176. After structure refinement by energy minimization, the final model presented good overall stereochemistry.

RESULTS

Crystal structure of Pyrococcus abyssi Nip7 and Comparison with Eukaryotic Orthologues. Structural analyses were performed in order to obtain information on the mechanism of Nip7p PUA domain interaction with RNA. The crystal structure of the human Nip7p orthologue (HsNip7) has already been described (*35*; PDB code 1SQW), showing a two-domain architecture in which the C-terminal domain corresponds to the conserved PUA domain. In this work, we describe the crystal structure of the *Pyrococcus abyssi* Nip7 orthologue, PaNip7, which was solved by single isomorphous replacement methods with anomalous scattering (SIRAS) using diffraction data from a native crystal and from an iodide derivative (*21*). The model was refined at 1.8 Å

Table 2: Refinement Statistics

resolution range (Å)	51.99−1.80
no. of reflections	31334
protein atoms	2443
water molecules	252
R_{factor}/R_{free} (%)	20.7/25.7
rms deviation from ideality	
bonds (Å)	0.016
angles (deg)	1.710
mean B-values (whole chain) (Å^2)	
monomer A	28.7
monomer B	28.8
solvent atoms	39.2
Ramachandran plot (%)	
most favored regions	92.0
additional allowed regions	8.0

resolution to a final R_{factor} of 20.7% (R_{free} = 25.7%). The final atomic model of PaNip7 includes two crystallographically independent monomers and 252 water molecules. The quality of the electron density allowed modeling of residues 5 to 159 (out of 166) in both monomers. A superposition of the symmetrically independent monomers shows no structural differences and results in an overall rms deviation of 0.11 Å for the 154 common Cα atoms. The two independent monomers associate in a head-to-tail orientation generating a dimer. The interface between the monomers buries a total of ~700 Å^2 of solvent-accessible area per molecule, or ~8% of its total surface. These values led us to suppose that the dimer formation was induced by crystallization and has no biological relevance. In fact, results of gel filtration experiments and dynamic light scattering support this hypothesis (data not shown). The PaNip7 monomer is composed of two alpha-beta domains (Figure 1). The larger N-terminal domain contains a five-stranded antiparallel β-sheet surrounded by three α-helices and one 3_{10} helix (α3). The C-terminal domain that corresponds to the putative RNA-binding domain (PUA) comprises residues 95 to 159 and contains a mixed β-sheet composed of strands β8 to β12, one α-helix, and one short 3_{10} helix (α6) (Figure 1).

A comparison of the PaNip7 atomic coordinates with the contents of the Protein Data Bank using the SSM service (*36*) identified structural alignment with HsNip7, the human Nip7p orthologue (PDB code 1SQW) (22% amino acid identity) and with a conserved hypothetical protein from *Thermoplasma acidophilum* (15% amino acid identity) (not published, PDB code 1Q7H). Superposition of the PaNip7 structure with the orthologues from *H. sapiens* and *T. acidophilum* resulted in overall rms deviations of 2.13 Å (114 Cα aligned) and 1.92 Å (102 Cα aligned), respectively. Despite the overall structural similarity HsNip7 and PaNip7 differ in the C-terminal PUA domain, where HsNip7 presents a large insertion between β-sheets β11 and β12 including residues 149 to 156, which form helix α7, not present in the PaNip7 structure (Figure 1). Yeast and human Nip7 orthologues share an overall 56.8% amino acid identity and 75% similarity. Since there is no crystal structure available for Nip7p, we took advantage of this high similarity and constructed a homology model of Nip7p to help us interpret the RNA interaction data. As expected, the *S. cerevisiae* Nip7p homology model and the HsNip7 crystallographic structure show a perfect superposition, with overall rms deviation of 0.09 Å (all Cα aligned) (Figure 1B).

Nip7p PUA Domain Structure Analysis and RNA-Interacting Residues. Despite the low sequence similarity among proteins from eukaryotes and *Archaea*, the PUA domain presents a conserved three-dimensional structure (Figure 1C). Superposition of PaNip7 and HsNip7 PUA domain structures resulted in overall rms deviations of 0.90 Å for 58 Cα aligned. Comparison with other PUA domains also resulted in a good structural superposition (*P. horikoshii* tRNA-guanine transglycosylase, PDB code 1J2B: rmsd = 1.15 Å for 58 Cα aligned; *T. maritima* tRNA pseudouridine synthase, PDB code 1ZE1: rmsd = 1.40 Å for 61 Cα aligned; *P. abyssi* Cbf5, PDB code 2AUS: rmsd = 1.08 Å for 58 Cα aligned). Interestingly, helix α7, the main structural difference between PaNip7 and HsNip7p PUA domains, is also found in PUA domains from other archaeal proteins (Figure 1C).

The crystal structure of *P. horikoshii* tRNA-guanine transglycosylase (ArcTGT) in complex with tRNA revealed the residues from domain C3 (the PUA domain) involved in RNA interaction (*37*; PDB code 1J2B). Structural comparison of PUA domains shows that most of the ArcTGT residues which participate in RNA interaction are structurally conserved in PaNip7 (Figure 2, Table 3). In the PaNip7 structure, arginine and lysine residues (R151, R152, K155, K158) form a positively charged path which may be

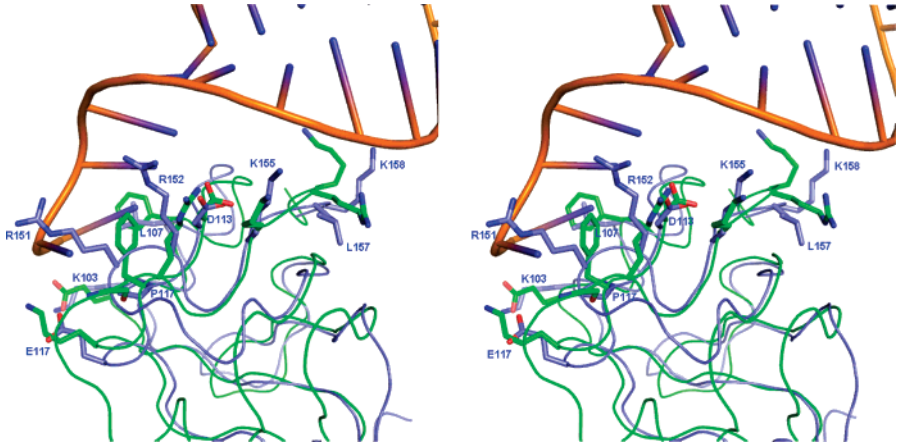

FIGURE 2: Residues of PUA domain involved in RNA interaction. Stereoview of a structural comparison of PUA domains of PaNip7 (blue) and archaeosine tRNA-guanine transglycosylase in complex with tRNA (ArcTGT, green). The ArcTGT residues involved in tRNA interactions and the structurally correspondent side-chains in PaNip7 structure are shown in sticks. The labels refer to PaNip7 residues and the RNA molecule is represented in orange-blue.

Table 3: Residues of Archaeosine tRNA-Guanine Transglycosylase (ArcTGT) PUA Domain Involved in RNA Interactions and Structurally Equivalent Residues in Nip7p Proteins from *P. abyssi*, *S. cerevisiae*, and *H. sapiens*

protein	residue									
ArcTGT	E515	F519	D525	F527	K529	G572	R573	K576	R578	K579
PaNip7	K103	L107	D113	P117	E117	R151	R152	K155	L157	K158
ScNip7	N102	P106	H112	L114	A116	G160	I161	F164	Q166	A167
HsNip7	G102	S106	H112	L114	S116	A160	I161	F164	Q166	A167

implicated in RNA binding, in a similar manner as described for the tRNA-ArcTGT complex (Figure 2, Table 3). Interestingly, analysis of the HsNip7 crystallographic structure and the Nip7p homology model revealed a charge pattern different from PaNip7 (Figure 3). In particular, PaNip7 arginine and lysine residues putatively involved in RNA interaction are not structurally conserved in the yeast and human counterparts, the same region being occupied by a glycine and three residues with hydrophobic side chain (Table 3). As shown in Figure 3B, the PUA domain of PaNip7 displays a highly positive electrostatic surface in the predicted RNA-interacting region, whereas the PUA domain of Nip7p displays an overall hydrophobic surface with a positively charged patch restricted to the region containing residues K100, K115, and R154 that are not conserved in PaNip7. This finding indicates that in these proteins, the PUA domain−RNA contacts might be mediated by different interactions.

Nip7p Interacts Directly with Polyuridine. Given the requirement of Nip7p for 27S pre-rRNA processing in yeast, Nip7p was expected to interact with regions of the pre-rRNA or with sequences corresponding to the mature rRNAs. In order to test this hypothesis, a series of *in vitro* RNA interaction assays were initially performed by using recombinant histidine-tagged Nip7p and *in vitro* transcribed RNAs corresponding to the 5.8S rRNA, ITS2 and 5′-ETS regions of the yeast pre-rRNA. An unrelated RNA transcribed from vector pBluescript (pBS) was used as a nonspecific competitor. Nip7p did not produce shifted bands on electrophoretic mobility shift assays with these RNAs under native conditions (data not shown), indicating that the affinity of Nip7p for the pre-rRNAs sequences tested is low. However, Nip7p interaction with RNAs derived from the 35S yeast pre-rRNA can be observed in RNase protection assays, in which RNA-Nip7p complexes were UV-cross-linked and treated with RNase A prior to denaturing polyacrylamide gel electrophoresis (Figure 4). In an attempt to determine whether Nip7p shows a higher affinity for a particular pre-rRNA region, we performed competition experiments. In these assays, 20 pmol Nip7p bound to 1 pmol of [^{32}P]-labeled RNA were incubated with unlabeled RNAs at concentrations of 5, 10, and 20 pmol (Figure 4). Although ITS2 was a somewhat more efficient competitor relative to the other RNAs, particularly relative to the unrelated RNA derived from the pBluescript plasmid (Figure 4), this experiment does not indicate that Nip7p recognizes a specific sequence of the RNAs tested.

In order to determine whether Nip7p shows a higher affinity to a particular RNA sequence, we performed a second round of experiments using homo-oligoribonucleotides in native electrophoretic mobility shift assays. Interestingly, these assays revealed that Nip7p binds specifically to poly-U (Figure 5A). Parallel assays were performed also with PaNip7, which also showed specific binding to poly-U. No

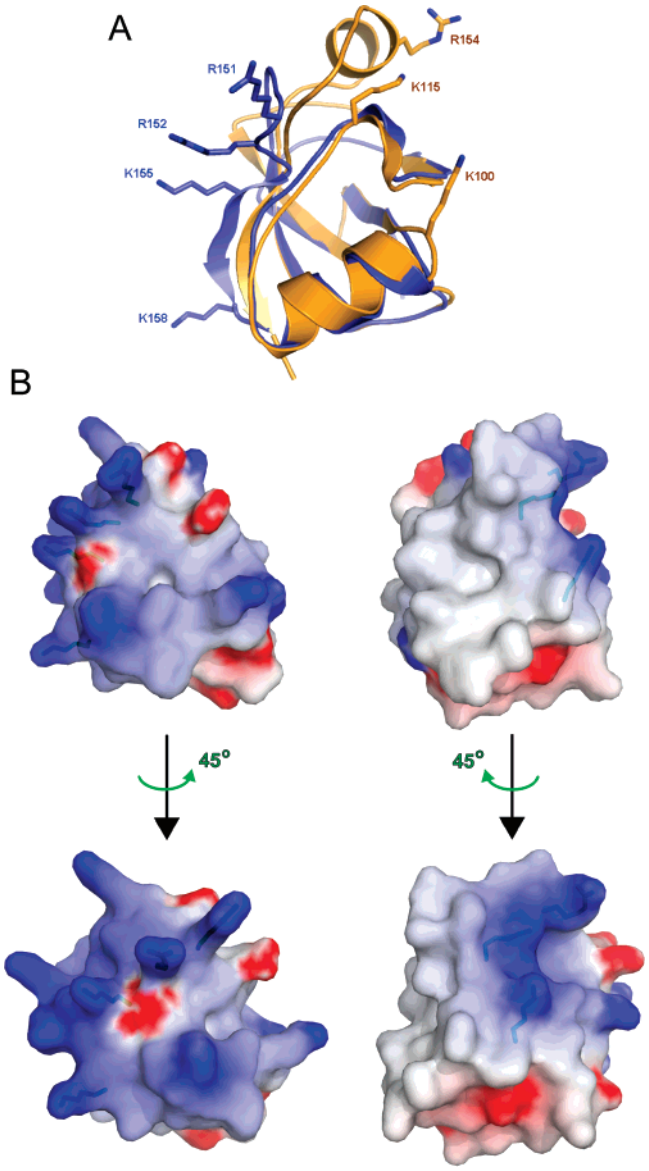

FIGURE 3: Structural comparison of the *P. abyssi* and *S. cerevisiae* Nip7 PUA domains. (A) Overlay of the PaNip7 (blue) and Nip7p (orange) PUA domains. Positively charged residues which could form a basic pathway for RNA interaction are showed in sticks and labeled. (B) Electrostatic surfaces of the PaNip7 (left) and Nip7p (right) PUA domains colored by charge, from red (negative) to blue (positive). The upper panel shows the electrostatic surface in the same position as shown in A. The lower panel shows the domains rotated by 90°, resulting from a 45° rotation to the right for the PaNip7 PUA domain (left) and from a 45° rotation to the left for the Nip7p (right) PUA domain, as indicated by the green arrows, to better view the positively charged regions. Residues indicated in A are represented in sticks.

band corresponding to a mobility shift equivalent to the one observed for poly-U was detected for the poly-C, poly-A, and poly-G probes, although in the case of yeast Nip7p, the signal of the probe disappeared from the free probe region

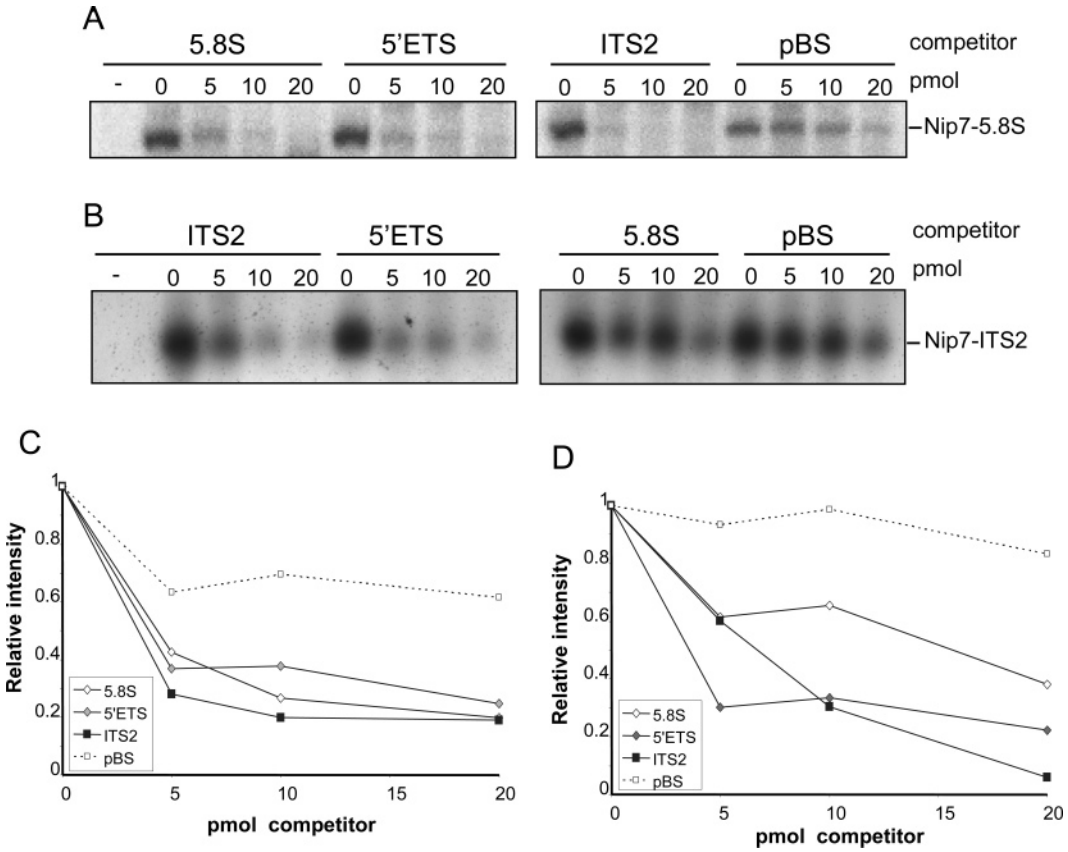

FIGURE 4: Analysis of yeast Nip7p interaction with pre-rRNA sequences. (A and B) 20 pmol of Nip7p was incubated with 1 pmol of *in vitro* transcribed [^{32}P]-labeled 5.8S RNA and [^{32}P]-labeled ITS2 RNA, respectively. Subsequently the reactions were incubated with increasing amounts (0, 5, 10, and 20 pmol) of unlabeled competitor RNAs as indicated. Samples were submitted to UV cross-linking for 5 min, treated with RNase A, and resolved on denaturing polyacrylamide gels using 20 mM CAPS pH 11.0 both as electrophoresis and gel buffer. Protein−RNA complexes were visualized by autoradiography. Lanes marked with "−" indicate the controls without Nip7p. (C and D) Quantitation of the assays shown in A and B, respectively. The graphs show the relative intensity of the bands in the competition reactions as compared to the reaction where no unlabeled competitor was added (lane 0).

and a band appeared in the well region (Figure 5A, arrowhead). We interpreted the presence of the band in the well as resulting from unspecific binding and aggregation. Although poly-G is known to adopt higher order structures that may affect protein interaction, it was included in the assay to have a complete set of RNA homopolymers tested. Binding of Nip7p and PaNip7 to poly-U was concentration-dependent (Figure 5B). Although equivalent amounts of protein and of ^{32}P-labeled poly-U probe were used for both Nip7p and PaNip7, the signal for Nip7p-poly-U complexes was consistently weaker in all assays performed. The signal of the free probe diminishes with the increase of the Nip7p concentration in the binding reaction, and part of the material is retained in the well, suggesting that part of the sample does not enter the gel.

Mutation Analysis of RNA-Interacting Residues of the Nip7 PUA Domain. The fact that both *P. abyssi* and *S. cerevisiae* Nip7 orthologues show preference for binding to poly-U RNAs is quite intriguing (Figure 5). In the case of PaNip7, evidence from structure comparison of its PUA domain with the PUA domain of ArcTGT indicates that RNA interaction is mediated by contacts of positively charged residues (R151, R152, K155, K158) with phosphates of the RNA (Figure 2, Table 3). In order to test whether these residues are involved in RNA interaction, two mutant clones were generated. Both are double mutants, one containing alanine residues at positions 151 and 152 (PaNip7$^{R151A/R152A}$) and the other containing alanine residues at positions 155 and 158 (PaNip7$^{K155A/K158A}$). The mutant proteins were expressed in *E. coli* and purified for RNA binding assays. Binding of both mutant proteins to poly-U was drastically reduced as determined by EMSA (Figure 6), which strongly supports the hypothesis that residues R151, R152, K155, and K158 of PaNip7 are directly involved in RNA binding.

As described above and in Table 3, PaNip7 residues R151, R152, K155, and K158 are not conserved in the PUA domain of Nip7p and HsNip7 proteins, with equivalent positions being occupied by residues G160, I161, F164, and A167. We hypothesized that if involved in RNA interaction, residues I161 and F164 should play an important role since they contain larger side chains relative to glycine and alanine residues of positions 160 and 167, respectively. A mutant clone was constructed in which residues I161 and F164 were replaced by alanine. The recombinant mutant protein (Nip7p$^{I161A/F164A}$) was assayed for poly-U binding and, similarly to PaNip7 mutants, showed reduced RNA binding activity (Figure 6). This result is consistent with the direct involvement of residues I161 and F164 with RNA interaction.

DISCUSSION

The PUA domain has already been identified in approximately 600 proteins of different families (*38*), including a large number of uncharacterized proteins. In RNA-

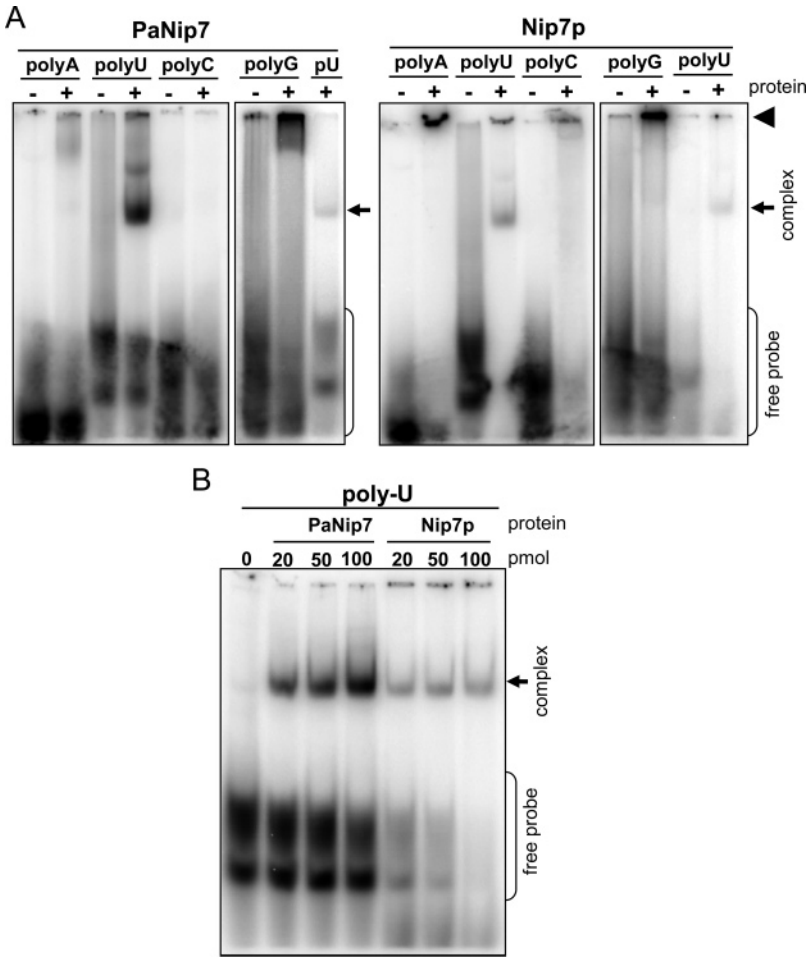

FIGURE 5: Analysis of yeast Nip7p and PaNip7 interaction with oligoribonucleotides. The panels show protein-RNA complexes resolved by electrophoretic mobility shift assays under native conditions on polyacrylamide gels and visualized by autoradiography as described in Experimental Procedures. (A) One picomole of the indicated oligoribonucleotides (poly-$A_{(25)}$, poly-$U_{(25)}$, poly-$C_{(25)}$ and poly-$G_{(18)}$) was incubated with 50 pmol of recombinant PaNip7 (left panel) or with recombinant yeast Nip7p (right panel). (B) One picomole of [^{32}P]-labeled poly-$U_{(25)}$ was incubated with increasing concentrations of recombinant PaNip7 or with recombinant yeast Nip7p. Arrows indicate the shifted bands corresponding to the complexes formed by PaNip7 and yeast Nip7p proteins with poly-U oligoribonucleotides. The arrowhead indicates the samples trapped in the wells.

modifying enzymes, the PUA domain function has been associated with RNA interaction. However, increasing evidence suggests that the PUA domain fold provides a structural scaffold for more general macromolecular interactions than initially thought (*38*). In *E. coli* glutamate 5-kinase, which displays a two-domain architecture with an N-terminal amino acid kinase (AAK) domain and a C-terminal PUA domain, the PUA domain has apparently assumed a role nonrelated to RNA processing, taking part in monomer interaction, in formation of a cavity at the dimer interface involved in magnesium binding, and binding a glutamate residue (*20*). The human candidate oncogene MCT1 shows a molecular weight similar to Nip7 proteins and contains a PUA domain in the C-terminal region. Unlike Nip7 PUA domains, this particular PUA domain was reported to interact with the mRNA cap translation factor complex, linking the MCT1 protein to translational control (*19*). In the *E. coli* methyltransferase YebU, which methylates cytidine$_{1407}$ of the 16S rRNA, the PUA domain forms a tight interface with the methyltransferase domain, and although there is no straightforward model that explains the mechanistic role played by the PUA domain of YebU (*17*), it still could be involved in RNA interaction during methylation of the 16S rRNA.

The experimental evidence for the mechanism of PUA domain interaction with RNA is based mostly on the crystal structures of the archaeal Cbf5 (*39*), TruB (*40*), and ArcTGT (*37*) proteins in complex with RNA that are currently available at PDB. In these complexes, the PUA domain contacts the RNA molecule using a glycine-containing loop which connects the first α-helix and the second β-strand and via residues from the sixth β-strand. RNA recognition depends on the identity of the $\alpha1-\beta2$ and $\beta6$ side chains involved in RNA interactions (reviewed in ref *38*). Corresponding regions in PaNip7 include helix α5 (PUA α1), the loop between α5 and the 3_{10} helix α6, and β-strand $\beta12$ (Figure 1). In Cbf5 and TruB, the PUA domains mediate the interaction with the minor groove of double-stranded RNA (*39*, *40*) whereas the ArcTGT PUA domain binds to the bottom of the $tRNA^{Val}$ acceptor stem, through the major groove (*37*). The structural alignment suggests that PaNip7 uses a mechanism similar to ArcTGT for RNA interaction, involving the positively charged residues R151, R152, K155, K158 from β-strand $\beta12$ (Figure 2). However, these residues are not structurally conserved in the yeast and human Nip7p counterparts, which are replaced by a glycine and three residues with hydrophobic side chain (Figure 3B, Table 3). In fact, the structure of the PUA domain from PaNip7

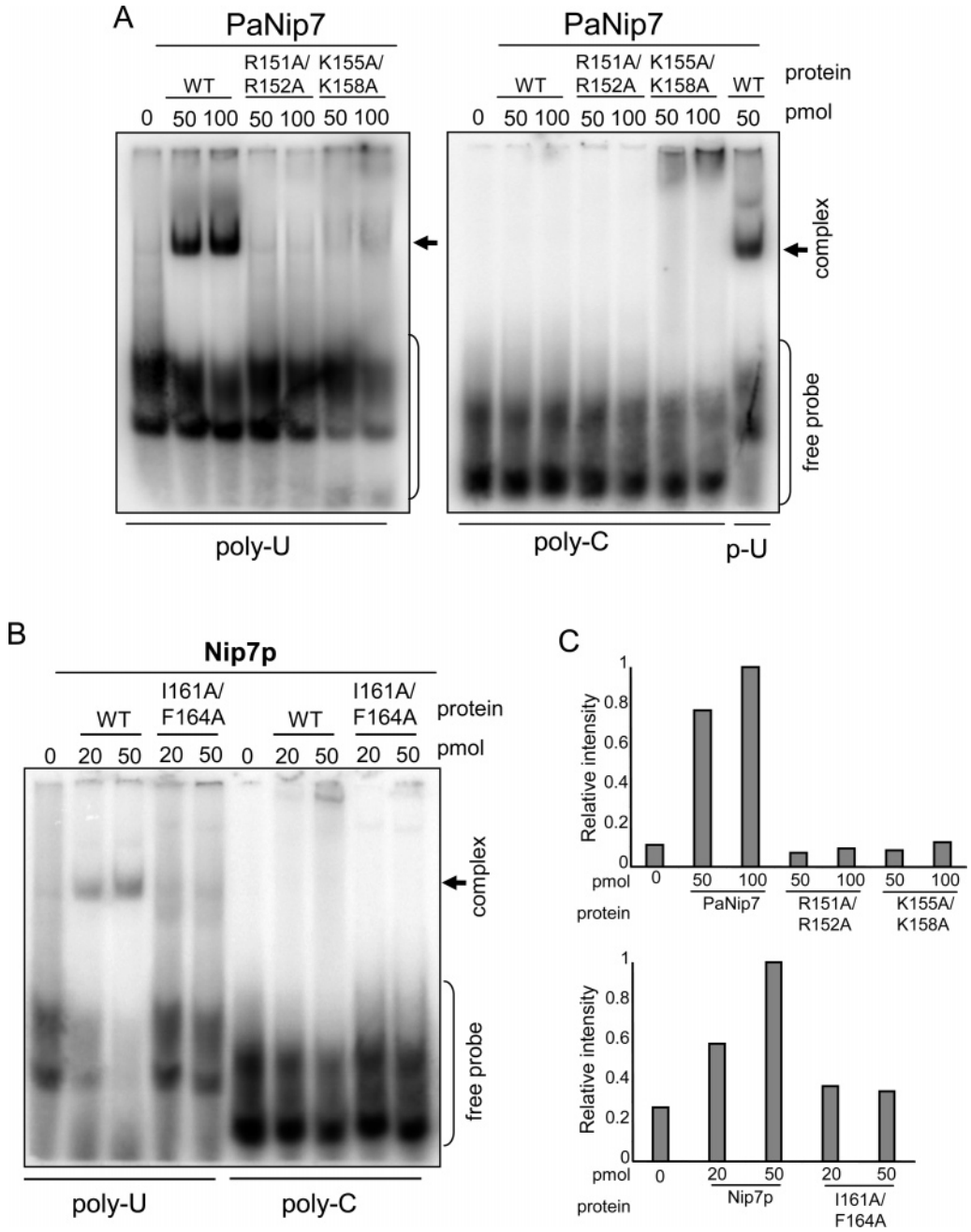

FIGURE 6: Analysis of the interaction of Nip7p and PaNip7 mutants with oligoribonucleotides. The panels show protein−RNA complexes resolved by electrophoretic mobility shift assays on polyacrylamide gels and visualized by autoradiography as described in Experimental Procedures. (A) One picomole of [^{32}P]-labeled poly-$U_{(25)}$ or poly-$C_{(25)}$ was incubated with 50 and 100 pmol of the recombinant wild type PaNip7 (WT) and of the mutant PaNip7$^{R151A/R152A}$ and PaNip7$^{K155A/K158A}$. p-U indicates the positive control in the assay containing [^{32}P]-labeled poly-$U_{(25)}$ and wild type PaNip7. (B) One picomole of [^{32}P]-labeled poly-$U_{(25)}$ or poly-$C_{(25)}$ was incubated with 20 and 50 pmol of the recombinant yeast wild type Nip7p (WT) and of the mutant Nip7$^{I161A/F164A}$. Arrows indicate the shifted bands corresponding to the complexes formed by PaNip7 and yeast Nip7p with poly-U. (C) Graphs showing the quantitation of the PaNip7-poly-U (top) and Nip7p-poly-U (bottom) complexes of the assays shown in A and B, respectively. The graphs show the intensity of the complexes relative to the lanes containing 100 pmol of PaNip7 or 50 of Nip7p, respectively, which were set to one.

revealed two differences relative to eukaryotic Nip7p and other archaeal PUA domains, which possess an insertion between β-strands β11 and β12 as compared to PaNip7 (residues 149 to 156 which form helix α7). The second difference involves the composition and distribution of positively charged residues that renders the PaNip7 PUA domain with a highly positive electrostatic surface and the Nip7p PUA domain with a predominantly hydrophobic surface. In Nip7p and HsNip7, electrostatic interaction between positively charged residues and phosphates of the RNA backbone would only be possible through a different region of the PUA domain involving residues K100, K115, and R154. In accordance with the structural comparisons, mutational analyses (Figure 6) have shown that residues R151, R152, K155, and K158 of PaNip7 are involved in RNA interaction. Mutational analysis of the yeast Nip7p has also shown that residues I161 and F164 are required for RNA interaction, indicating that the same region of the PUA domain interacts with poly-U in archaeal and yeast Nip7p proteins but probably via different contacts.

The *S. cerevisiae* ribosome biogenesis Rrp5p protein has also been described to preferentially bind poly-U and U-rich sequences (*41*). Rrp5p contains twelve tandem repeats of the S1 RNA binding domain in the N-terminal region that is responsible for RNA binding *in vitro* with a higher affinity to poly-U (*41*). Genetic depletion of Rrp5p results in accumulation of pre-rRNA species with extended 5′ end, affecting biogenesis of both ribosomal subunits. Based on deletion analyses of the pre-rRNA, de Boer and co-workers (*41*) have proposed that Rrp5p may bind to a conserved single-stranded U-rich sequence upstream from the pre-rRNA cleavage site A2 in ITS1. Genetic depletion of Nip7p results in accumulation of unprocessed 27S pre-rRNA (*7*), indicating that it is required for processing of ITS2. As many 60S biogenesis factors, Nip7p is not found in 90S preribosomes (*3*), and, consistent with the genetic depletion data, it cosediments with the 60S subunit peak in sucrose density gradients (*7*) and has been found associated with pre-60S complexes (*5*, *6*). Although the *in vitro* interaction assays indicated a low Nip7p affinity for the ITS2 region (Figure 4) even though it contains several U-rich stretches, Nip7p interacts with the nucleolar proteins, Nop8p and Nop53p (*9*, *10*), both containing RNA interaction domains, that may bind the pre-rRNA and help stabilize Nip7p on ITS2 *in vivo*. However, one has to consider also that the Nip7p preference for binding to poly-U raises the question whether *in vivo* Nip7 proteins might bind to U-rich snoRNAs instead of pre-rRNA sequences. Nip7p does not possess intrinsic catalytic activity and might function as an adaptor since it has the ability to bind to RNA via the C-terminal PUA domain and interacts with proteins involved in pre-rRNA processing, such as Rrp43p, Nop8p, and Nop53p (*9*, *10*), possibly via its N-terminal domain. The temperature sensitive *nip7-1* allele results from mutation of a conserved glycine residue at position 71 which is replaced by an aspartic acid (*7*), affecting Nip7p stability and interaction with other proteins in the yeast two-hybrid system (data not shown).

In conclusion, we have shown that the PUA domain of Nip7 proteins mediates interaction with RNA. Although RNA-binding assays did not identify a 35S pre-rRNA sequence to which Nip7p could bind specifically, we found that Nip7 proteins bind specifically to poly-U RNAs *in vitro*. Structural and mutational analyses revealed that equivalent regions, including residues R151, R152, K155, and K158 in PaNip7 and residues I161 and F164 in yeast Nip7p PUA domains, are involved in RNA interaction.

ACKNOWLEDGMENT

The authors are grateful to Zildene G. Correa for technical assistance. P.P.C., D.C.G., and J.S.L. are recipients of FAPESP fellowships.

SUPPORTING INFORMATION AVAILABLE

One figure showing the $2F_o - F_c$ electron density map calculated from experimental phases (contour level 1.2σ) of the PaNip7 refined model superposed to the experimental map, showing a region of the β9, β8, and β10 strands of the PUA domain (from left to right). This material is available free of charge via the Internet at http://pubs.acs.org

REFERENCES

1. Fromont-Racine, M., Senger, B., Saveanu, C., and Fasiolo, F. (2003) Ribosome assembly in eukaryotes, *Gene 313*, 17−42.
2. Peng, W. T., Robinson, M. D., Mnaimneh, S., Krogan, N. J., Cagney, G., Morris, Q., et al. (2003) A panoramic view of yeast noncoding RNA processing, *Cell 113*, 919−933.
3. Grandi, P., Rybin, V., Bassler, J., Petfalski, E., Strauss, D., Marzioch, M., et al. (2002) 90S pre-ribosomes include the 35S pre-rRNA, the U3 snoRNP, and 40S subunit processing factors but predominantly lack 60S synthesis factors, *Mol. Cell 10*, 105−115.
4. Dragon, F., Gallagher, J. E., Compagnone-Post, P. A., Mitchell, B. M., Porwancher, K. A., Wehner, K. A., et al. (2002) A large nucleolar U3 ribonucleoprotein required for 18S ribosomal RNA biogenesis, *Nature 417*, 967−970.
5. Bassler, J., Grandi, P., Gadal, O., Lessmann, T., Petfalski, E., Tollervey, D., Lechner, J., and Hurt, E. (2001) Identification of a 60S preribosomal particle that is closely linked to nuclear export, *Mol. Cell 8*, 517−529.
6. Nissan, T. A., Bassler, J., Petfalski, E., Tollervey, D., and Hurt, E. (2002) 60S pre-ribosome formation viewed from assembly in the nucleolus until export to the cytoplasm, *EMBO J. 21*, 5539−5547.
7. Zanchin, N. I. T., Roberts, P., DeSilva, A., Sherman, F., and Goldfarb, D. S. (1997) *Saccharomyces cerevisiae* Nip7p is required for efficient 60S ribosome subunit biogenesis, *Mol. Cell. Biol. 17*, 5001−5015.
8. Zanchin, N. I. T., and Goldfarb, D. S. (1999a) The exosome subunit Rrp43p is required for the efficient maturation of 5.8S, 18S and 25S rRNA, *Nucl. Acids Res. 27*, 1283−1288.
9. Zanchin, N. I. T., and Goldfarb, D. S. (1999b) Nip7p interacts with Nop8p, an essential nucleolar protein required for 60S ribosome biogenesis, and the exosome subunit Rrp43p, *Mol. Cell. Biol. 19*, 1518−1525.
10. Granato, D. C., Gonzales, F. A., Luz, J. S., Cassiola, F., Machado-Santelli, G. M., and Oliveira, C. C. (2005) Nop53p, an essential nucleolar protein that interacts with Nop17p and Nip7p, is required for pre-rRNA processing in *Saccharomyces cerevisiae*, *FEBS J. 272*, 4450−4463.
11. van Hoof, A., Staples, R. R., Baker, R. E., and Parker, R. (2000) Function of the Ski4p (Csl4p) and Ski7p proteins in 3′-to-5′ degradation of mRNA, *Mol. Cell. Biol. 20*, 8230−8243.
12. Mitchell, P., Petfalski, E., Shevchenko, A., Mann, M., and Tollervey, D. (1997) The exosome: a conserved eukaryotic RNA processing complex containing multiple 3′→5′ exoribonucleases, *Cell 91*, 457−466.
13. Sekiguchi, T., Todaka, Y., Wang, Y., Hirose, E., Nakashima, N., and Nishimoto, T. (2004) A novel human nucleolar protein, Nop132, binds to the G proteins, RRAG A/C/D, *J. Biol. Chem. 279*, 8343−8350.
14. Hesling, C., Oliveira, C. C., Castilho, B. A., and Zanchin, N. I. T. (2007) The Shwachman-Bodian-Diamond syndrome associated protein interacts with HsNip7 and its down-regulation affects gene expression at the transcriptional and translational levels, *Exp. Cell Res.*, in press.
15. Aravind, L., and Koonin, E. (1999) Novel predicted RNA-binding Domains Associated with the Translation Machinery, *J. Mol. Biol. 48*, 291−302.
16. Ishitani, R., Nureki, O., Fukai, S., Kijimoto, T., Nameki, N., Watanabe, M., et al. (2002) Crystal structure of archaeosine tRNA-guanine transglycosylase, *J. Mol. Biol. 318*, 665−677.
17. Hallberg, B. M., Ericsson, U. B., Johnson, K. A., Andersen, N. M., Douthwaite, S., Nordlund, P., Beuscher, A. E., IV, and Erlandsen, H. (2006) The structure of the RNA m^5C methyltransferase YebU from *Escherichia coli* reveals a C-terminal RNA-recruiting PUA domain, *J. Mol. Biol. 360*, 774−787.
18. Manival, X., Charron, C., Fourmann, J. B., Godard, F., Charpentier, B., and Branlant, C. (2006) Crystal structure determination and site-directed mutagenesis of the *Pyrococcus abyssi* aCBF5-aNOP10 complex reveal crucial roles of the C-terminal domains of both proteins in H/ACA sRNP activity, *Nucl. Acids Res. 34*, 826−839.
19. Reinert, L. S., Shi, B., Nandi, S., Mazan-Mamczarz, K., Vitolo, M., Bachman, K. E., He, H., and Gartenhaus, R. B. (2006) MCT-1 protein interacts with the cap complex and modulates messenger RNA translational profiles, *Cancer Res. 66*, 8994−9001.
20. Marco-Marín, C., Gil-Ortiz, F., Pérez-Arellano, I., Cervera, J., Fita, I., and Rubio, V. (2007) A novel two-domain architecture within

the amino acid kinase enzyme family revealed by the crystal structure of *Escherichia coli* glutamate 5-kinase, *J. Mol. Biol. 367*, 1431−1446.
21. Coltri, P. P., Guimarães, B. G., Oliveira, C. C., and Zanchin, N. I. T. (2004) Expression, crystallization and preliminary X-ray analysis of the *Pyrococcus abyssi* protein homologue of *Saccharomyces cerevisiae* Nip7p, *Acta Crystallogr.Sect. D: Biol. Crystallogr. 60*, 1925−1928.
22. Carneiro, F. R., Silva, T. C., Alves, A. C., Haline-Vaz, T., Gozzo, F. C., and Zanchin, N. I. T. (2006) Spectroscopic characterization of the tumor antigen NY-REN-21 and identification of heterodimer formation with SCAND1, *Biochem. Biophys. Res. Commun. 343*, 260−268.
23. Sambrook, J., Fritsch, E. J., and Maniatis, T. (1989) in *Molecular cloning, a laboratory manual*, 2nd ed., Cold Spring Harbor Laboratory Press, Cold Spring Harbor, NY.
24. Dauter, Z., Dauter, M., and Rajashankar, K. R. (2000) Novel approach to phasing proteins: derivatization by short cryo-soaking with halides, *Acta Crystallogr.Sect. D: Biol. Crystallogr. 56*, 232−237.
25. Nagem, R. A. P., Dauter, Z., and Polikarpov, I. (2001) Protein crystal structure solution by fast incorporation of negatively and positively charged anomalous scatterers, *Acta Crystallogr.Sect. D: Biol. Crystallogr. 57*, 996−1002.
26. Sheldrick, G. M., and Schneider, T. R. (2001) in *Methods in Macromolecular Crystallography* (Turk, D., and Johnson, L., Eds.) pp 72−81, IOS Press, Amsterdam.
27. La Fortelle, E., and Bricogne, G. (1997) Maximum-likelihood heavy-atom parameter refinement for multiple isomorphous replacement and multiwavelength anomalous diffraction methods, *Methods Enzymol. 276*, 472−494.
28. Abrahams, J. P., and Leslie, A. G. W. (1996) Methods used in the structure determination of bovine mitochondrial F1 ATPase, *Acta Crystallogr.Sect. D: Biol. Crystallogr. 52*, 30−42.
29. Perrakis, A., Morris, R., and Lamzin, V. S. (1999) Automated protein model building combined with iterative structure refinement, *Nat. Struct. Biol. 6*, 458−463.
30. Jones, T., Zou, J., Cowan, S., and Kjeldgaard, M. (1991) Improved methods for building protein models in electron density maps and the location of errors in these models, *Acta Crystallogr Sect. A: Found. Crystallogr. 47*, 110−119.
31. Murshudov, G. N., Vagin, A. A., and Dodson, E. J. (1997) Refinement of macromolecular structures by the maximum-likelihood method, *Acta Crystallogr.Sect. D: Biol. Crystallogr. 53*, 240−255.
32. Collaborative Computational Project, Number 4 (1994) The CCP4 suite: programs for protein crystallography, *Acta Crystallogr.Sect. D: Biol. Crystallogr. 50*, 760−763.
33. Laskowski, R. A., MacArthur, M. W., Moss, D. S., and Thornton., J. M. (1993) PROCHECK: a program to check the stereochemical quality of protein structures, *J. Appl. Crystallogr. 26*, 283−291.
34. Schwede, T., Kopp, J., Guex, N., and Peitsch, M. C. (2003) SWISS-MODEL: An automated protein homology-modeling server, *Nucl. Acids Res. 31*, 3381−3385.
35. Liu, J. F., Wang, X. Q., Wang, Z. X., Chen, J. R., Jiang, T., An, X. M., Chang, W. R., and Liang, D. C. (2004) Crystal structure of KD93, a novel protein expressed in human hematopoietic stem/progenitor cells, *J. Struct. Biol. 148*, 370−374.
36. Krissinel, E., and Henrick, K. (2004) Secondary-structure matching (SSM), a new tool for fast protein structure alignment in three dimensions, *Acta Crystallogr.Sect. D: Biol. Crystallogr. 60*, 2256−2268.
37. Ishitani, R., Nureki, O., Nameki, N., Okada, N., Nishimura, S., and Yokoyama, S. (2003) Alternative tertiary structure of tRNA for recognition by a posttranscriptional modification enzyme, *Cell 113*, 383−394.
38. Perez-Arellano, I., Gallego, J., and Cervera, J. (2007) The PUA domain - a structural and functional overview, *FEBS J.*, in press.
39. Li, L., and Ye, K. (2006) Crystal structure of an H/ACA box ribonucleoprotein particle, *Nature 443*, 302−307.
40. Pan. H., Agarwalla, S., Moustakas, D. T., Finer-Moore, J., and Stroud, R. M. (2003) Structure of tRNA pseudouridine synthase TruB and its RNA complex: RNA recognition through a combination of rigid docking and induced fit, *Proc. Natl. Acad. Sci. U.S.A. 100*, 12648−12653.
41. de Boer, P., Vos, H. R., Faber, A. W., Vos, J. C., and Raué, H. A. (2006) Rrp5p, a trans-acting factor in yeast ribosome biogenesis, is an RNA-binding protein with a pronounced preference for U-rich sequences, *RNA 12*, 263−271.

BI7015876

3.3. Capítulo 3

Saccharomyces cerevisiae Nip7p interacts with box H/ACA proteins and RNA during 60S subunit biogenesis

Patrícia P. Coltri, Beatriz G. Guimarães, Daniela C. Granato, Tereza C. L. Silva, Juliana S. Luz, Carla C. Oliveira and Nilson I. T. Zanchin

Saccharomyces cerevisiae Nip7p interacts with box H/ACA proteins and RNA during 60S subunit biogenesis

Patrícia P. Coltri[1], Beatriz G. Guimarães[1], Daniela C. Granato[2], Tereza C. L. Silva[1], Juliana S. Luz[2], Carla C. Oliveira[2] and Nilson I. T. Zanchin[1]*

[1]Center for Structural Molecular Biology
Brazilian Synchrotron Light Laboratory, LNLS
Rua Giuseppe Maximo Scolfaro 10000
PO Box 6192, CEP13083-970, Campinas SP, Brazil

[2]Department of Biochemistry, Institute of Chemistry, University of São Paulo
Av. Prof. Lineu Prestes, 748
São Paulo, SP, 05508-900, Brazil

Running title: Nip7p interacts with RNA and with a supramolecular complex

*Corresponding author: Nilson I. T. Zanchin
Centro de Biologia Molecular Estrutural
Laboratório Nacional de Luz Síncrotron
Campinas - SP
Caixa Postal (PO Box) 6192 -CEP 13084-971
Tel. 55 19 3512 1113
Fax. 55 19 3512 1004
e-mail:zanchin@lnls.br

ABSTRACT

Saccharomyces cerevisiae Nip7p is required for proper 27S pre-rRNA processing and 60S ribosome subunit biogenesis. In this work, we show that the PUA domain interacts with the same set of proteins that interact with full-length Nip7p, including Nop8p, Nop53p, Rrp43p, Rrp15p and the box H/ACA proteins Cbf5p, Gar1p, Nop10p and Nhp2p. Direct interaction of Nip7p was observed with Nop8p, Nop53p and Nop10p. Despite Nip7p interaction with box H/ACA subunits, its depletion resulted in a moderate defect in pre-rRNA pseudouridylation whereas cleavage of the 27S pre-rRNA is severely affected. Further analysis showed Nip7p interacts in vitro with ITS2 rRNA spacer sequence and co-precipitates 27S precursor. These results allow us to propose a model in which Nip7p is part of a ribonucleoprotein complex responsible for processing of 27S pre-rRNA where it binds directly to RNA and regulates excision of ITS2.

Key words: box H/ACA, Nip7p, pre-rRNA processing, PUA domain, ribosome biogenesis, *S. cerevisiae*

INTRODUCTION

Saccharomyces cerevisiae has been the favorite model system to study the molecular events involved in pre-ribosomal RNA processing and eukaryotic ribosome biogenesis. Major processing and assembly steps have already been described and a large number of factors identified. Ribosome biogenesis takes place mainly in the nucleolus where a precursor of the 18S, 5.8S and 25S rRNAs, the 35S pre-rRNA, is transcribed by RNA polymerase I and the 5S rRNA is transcribed by RNA polymerase III. Concomitantly with its transcription, the pre-rRNA is assembled with processing factors, undergoing extensive endo- and exonucleolytic cleavage and covalent modification to generate the mature rRNAs (1, 2). The large 35S precursor is assembled into a 90S particle containing U3 snoRNP, which is rapidly converted into the pre-40S and the pre-60S pre-ribosomal particles. Whereas the pre-40S particles are further processed in the cytoplasm, pre-60S pre-rRNAs go through several endo- and exonucleolytic digestions before export to the cytoplasm, where ribosome assembly terminates (1, 3, 4).

Major pre-rRNA processing events are carried out by supramolecular complexes formed by proteins and snoRNAs. For instance, ribose and base methylation at specific sites is directed by box C/D guide snoRNAs associated with the core proteins Nop1p, Nop56p, Nop58p and Snu13p (5, 6). Pseudouridylation is guided by box H/ACA snoRNAs in complex with four core proteins, Cbf5p, Nop10p, Nhp2p and Gar1p (1, 7-9). Although the precise function of these modifications in the mature rRNA is still unclear, ribose methylation and uridine conversion to pseudouridine may have a role in stabilization of the rRNA conformation. They may also be important to promote the

correct ribosome activity (1, 9), since most modification sites are found close to active regions in the ribosome (10).

Ribonucleoprotein complexes are also involved in pre-rRNA cleavage of the external and internal transcribed spacer sequences, ETS and ITS, respectively. U3 snoRNP directs the early pre-rRNA cleavages (11, 12), reactions in which U14, snR10 and snR30 also participate (13-15). The yeast RNases MRP and P are formed by different RNA molecules but share a common set of proteins (16). The RNase MRP has been directly implicated in endonucleolytic processing at site A_3 (17-19). However, one of the most intriguing protein complexes involved in pre-rRNA processing is the exosome. The exosome has a broad function in RNA metabolism that includes also snoRNA maturation and mRNA turnover (20). In yeast, it is formed by 11 subunits and an intact exosome is required for maturation of the 3'-end of the 5.8S rRNA following cleavage of the 27S pre-rRNA in ITS2 and for degradation of the 5'-ETS (20, 21).

Despite the identification of nearly 30 non-ribosomal factors components of pre-60S particles required for 60S subunit maturation (22, 23), key players in ITS2 processing, such as the endonuclease responsible for cleavage at site C_2, remain to be discovered. Among the proteins identified in the pre-60S particle is Nip7p, which is required for accurate processing of the 27S precursor to form the mature 25S and 5.8S rRNAs (22, 24). Nip7p interacts with the exosome subunit Rrp43p and the nucleolar proteins Nop8p and Nop53p (25-27). Despite this information, the function of Nip7p remains elusive and the scope of this work was to further investigate the role played by Nip7p and its conserved C-terminal PUA domain in rRNA processing and protein-protein interaction. The PUA domain, after *P*seudo-*U*ridine synthases and *A*rchaeosine-specific

transglicosilases (28), mediates protein-RNA interaction and is present in tRNA modifying enzymes and in pseudo-uridine synthases from Archaea and eukaryotes (29-32) raising the hypothesis that Nip7p might be associated to pseudo-uridine formation in yeast. In this work, a series of protein interaction assays detected Nip7p interaction with box H/ACA and with other nucleolar proteins involved in ribosome biogenesis. Interestingly, Nip7p interacts directly just with a subset of the proteins that are positive in the yeast two-hybrid system, including Nop8p, Nop53p and box H/ACA core component Nop10p. Based on the structural arrangement of the human and archaeal Nip7p orthologs (33), we investigated both the Nip7p N- and C-terminal (PUA) domains involvement in protein interaction. Surprisingly, the PUA domain mediates all the interactions tested. We also analyzed the effect of Nip7p depletion on pre-rRNA pseudouridylation and cleavage. Pre-rRNA cleavage is more severely affected than pseudouridine formation in Nip7p-depleted cells. *In vitro* RNA binding studies revealed Nip7p can bind to ITS2 spacer sequence. Consistently, further analysis showed Nip7p co-precipitates 27S precursor. Based on these results we propose a model in which Nip7p interacts directly with the pre-rRNA and is part of the pre-60S complex which contains the RNA processing and modifying factors required for maturation of the 25S and 5.8S rRNAs and 60S subunit biogenesis.

MATERIALS AND METHODS

1. Plasmids, strains and media

Plasmids used in this study are listed in Table 1 and cloning procedures are summarized below. pTL1-NIP7 was generated by replacing the ampicilin *E. coli* selection marker of vector pBTM-NIP7 (26) to kanamycin. DNA fragments coding for *NIP7* N-terminal (containing amino-acid 1 to 93) and C-terminal (from amino-acid 94 to 181) regions were PCR-amplified and cloned into vector pGEM-T (Promega). Subsequently, these fragments were subcloned into pTL1 (34) using the BamHI/SalI restriction sites, generating vectors pTL1-NIP7-Nter and pTL1-PUA, respectively. pACT-RRP15 was isolated in a yeast two-hybrid assay using Nip7p as a bait. Activation domain fusions of *CBF5*, *GAR1*, *NOP10* and *NHP2* for yeast two-hybrid assays were constructed by inserting the respective coding sequences PCR-amplified from *S. cerevisiae* genomic DNA into the cloning vector pGEM-T (Promega) and subcloning into $pGADC_2$ using BamHI/SalI restriction sites. The *CBF5* coding sequence was isolated from pCRII-CBF5 using XbaI/SalI restriction enzymes and inserted into YCpGAL (26) generating plasmid YCpGAL-CBF5. *GAR1*, *NOP10*, *NHP2* and *RRP15* coding sequences were isolated from the respective $pGADC_2$ vectors using BamHI/SalI and inserted into YCpGAL (26), which contain the protein A tag (ProtA) fused to the proteins N-termini under the control of the *GAL1* promoter. The GST-Nip7p fusion was constructed by isolating the EcoRI/SalI *NIP7* sequence from pTL1-NIP7 and inserting into pGEX-4T1 (GE Healthcare). The plasmid pET29-A-NOP8 was constructed by transferring the protein A-NOP8 fusion from YCpGALNOP8 (26) to vector pET29a

using NdeI/SalI restriction sites. *NOP10* and *NHP2* coding sequences were isolated from respective $pGADC_2$ vectors using BamHI/SalI and inserted into pGEX-5X2 (GE Healthcare), generating *E. coli* expression vectors with GST fused to the proteins N-termini. Plasmids $pGADC_2$-NOP53, pET28-NOP53, pGEM-5.8S have been described elsewhere (27). Plasmids pET28-NIP7 and pGEM-ITS2 have been described previously (35). *E. coli* strains DH5α and BL21(DE3) were manipulated according to standard techniques (36). Growth and handling of *S. cerevisiae* strains were performed as previously described (37). Two-hybrid assays were performed essentially as previously described (26). A list of the yeast strains used in this work with a brief description of the relevant genetic markers is shown in Table 2.

2. Recombinant Nip7p expression and purification

Nip7p was expressed in *E. coli* BL21(DE3) harboring plasmid pET28-NIP7 at 30°C for 6h. Cellular extract preparation and His-Nip7 purification were described previously (35).

Table 1. Plasmids used in this study

Plasmid	Relevant features	Reference
pBTM116-NIP7	*lexADBD::NIP7 TRP1 2 μm*	26
pTL1- NIP7	*lexADBD::NIP7 TRP1 2 μm*	This study
pTL1- NIP7-N	*lexADBD::NIP7-N TRP1 2 μm*	This study
pTL1-PUA	*lexADBD::PUA TRP1 2 μm*	This study
pACT-NOP8	*GAL4AD::NOP8 LEU2 2 μm*	26
pACT-RRP43	*GAL4AD::RRP43 LEU2 2 μm*	26
pACT-RRP15	*GAL4AD::RRP15 LEU2 2 μm*	This study
$pGADC_2$-NOP53	*GAL4AD::NOP53 LEU2 2 μm*	27
$pGADC_2$-CBF5	*GAL4AD::CBF5 LEU2 2 μm*	This study
$pGADC_2$-GAR1	*GAL4AD::GAR1 LEU2 2 μm*	This study
$pGADC_2$-NOP10	*GAL4AD::NOP10 LEU2 2 μm*	This study
$pGADC_2$-NHP2	*GAL4AD::NHP2 LEU2 2 μm*	This study
YCpGALNOP8	*GAL::PrtA::NOP8 URA3 CEN4*	26
YCpGALRRP43	*GAL::PrtA::RRP43 URA3 CEN4*	26
YCpGALCBF5	*GAL::PrtA::CBF5 URA3 CEN4*	This study
YCpGALGAR1	*GAL::PrtA::GAR1 URA3 CEN4*	This study
YCpGALNOP10	*GAL::PrtA::NOP10 URA3 CEN4*	This study
YCpGALNHP2	*GAL::PrtA::NHP2 URA3 CEN4*	This study
YCpGALRRP15	*GAL::PrtA::RRP15 URA3 CEN4*	This study
pET28-NIP7	*His::NIP7, Kan^R*	35
pGEX-NIP7	*GST::NIP7, Amp^R*	This study
pET28-NOP53	*His::NOP53, Kan^R*	27
pET29-PrtANOP8	*PrtA::NOP8, Kan^R*	This study
pGEX-NOP10	*GST::NOP10, Amp^R*	This study
pGEX-NHP2	*GST:: NHP2, Amp^R*	This study
pGEM-5.8S	*5.8S, Amp^R*	27
pGEM-ITS2	*ITS2, Amp^R*	35

Table 2. *S. cerevisiae* strains used in this study

Strain	Genotype	Reference
L40	*MAT*a *his3*D*200 trp1-901 leu2-3,311 ade2 lys2801am URA3*::(*lexAop*)$_8$-*lacZ LYS2*::(*lexAop*)$_4$-*HIS3*	38
L40/NIP7-pGAD	L40 pKTM-NIP7, pGADC2	This study
L40/NIP7-NOP8	L40 pKTM-NIP7, pACT-NOP8	This study
L40/NIP7-RRP43	L40 pKTM-NIP7, pACT-RRP43	This study
L40/NIP7-NOP53	L40 pKTM-NIP7, pGAD-NOP53	This study
L40/NIP7-RRP15	L40 pKTM-NIP7, pACT-RRP15	This study
L40/NIP7-CBF5	L40 pKTM-NIP7, pGAD-CBF5	This study
L40/NIP7-GAR1	L40 pKTM-NIP7, pGAD-GAR1	This study
L40/NIP7-NOP10	L40 pKTM-NIP7, pGAD-NOP10	This study
L40/NIP7-NHP2	L40 pKTM-NIP7, pGAD-NHP2	This study
L40/NIP7-N-pGAD	L40 pTL1-NIP7-N, pGADC2	This study
L40/NIP7-N-NOP8	L40 pTL1-NIP7-N, pACT-NOP8	This study
L40/NIP7-N-RRP43	L40 pTL1-NIP7-N, pACT-RRP43	This study
L40/NIP7-N-NOP53	L40 pTL1-NIP7-N, pGAD-NOP53	This study
L40/NIP7-N-RRP15	L40 pTL1-NIP7-N, pACT-RRP15	This study
L40/NIP7-N-CBF5	L40 pTL1-NIP7-N, pGAD-CBF5	This study
L40/NIP7-N-GAR1	L40 pTL1-NIP7-N, pGAD-GAR1	This study
L40/NIP7-N-NOP10	L40 pTL1-NIP7-N, pGAD-NOP10	This study
L40/NIP7-N-NHP2	L40 pTL1-NIP7-N, pGAD-NHP2	This study
L40/PUA-pGAD	L40 pTL1-PUA, pGADC2	This study
L40/PUA-NOP8	L40 pTL1-PUA, pACT-NOP8	This study
L40/PUA-RRP43	L40 pTL1-PUA, pACT-RRP43	This study
L40/PUA-NOP53	L40 pTL1-PUA, pGAD-NOP53	This study
L40/PUA-RRP15	L40 pTL1-PUA, pACT-RRP15	This study
L40/PUA-CBF5	L40 pTL1-PUA, pGAD-CBF5	This study
L40/PUA-GAR1	L40 pTL1-PUA, pGAD-GAR1	This study
L40/PUA-NOP10	L40 pTL1-PUA, pGAD-NOP10	This study
L40/PUA-NHP2	L40 pTL1-PUA, pGAD-NHP2	This study
W303-1a	*MAT*a *ade2-1 leu2-3,112 his3-11,15 trp1-1 ura3-1 can1-100*	N. Nomura
DG440	*MAT*a *ade2-1 leu2-3,112 trp1-1 ura3-1 nip7::HIS3* p[*LEU2 ARS1 NIP7*]	24
DG442	*MAT*a *ade2-1 leu2-3,112 trp1-1 ura3-1 nip7::HIS3* p[*LEU2 ARS1 GAL1::nip7-1*]	24
DG456	*MAT*a *ade2-1 leu2-3,112 his3-11,15 trp1-1 ura3-1 can1-100 Nop8*::*KAN* p(*URA3 GAL::PrtA::NOP8*)	26
DG439/GAL::A-NIP7	DG439, YCp111GAL::PrtA::NIP7	This study
W303-1a/ YCpGALCBF5	W303-1a, YCpGALCBF5	This study
W303-1a/ YCpGALGAR1	W303-1a, YCpGALGAR1	This study
W303-1a/ YCpGALNOP10	W303-1a, YCpGALNOP10	This study
W303-1a/ YCpGALNHP2	W303-1a, YCpGALNHP2	This study
W303-1a/ YCpGALRRP15	W303-1a, YCpGALRRP15	This study
W303-1a/PUA	W303-1a, pTL1-PUA	This study
W303-1a/PUA-YCpGALNOP8	W303-1a, pTL1-PUA, YCpGALNOP8	This study
W303-1a/PUA–YCpGALRRP43	W303-1a, pTL1-PUA, YCpGALRRP43	This study
W303-1a/PUA-YCpGALCBF5	W303-1a, pTL1-PUA, YCpGALCBF5	This study
W303-1a/PUA-YCpGALNOP10	W303-1a, pTL1-PUA, YCpGALNOP10	This study

3. RNA binding and primer extension assays

RNA fragments corresponding to the 5.8S rRNA, the ITS2 spacer and an unrelated control derived from pBluescript plasmid (Stratagene) RNA were transcribed *in vitro* with T7 or SP6 RNA polymerase using linearized vectors pGEM-5.8S, pGEM-ITS2 and pBlueScript as templates in the presence of 10 μCi of [α-^{32}P]-UTP (27). One pmol of radiolabelled RNA was incubated with different amounts of purified His-Nip7p in buffer A (20 mM Tris-Cl pH 8.0, 5 mM magnesium acetate, 150 mM potassium acetate, 0.2% v/v Triton X-100, 1 mM DTT, 1 mM PMSF, 1 mg/ml aprotinin, 1 mg/ml pepstatin A and 1 mg/ml leupeptin) containing 0.8U RNAseOUT (Invitrogen) for 30 min at 37°C. 5-20 pmol of cold RNAs generated by parallel in vitro transcription of the plasmids cited above were used in the assays. UV cross-linking was performed by placing RNA-protein complexes on ice and irradiation for 5 min at 260 nm using a Fotodyne transilluminator. Subsequently, samples were treated with 10 μg of RNaseA for 30 min at 37°C. Samples were resolved on a 6% denaturing polyacrylamide gels using 20 mM CAPS pH 11.0 (N-Cyclohexyl-3-aminopropanesulfonic acid) as buffer and visualized on a Phosphorimager. For primer extension analyses, exponentially growing cultures of yeast strains DG440 and DG442 were transferred from YP medium containing galactose to YP medium containing glucose. Samples were collected at the time of the shift and 9 h after the shift and total RNA was isolated through a modified hot phenol method (27, 39). For pre-rRNA pseudouridylation analysis, RNAs were treated with CMCT (1-Cyclohexyl-3-[2-morpholinoethyl] carbodiicarbonate, Sigma) as described previously (40). Primer extension reactions were performed by annealing 1 pmol of [^{32}P]-labeled primer to 5 μg of total RNA as described previously (27). Control sequencing reactions were performed

using the Thermo-Sequenase kit (GE Healthcare). Primers used in the analysis are listed in Table 3.

Table 3. Primers used in this work

Primer	Sequence	Reference
P1	5' TAATCTTTGAGACAAGCATATG 3'	This study
P2	5' CATGGCTTAATCTTTGAGAC 3'	41
P3	5' CGTATCGCATTTCGCTGCGTTC 3'	24
P4	5' GTTCGCCTAGACGCTCTCTTC 3'	24
P5	5' GCCGCTTCACTCGCCGTTACTAAGGC 3'	42
P6	5' TCAAGGTCATTTCGACCCCGG 3'	This study
P7	5' GTTCAATTAAGTAACAAGG 3'	This study
P8	5' TTACCGAATTCTGCTTCGG 3'	This study
anti-5S	5' GGTCACCCACTACACTACTCGG 3'	This study
Anti-snR37	5'-GATAGTATTAACCACTACTG-3'	6
Anti-U3	5'-ATGGGGCTCATCAACCAAGTTGG-3'	39

4. "*Pull-down*" assays

GST pull-down assays using recombinant proteins were performed by co-expressing fusion proteins in *E. coli* BL21(DE3) at 25°C for 4h followed by purification using glutathione-sepharose beads (GE Healthcare). Cells expressing GST-Nop10p and GST-Nhp2p were mixed to cells expressing Nip7p prior to the lysis. Cell extracts were prepared in PBS buffer pH 7.5 (140 mM NaCl, 2.7 mM KCl, 10 mM Na_2HPO_4, 1.8 mM KH_2PO_4), containing 1 mM dithiothrietol (DTT), 1 mM phenylmethylsulfonyl fluoride (PMSF), 0.5% v/v Nonidet-40 and 5% v/v glycerol followed by incubation with glutathione-sepharose beads (GE Healthcare) for 1h at 4°C. After washing with PBS buffer containing 1 mM DTT and 1 mM PMSF, the beads were suspended in 100 µl of SDS-PAGE sample buffer (36). Whole-cell yeast extracts were prepared by suspending cells in 1 ml of ice-cold buffer A and the cells disrupted by vortexing with 1 volume of glass beads and 2 sequential centrifugations at 16,000 g for 20 minutes at 4°C (26).

Extracts containing protein A-fusion proteins were incubated with IgG-sepharose beads (GE Healthcare) for 2 h at 4°C. Nip7p PUA pull-down assays were performed with higher potassium acetate concentration (300 mM). After washing with ice-cold buffer A, IgG-sepharose beads were divided in two aliquots for protein or RNA analysis. For protein analysis, the beads were suspended in 80 µl of SDS-PAGE sample buffer and analyzed by immunoblot, as described previously (24). Membranes were probed with mouse antibodies directed against the poly-histidine tag (GE Healthcare) or against GST and with rabbit polyclonal antiserum raised against Nip7p (24) or against lexA (Invitrogen). Subsequently, membranes were incubated with alkaline phosphatase-conjugated immunoglobulin G (Sigma) and visualized by using 5-bromo-4-chloro-3-indolylphosphate (BCIP) and nitroblue tetrazolium (NBT) as previously described (36). RNA was isolated from bound fractions by adding phenol directly to the beads. After precipitation, the recovered RNA was denatured and separated by electrophoresis on 6% polyacrylamide or 1.5% agarose gels following northern blot, as described previously (27, 42). For comparison, 1% of RNA recovered from total extract was loaded on gels.

RESULTS

1. Nip7p interaction with box H/ACA snoRNP subunits and with other nucleolar proteins is mediated by the PUA domain region

In yeast, pseudouridylation of ribosomal RNA is carried out by the box H/ACA snoRNP which in yeast comprises the protein subunits Cbf5p, Gar1p, Nop10p and Nhp2p (7, 8). To test the involvement of Nip7p in rRNA pseudouridylation, the yeast two-hybrid system was used to test the interaction between Nip7p and the core subunits of box H/ACA snoRNPs, as well as with other cellular proteins. Two-hybrid assays were positive for Nip7p interaction with all H/ACA snoRNPs proteins, among which interaction with Cbf5p and Nop10p were stronger (Figure 1A and B). Association of Nip7p with these proteins and Rrp15p was verified by protein A pull-down assays with IgG sepharose. Nip7p was pulled down by all four protein subunits of the snoRNP complex fused to protein A (Figure 1C). Consistently with its association with box H/ACA proteins, Nip7p also interacts with Naf1p in the two-hybrid system (data not shown), which is required for assembly and stability of the box H/ACA snoRNP (39, 41). Nip7p also interacts in vivo with Rrp15p, a nucleolar protein involved in 60S biogenesis (43).

The question whether Nip7p is able to interact directly with all of these proteins was addressed by using recombinant proteins expressed in *E. coli*. The fusions Protein A-Nop8p and His-Nop53p interact directly with GST-Nip7p in GST-pull down assays (Figure 1D and E). Nip7p also interacts directly the box H/ACA snoRNP subunit Nop10p but not with Nhp2p in GST-pull down assays (Figure 1F). It was not possible to test

Cbf5p because it is insoluble in *E. coli*. This assay showed that Nip7p binds directly only to a subset of positive baits for Nip7p interaction in the two-hybrid. This result indicates that for several of these baits, which are parts of a complex located in the nucleus such as the box H/ACA snoRNP, two-hybrid assays might artificially bring the whole complex in association with the bait and therefore activate the reporter genes.

The approach used to map the region of Nip7p required for its interaction with other proteins involved construction of two deletion mutants. Yeast two-hybrid vectors pTL1-NTer and pTL1-PUA were constructed containing lexA fused to the amino acids 1 to 93 and 94 to 181 of Nip7p, respectively. The N-terminal and PUA domains were assayed for interaction with Nop8p, Nop53p, Rrp43p and Rrp15p in the two-hybrid system and the results revealed that the interactions are mediated by the PUA domain in all cases (Figure 2A and B). Consistently with these results, lexA-PUA was found in pull-down assays with Protein A fusions of Nop8p, Rrp43p and the box H/ACA subunits Cbf5p and Nop10p (Figure 2C).

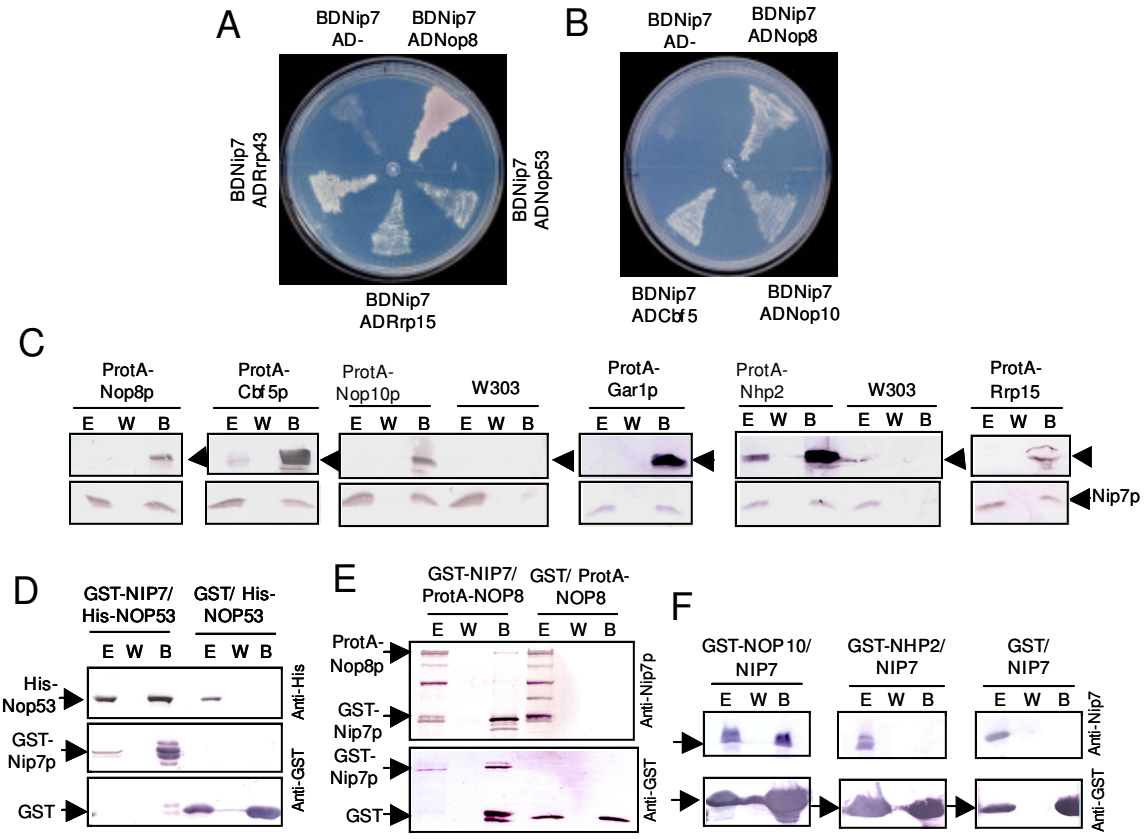

Figure 1. Analysis of Nip7p interaction with other proteins. (**A**) and (**B**) Nip7p interaction analysis using the yeast two-hybrid system. Nip7p fused to the DNA binding domain of *lex*A (BD fusions) was assayed in combination with activation domain fusions (AD fusions) of the indicated proteins. *lex*A-Nip7p and the activation domain alone (BDNip7, AD-) were used as a negative control in the assays. (**C**) Protein A-pull down assays. Protein A fusions were immobilized with IgG-sepharose beads and the bound fractions were analyzed by immunoblot using an antiserum against Nip7p. W303-1a extracts were used as negative controls in the assays. Nip7p and the protein A fusion proteins positions are indicated by arrows. (**D**) Direct interaction of GST-Nip7p with His-Nop53p. GST-Nip7p or GST were co-expressed with His-Nop53p in *E. coli* and isolated by binding to glutathione-sepharose beads. Bound His-Nop53p was probed by using an antibody against polihistidine. (**E**) Direct interaction of GST-Nip7p with Protein A-Nop8p. GST-Nip7p or GST were co-expressed with ProteinA-Nop8p in *E. coli* and isolated by binding to glutathione-sepharose beads. Bound Protein A-Nop8p was probed by using antibodies against Nip7p and GST. (**F**) Analysis of recombinant Nip7p interaction with box H/ACA proteins. *E. coli* cell extracts containing GST-Nop10p and GST-Nhp2p fusion proteins or GST alone were mixed to Nip7p extracts and the GST fusion proteins isolated by pull-down with glutathione-sepharose beads. The upper panel shows an immunoblot against Nip7p showing that Nip7p co-precipitates with GST-Nop10p but not with GST-Nhp2p nor with GST alone. The lower panel shows an immunoblot against GST showing the purified GST fusion proteins. E, whole cell extract, W, last wash, B, bound fraction.

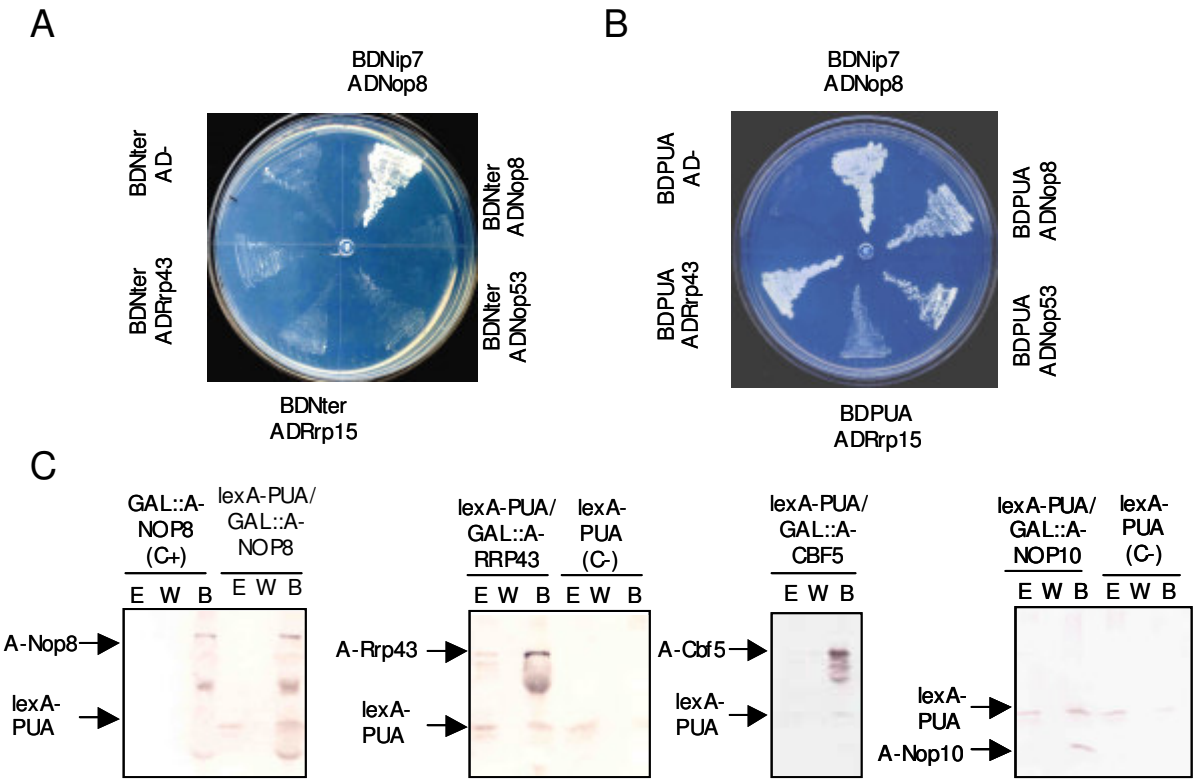

Figure 2. Interaction analysis of the Nip7p domains. (**A**) and (**B**) Two-hybrid interactions of the N-terminal and PUA domains of Nip7p, respectively. The assay was performed using either the N-terminal (NTer) or C-terminal (PUA) domains fused to *lex*A (BD fusions) and assayed in combination with activation domain fusions (AD fusions) of the indicated proteins. lexA-PUA and lexA-NTer and the activation domain combinations (BDPUA/AD-; ADNTer/AD-) were used as negative controls in the assays. Strain L40 carrying vectors pBTM116-NIP7 and pACT-NOP8 was used as a positive control. (**C**) Protein A-pull down assays. Protein A fusions and BD-PUA were immobilized in IgG-sepharose beads and bound fraction analyzed by immunoblot using an antiserum raised against lexA. Extracts of strain W303-1a carrying either vector YCpGALNOP8 or pTL1-PUA were used as negative controls. The immunoblots reveal the position of lexA-PUA as well as the protein A fusion proteins as indicated. E, whole cell extract, W, last wash, B, bound fraction.

2. Nip7p-depletion causes a moderate reduction in rRNA pseudouridylation

A major question raised by the interactions identified for Nip7p concerns the role played by Nip7p regarding its association to the box H/ACA snoRNP subunits. This association, along with the PUA domain, pointed to a role for Nip7p in pseudouridine formation. Therefore, extensive analyses of pseudouridine formation in Nip7p-depleted cells were performed and the level of pseudouridylation of 11 sites inside the 25S rRNA is shown in Figure 3. Depletion of Nip7p leads to accumulation of unprocessed 27S pre-rRNA and a general defect in pre-rRNA processing that causes a drastic reduction in the total amount of mature 18S and 25S rRNAs. To avoid discrepancies in the experiments, primer extension assays were performed with equal amounts of 25S rRNA, normalized by ethidium bromide staining. These analyses showed that cells depleted of Nip7p show a moderate reduction in the level of pseudouridine formation (Figure 3). Corroborating these results, depletion of Nip7p does not affect the levels of the box H/ACA snR37 in the cell, which is involved in pseudouridylation of 25S rRNA (9) (Figure 3D).

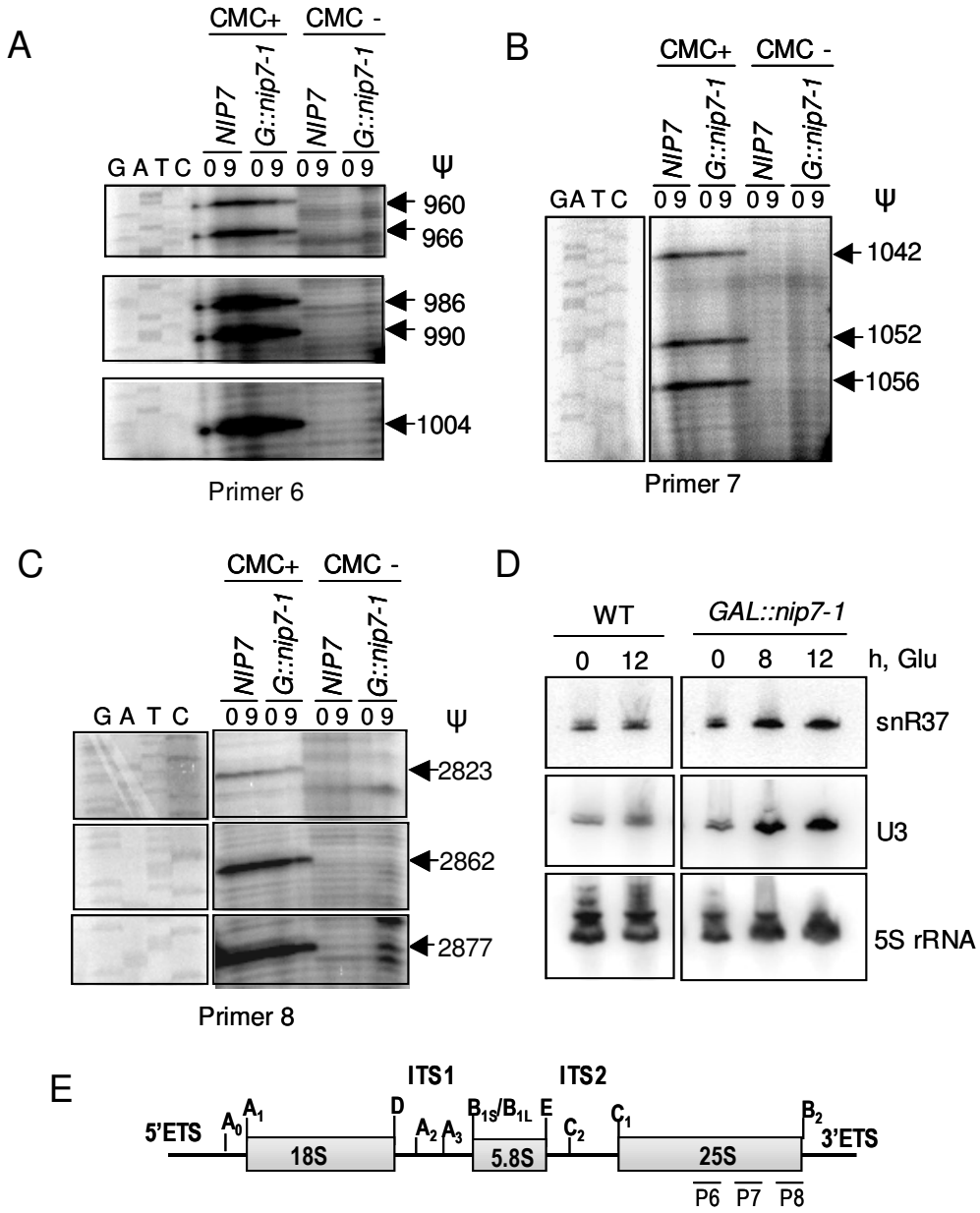

Figure 3. Primer extension analysis of rRNA pseudouridylation in Nip7p deficient cells. Control strain DG440 (*NIP7*) and test strain DG442 (*GAL::nip7-1*) were incubated in YPD medium for the indicated times to deplete nip7-1p. Total RNA was extracted and divided into two fractions for primer extension analysis. One fraction was pre-treated with CMCT (indicated as CMC+) before performing the primer extension reactions using primers 6 (**A**), 7 (**B**) and 8 (**C**), which cover 11 pseudouridylation sites in the 25S rRNA. Sequencing reactions were performed in parallel (indicated by GATC) to determine the position of the pseudouridylation sites that are indicated (ψ). (**D**) Analysis of steady-state levels of H/ACA box snR37 in strains DG440 and DG442. Cells were incubated in YPD medium for the indicated times to deplete nip7-1p and total RNA was extracted and analyzed by Northern blot using probes to detect snR37, and the controls U3 snoRNA and 5S rRNA. (**E**) Diagram showing the 35S pre-rRNA (not to scale) with the major processing sites and relative position of the primers used in the analyses of pseudouridylation sites.

3. Nip7p-depletion affects pre-rRNA cleavage

Taking into account that the results described above do not directly implicate Nip7p in pseudouridine formation, we turned our attention to the fact that Nip7p depletion causes a strong accumulation of unprocessed 27S pre-rRNA. This is the major defect in pre-rRNA processing observed in absence of Nip7p (24) indicating that Nip7p might be involved in ITS2 cleavage reactions. Aiming to find a specific defect in 27S pre-rRNA cleavage, we performed primer extension analysis, which is an indirect approach to evaluate the defects in the cleavages sites caused by Nip7p deficiency (Figure 4). Processing at site A_1 was analyzed with primers P1 and P2 and, consistently with reduced formation of mature 5' end of the 18S rRNA, there is a reduction in the band corresponding to the A_1 site upon depletion of Nip7p (Figure 4A). Two additional bands corresponding to shorter forms are also detected. Reduction in site A_1 processing can be explained due to accumulation of the aberrant 23S pre-rRNA in Nip7p-depleted cells (24), which is typical of deficient processing of sites A_0, A_1 and A_2. Formation of the 5'-end of the $58.S_S$ and $5.8S_L$ rRNAs was analyzed with primer P3, revealing a moderate reduction in the bands corresponding to the 5' end and an additional shorter product (Figure 4B). This defect is relatively mild and, accordingly, Nip7p is not predicted to directly participate in the 5'-end formation of the 5.8S rRNAs. Primer extension with P4 that hybridizes in ITS2 downstream of site C_2 identified a ladder-like pattern of larger aberrant products (Figure 4C) whereas primer P5 that hybridizes in the 25S rRNA downstream of site C_1, revealed shorter aberrant products in Nip7p-depleted cells (Figure 4D). These bands indicate the 5' ends of products that have been generated either by defective processing of sites C_1 and C_2 or from 5' to 3' degradation of the pre-rRNAs.

These results indicate that accumulation of 27S unprocessed precursors on Nip7-depleted cells might be due to failure on excision reactions of ITS2 spacer, suggesting a role for Nip7p on this process.

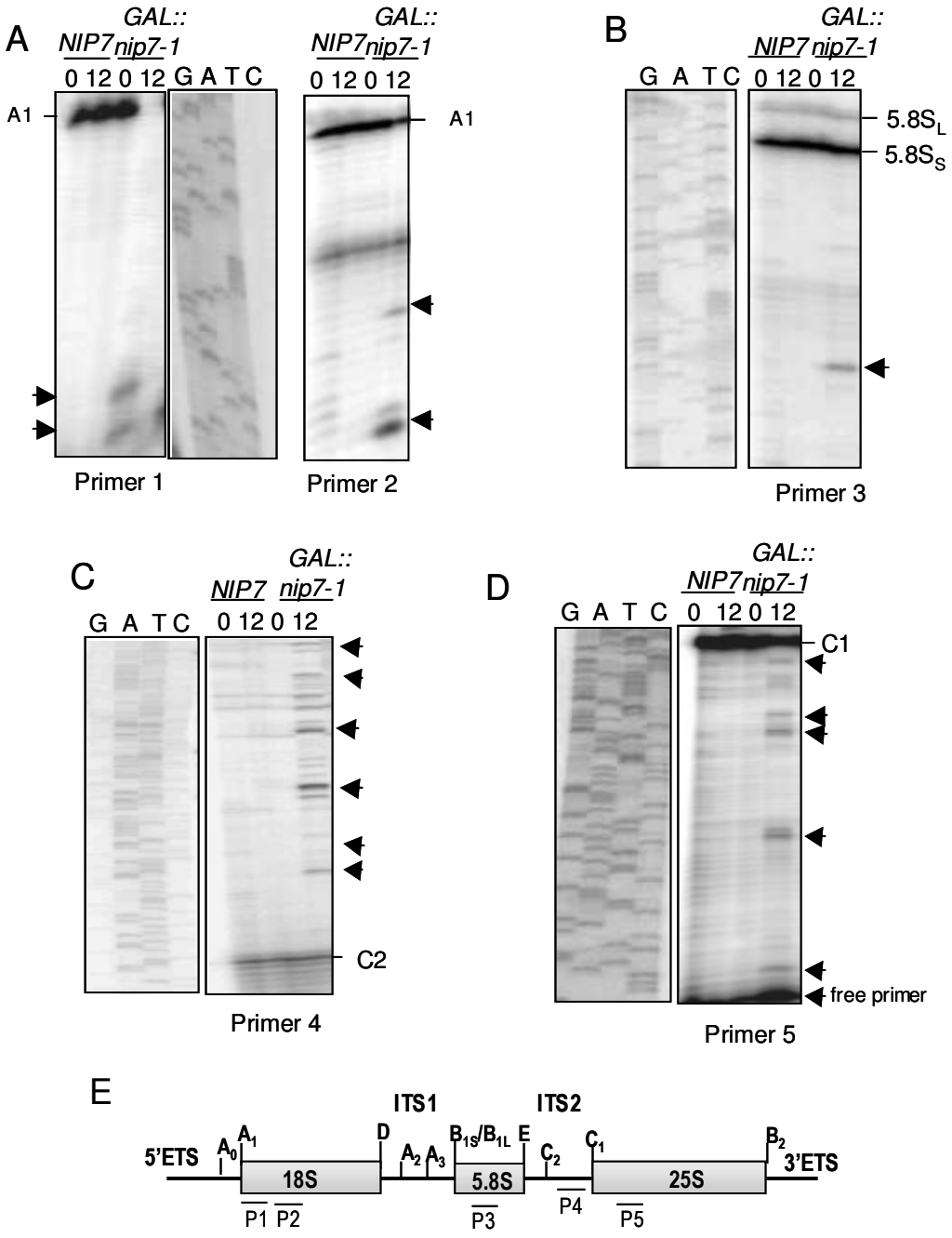

Figure 4. Primer extension analysis of pre-rRNA processing sites in Nip7p deficient cells. Control strain DG440 (*NIP7*) and test strain DG442 (*GAL::nip7-1*) were incubated in YPD medium for the indicated times to deplete nip7-1p. Total RNA was analyzed by primer extension. Sequencing reactions (indicated by GATC) were performed in parallel to determine the position of the unusual 5' ends of the pre-rRNA. (**A**) Analysis of pre-rRNA cleavage at site A_1 using primers 1 (left panel) and 2 (right panel). (**B**) Analysis of processing at site B_1 that corresponds to the 5' ends of the 5.8S rRNA ($5.8S_S$ and $5.8S_L$). (**C**) Analysis of processing at site C_2 in ITS2. (**D**) Analysis of processing at site C_1 that corresponds to the 5' end of the 25S rRNA. (**E**) Diagram showing the 35S pre-rRNA (not to scale) with the major processing sites and relative position of the primers used in the analyses cleavage sites.

4. Nip7p interacts directly with RNA

Considering the role of Nip7p in ribosome biogenesis and the presence of PUA domain, found in a number of RNA-interacting proteins, we performed a series of pull-down and RNA interaction assays. W303-1a cells expressing either Protein A or the Protein A-Nip7p fusion were used to test co-immunoprecipitation of rRNAs on IgG-sepharose affinity columns. The results obtained showed that Protein A-Nip7p co-precipitates the 27S pre-rRNA and the mature 5.8S and 5S rRNAs (Figure 5), consistent with the presence of Nip7p in pre-60S complex.

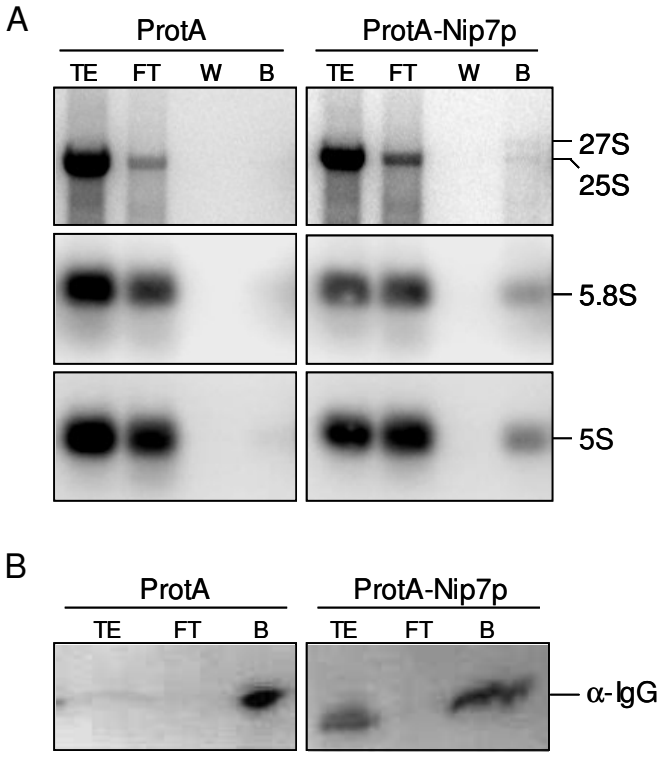

Figure 5. Co-immunoprecipitation of rRNA with protein A-Nip7p. (**A)** Total cell extracts from strains W303-1a/A and DG439/YCp111-*GAL*::protein A-NIP7 were mixed with IgG-sepharose beads for co-immunoprecipitation of rRNAs. RNA extracted from different fractions was separated on an agarose gel and bound RNA was detected by northern hybridization using probes specific to the indicated rRNAs. (**B**) Immunoblot of the same fractions as in (A) showing the bands corresponding to Protein A and Protein A-Nip7p. TE, total extract; FT, flow through; W, last wash; B, bound fraction (beads).

In vitro RNA interaction assays were performed by using recombinant histidine-tagged yeast Nip7p and *in vitro* transcribed RNAs corresponding to two different regions of the pre-rRNA: the 5.8S rRNA and the ITS2 spacer sequences. An unrelated RNA transcribed from vector pBluescript was used as a non specific competitor (pBS). Yeast Nip7p is a basic protein (pI 9.28) and regular EMSA using TBE buffer pH 8.0 was not suitable to resolve Nip7p-RNA complexes. Best results were obtained by changing the buffer to 20 mM CAPS pH 11.0, in which the pH is higher than Nip7p isoelectric point. UV-crosslinking followed by RNase digestion assays showed that Nip7p can bind directly to RNA in a concentration-dependent manner (Figure 6). We have previously reported that Nip7p has strong preference for U-rich RNA sequences. This is consistent with the higher affinity for ITS2 sequence, which is also U-rich (35). It is tempting to speculate a role for Nip7p in ITS2 cleavage reactions, which is supported by *in vitro* RNA interaction and primer extension analysis described above. However, further experimental evidence is still required to allow us to propose a direct function for Nip7p in ITS2 cleavage. Future studies should focus on the catalytic activity of Nip7p partners in an attempt to investigate the cleavage reactions.

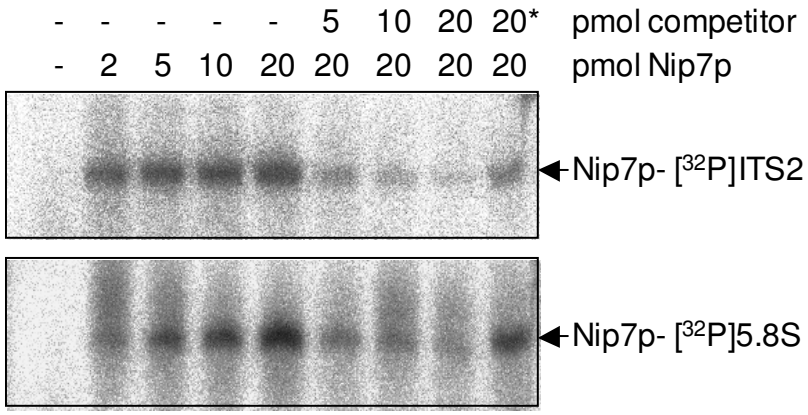

Figure 6. Analysis of Nip7p interaction with RNA *in vitro*. Increasing amounts of recombinant Nip7p (2-20 pmol) were incubated with 1 pmol of in vitro transcribed [^{32}P]-labeled ITS2 RNA and [^{32}P]-labeled 5.8S RNA (indicated by arrows). Subsequently the reactions were incubated with 5-20 pmol of unlabeled competitor RNAs as indicated. An RNA was *in vitro* transcribed from pBluescript plasmid and used as unspecific competitor (indicated by *). Samples were submitted to UV cross-linking for 5 min, treated with RNase A and resolved on denaturing polyacrylamide gels using 20 mM CAPS pH 11.0 both as electrophoresis and gel buffer.

DISCUSSION

Previous studies showed that depletion of *S. cerevisiae* Nip7p blocks processing of the 27S pre-rRNA, leading to an unbalanced ratio of ribosomal subunits (24, 26). Taking into account its essential role in ribosome biogenesis, experimental analysis is still needed to further characterize the function played by Nip7p during rRNA processing. In order to determine whether Nip7p binds a specific sequence of the 35S pre-rRNA, Nip7p interaction with rRNA was assessed both *in vivo* and *in vitro*. Nip7p co-precipitates 27S pre-rRNA and the mature 25S, 5.8S and 5S rRNAs, which is consistent with its presence in the pre-60S complex. The previously reported Nip7p preference for poly-U binding is intriguing (35). Nip7p may bind to a U-rich snRNA or snoRNA on the nucleolus during rRNA processing or, the preference for U-rich sequences might explain its high affinity for ITS2 spacer. Interestingly, Nip7p co-precipitated H/ACA snR37, albeit probably as part of the pre-60S complex (C. C. Oliveira, unpublished data).

In the yeast two-hybrid system, the Nip7p interactions with Nop8p, Rrp43p and Nop53p had previously been demonstrated (25-27) and here we show that Nip7p also interacts with Rrp15p and with box H/ACA snoRNP subunits. All proteins interacting with Nip7p are involved in pre-60S maturation, although at different steps. It is difficult to envision how all these interactions could take place in the cell. However, taking into account that Nip7p can bind rRNA directly, all protein interactions could occur in the context of the pre-60S processing pathway, not necessarily, and most probably, not at the same time (Figure 7). Interestingly, two-hybrid analysis and pull-down assays using separate domains showed that PUA is responsible for all the Nip7p interactions observed

and are consistent with the hypothesis that, during maturation of the 25S and 5.8S rRNAs, Nip7p is part of a closely associated RNP complex that includes components of the pre-rRNA processing machinery required for both covalent modification, such as the box H/ACA snoRNP complex, and for exonucleolytic cleavage, such as the exosome complex (Figure 7).

The Nip7p interaction with box H/ACA core components along with the presence of PUA domain in other pseudo-uridine synthases (29-32) led us to investigate the defects in pseudouridylation in cells deficient for Nip7p. The moderate impact of Nip7p depletion on rRNA pseudouridylation indicates that its primary function is not directly related to this process. Interestingly, Rnt1p was also found to interact with Gar1p and an *RNT1* mutant strain was also shown to have a moderate effect on pre-rRNA pseudouridylation (44). In addition, the impact of Nip7p depletion on accumulation of unprocessed 27S pre-rRNA strongly suggests a role for Nip7p in ITS2 cleavage (24). Therefore, it was reasonable to predict that among the Nip7p-interacting partners there should be some which are involved in ITS2 endonucleolytic cleavage. As a subunit of the exosome, Rrp43p can be excluded from the list of candidates (21, 25). Nop8p possesses canonical RNA binding motifs and Nop53p was shown to bind RNA (27), but none of these proteins contain domains related to catalytic cleavage of RNA. Nip7p was also found in complexes isolated with tap-tagged Rrp1p. Tap-tagged Rrp15p in its turn precipitated Rrp1p, both of which are required for 27S pre-rRNA processing and 60S subunit biogenesis (23, 43).

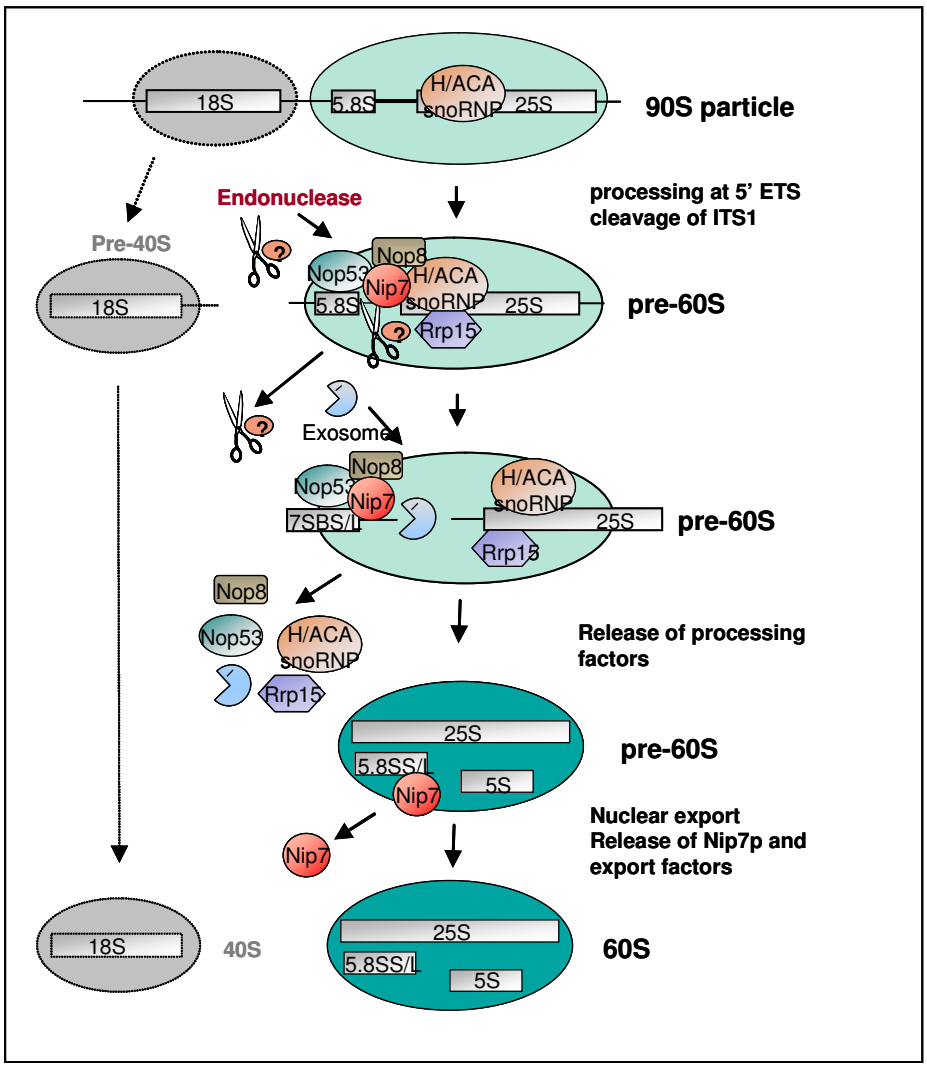

Figure 7. Cartoon of the processing steps involving Nip7p and Nip7p-interacting proteins during 60S ribosome subunit biogenesis. Nip7p binds to the early 60S pre-ribosomal particle, probably in ITS2 region, and remains associated to pre-60S complexes up to the late processing steps required for maturation of 60S ribosome subunits.

Conditional genetic depletion of over 30 non-ribosomal factors have already been described to affect processing of the 27S pre-rRNA, blocking formation of the 60S subunit. However, factors that directly function in endonucleolytic cleavage of ITS2 have not been identified yet, although it has been proposed that Rlp7p and Rea1p functions might be closely related to the initial processing steps of ITS2 (45,46). A limitation to study pre-rRNA processing mechanisms is that, so far, there is no straightforward *in vitro* assay to directly analyze the specific function of individual factors. Experimental approaches have been many times based on the characterization of defects in the pathway generated by conditional mutants, as in this case. Despite its limitations, this approach is quite robust and works very well even for mammalian cells (47). In fact, our work suggests that the primary defect caused by Nip7p depletion is the inhibition of ITS2 cleavage which leads to reduced formation of mature rRNAs. The analysis of pre-rRNA cleavage reactions in *nip7-1* strain through primer extension revealed that although precursor rRNAs accumulate in this strain, shorter bands are detected, probably due to 5'-3' degradation of the precursors. Similar phenotypes were described for Rrp43p and Nop53p mutants (27), two proteins that interact with Nip7p.

In conclusion, the interaction studies show that Nip7p is part of a closely related ribonucleoprotein complex that contains the 27S pre-rRNA and that the interactions are mediated by the PUA domain. Our data strongly suggest that Nip7p binds to ITS2 spacer sequence and that depletion causes a severe impact on processing of this spacer. Nip7p does not possess intrinsic RNA catalytic activity and our results suggest that it plays a regulatory role during processing of ITS2. Future studies should focus on the sequence elements in ITS2 and 5.8S rRNA that are important for processing of the 27S pre-rRNAs

and on *in vitro* assays to identify the specific elements that might be recognized by Nip7p during processing of the 27S pre-rRNAs and formation of the mature 5.8S and 25S rRNAs. In addition, it will be important to test Nip7p interaction with nucleases potentially involved in ITS2 endonucleolytic cleavage.

ACKNOWLEDGEMENTS

The authors are grateful to Zildene G. Correa for technical assistance and to Jörg Kobarg for providing the GST anti-serum. This work was supported by FAPESP grants (CEPID/CBME 98/14138-2; SMolBNet 00/10266-8, 00/02788-4 and 06/02083-7 to NITZ and BGG, and 03/06031-3 to CCO). PPC, DCG and JSL are recipients of FAPESP PhD fellowships.

REFERENCES

1. Fromont-Racine, M., Senger, B., Saveanu, C. and Fasiolo, F. (2003). Ribosome assembly in eukaryotes. *Gene*, **313**, 17-42.

2. Peng, W. T., Robinson, M. D., Mnaimneh, S., Krogan, N. J., Cagney, G., Morris, Q. *et al.* (2003). A panoramic view of yeast noncoding RNA processing. *Cell*, **113**, 919-933.

3. Grandi, P., Rybin, V., Bassler, J., Petfalski, E., Strauss, D., Marzioch, M. *et al.* (2002). 90S pre-ribosomes include the 35S pre-rRNA, the U3 snoRNP, and 40S subunit processing factors but predominantly lack 60S synthesis factors. *Mol. Cell*, **10**, 105-115.

4. Krogan, N. J., Peng, W.T., Cagney, G., Robinson, M. D., Haw, R., Zhong, G. *et al.* (2004). High-definition macromolecular composition of yeast RNA-processing complexes. *Mol. Cell*, **13**, 225-239.

5. Tollervey, D. and Kiss, T. (1997). Function and synthesis of small nucleolar RNAs. *Curr. Opin. Cell Biol.*, **9**, 337-342.

6. Lafontaine, D. L. and Tollervey, D. (2000). Synthesis and assembly of the box C+D small nucleolar RNPs. *Mol. Cell. Biol.*, **20**, 2650-2659.

7. Ganot, P., Bortolin, M. L. and Kiss, T. (1997). Site-specific pseudouridine formation in preribosomal RNA is guided by small nucleolar RNAs. *Cell*, **89**, 799-809.

8. Henras, A. K., Capeyrou, R., Henry, Y. and Caizergues-Ferrer, M. (2004). Cbf5p, the putative pseudouridine synthase of H/ACA-type snoRNPs, can form a complex with Gar1p and Nop10p in absence of Nhp2p and box H/ACA snoRNAs. *RNA*, **10**, 1704-1712.

9. Torchet, C., Badis, G., Devaux, F., Costanzo, G., Werner, M. and Jacquier, A. (2005). The complete set of H/ACA snoRNAs that guide rRNA pseudouridylations in *Saccharomyces cerevisiae*. *RNA*, **11**, 928-938.

10. King, T. H., Liu, B., McCully, R. R. and Fournier, M. J. (2003). Ribosome structure and activity are altered in cells lacking snoRNPs that form pseudouridines in the peptidyl transferase center. *Mol. Cell*, **11**, 425-435.

11. Hughes, J. M. and Ares Jr., M. (1991). Depletion of U3 small nucleolar RNA inhibits cleavage in the 5' external transcribed spacer of yeast pre-ribosomal RNA and impairs formation of 18S ribosomal RNA. *EMBO J.*, **10**, 4231-4239.

12. Dragon, F., Gallagher, J. E., Compagnone-Post, P. A., Mitchell, B. M., Porwancher, K. A., Wehner, K. A. *et al.* (2002). A large nucleolar U3 ribonucleoprotein required for 18S ribosomal RNA biogenesis. *Nature*, **417**, 967-970.

13. Tollervey, D. (1987). A yeast small nuclear RNA is required for normal processing of pre-ribosomal RNA. *EMBO J.*, **6**, 4169-4175.

14. Li, H. D., Zagorski, J. and Fournier, M. J. (1990). Depletion of U14 small nuclear RNA (snR128) disrupts production of 18S rRNA in *Saccharomyces cerevisiae*. *Mol. Cell. Biol.*, **10**, 1145-1152.

15. Morrissey, J. P. and Tollervey, D. (1993). Yeast snR30 is a small nucleolar RNA required for 18S rRNA synthesis. *Mol. Cell. Biol.*, **13**, 2469-2477.

16. Chamberlain, J. R., Lee, Y., Lane, W. S. and Engelke, D. R. (1998). Purification and characterization of the nuclear RNase P holoenzyme complex reveals extensive subunit overlap with RNase MRP. *Genes Dev.*, **12**, 1678-1690.

17. Lygerou, Z., Mitchell, P., Petfalski, E., Seraphin, B. and Tollervey, D. (1994). The POP1 gene encodes a protein component common to the RNase MRP and RNase P ribonucleoproteins. *Genes Dev.*, **8**, 1423-1433.

18. Chamberlain, J. R., Pagan-Ramos, Kindelberger, D. W. and Engelke, D. R. (1996). An RNase P RNA subunit mutation affects ribosomal RNA processing. *Nucleic Acids Res.*, **24**, 3158-3166.

19. Dichtl, B. and Tollervey, D. (1997). Pop3p is essential for the activity of the RNase MRP and RNase P ribonucleoproteins *in vivo*. *EMBO J.*, **16**, 417-429.

20. van Hoof, A., Staples, R. R., Baker, R. E. and Parker, R. (2000). Function of the Ski4p (Csl4p) and Ski7p proteins in 3'-to-5' degradation of mRNA. *Mol. Cell. Biol.*, **20**, 8230-8243.

21. Mitchell, P., Petfalski, E., Shevchenko, A., Mann, M. and Tollervey, D. (1997). The exosome: a conserved eukaryotic RNA processing complex containing multiple 3'→5' exoribonucleases. *Cell*, **91**, 457-466.

22. Baßler, J., Grandi, P., Gadal, O., Leßmann, T., Petfalski, E., Tollervey, D., Lechner, J. and Hurt, E. (2001). Identification of a 60S preribosomal particle that is closely linked to nuclear export. *Mol. Cell*, **8**, 517-529.

23. Horsey, E.W., Jakovljevic, J., Miles, T. D., Harnpicharnchai, P. and Woolford Jr, J. L. (2004). Role of the yeast Rrp1p protein in the dynamics of pre-ribosome maturation. *RNA*, **10**, 813-827.

24. Zanchin, N. I. T., Roberts, P., DeSilva, A., Sherman, F. and Goldfarb, D. S. (1997). *Saccharomyces cerevisiae* Nip7p is required for efficient 60S ribosome subunit biogenesis. *Mol. Cell. Biol.*, **17**, 5001-5015.

25. Zanchin, N.I.T. and Goldfarb, D. S. (1999a). The exosome subunit Rrp43p is required for the efficient maturation of 5.8S, 18S and 25S rRNA. *Nucleic Acids Res.*, **27**, 1283-1288.

26. Zanchin, N.I.T. and Goldfarb, D. S. (1999b). Nip7p interacts with Nop8p, an essential nucleolar protein required for 60S ribosome biogenesis, and the exosome subunit Rrp43p. *Mol. Cell. Biol.*, **19**, 1518-1525.

27. Granato, D. C., Gonzales, F. A., Luz, J. S., Cassiola, F., Machado-Santelli, G. M. and Oliveira, C. C. (2005). Nop53p, an essential nucleolar protein that interacts with Nop17p and Nip7p, is required for pre-rRNA processing in *Saccharomyces cerevisiae*. *FEBS J.*, **272**, 4450-4463.

28. Aravind, L. and Koonin, E. (1999). Novel predicted RNA-binding Domains Associated with the Translation Machinery. *J. Mol. Biol.*, **48**, 291-302.

29. Ishitani, R., Nureki, O., Fukai, S., Kijimoto, T., Nameki, N., Watanabe, M. *et al.* (2002). Crystal structure of archaeosine tRNA-guanine transglycosylase. *J. Mol. Biol.*, **318**, 665-677.

30. Hallberg, B. M., Ericsson, U. B., Johnson, K. A., Andersen, N. M., Douthwaite, S., Nordlund, P., Beuscher, A. E. 4th and Erlandsen, H. (2006). The structure of the RNA m^{5}C methyltransferase YebU from *Escherichia coli* reveals a C-terminal RNA-recruiting PUA domain. *J. Mol. Biol.*, **360**, 774-787.

31. Manival, X., Charron, C., Fourmann, J. B., Godard, F., Charpentier, B. and Branlant, C. (2006). Crystal structure determination and site-directed mutagenesis of the *Pyrococcus abyssi* aCBF5-aNOP10 complex reveal crucial roles of the C-terminal domains of both proteins in H/ACA sRNP activity. *Nucleic Acids Res.*, **34**, 826-839.

32. Pérez-Arellano, I., Gallego, J., and Cervera, J. (2007) The PUA domain - a structural and functional overview, *FEBS J.*, **274**, 4972-4984.

33. Liu, J. F., Wang, X. Q., Wang, Z. X., Chen, J. R., Jiang, T., An, X. M., Chang, W. R. and Liang, D. C. (2004). Crystal structure of KD93, a novel protein expressed in human hematopoietic stem/progenitor cells. *J. Struct. Biol.*, **148**, 370-374.

34. Carneiro, F. R., Silva, T. C., Alves, A. C., Haline-Vaz, T., Gozzo, F. C. and Zanchin, N. I. T. (2006). Spectroscopic characterization of the tumor antigen NY-REN-21 and identification of heterodimer formation with SCAND1. *Biochem. Biophys. Res. Commun.*, **343**, 260-268.

35. Coltri, P. P., Guimarães, B. G., Granato, D. C., Luz, J., Teixeira, E., Oliveira, C. C. and Zanchin, N. I. T. Structural insights into the interaction of the Nip7 PUA domain with polyuridine RNA. *Biochemistry*, **46**, 14177-14187.

36. Sambrook, J., Fritsch, E. J. and Maniatis, T. (1989). Molecular cloning, a laboratory manual (2nd ed) Cold Spring Harbor Laboratory Press, Cold Spring Harbor, NY.

37. Ausubel, F.M., Brent, R., Kingston, R., Moore, D. D., Seidman, J. G., Smith, J. A., and Struha, K. (1998). Current Protocols in Molecular Biology. John Wiley and Sons, New York, NY.

38. Hollenberg, S. M., Sternglanz, R., Cheng, P. F. and Weintraub, H. (1995). Identification of a new family of tissue-specific basic helix-loop-helix proteins with a two-hybrid system. *Mol. Cell. Biol.*, **15**, 3813-3822.

39. Dez, C., Noaillac-Depeyre, J., Caizergues-Ferrer, M. and Henry, Y. (2002). Naf1p, an essential nucleoplasmic factor specifically required for accumulation of box H/ACA small nucleolar RNPs. *Mol. Cell. Biol.*, **22**, 7053-7065.

40. Ofengand, J., Del Campo, M. and Kaya, Y. (2001). Mapping pseudouridines in RNA molecules. *Methods*, **25**, 365-373.

41. Fatica, A., Cronshaw, A. D., Dlakiæ, M. and Tollervey, D. (2002). Ssf1p prevents premature processing of an early pre-60S ribosomal particle. *Mol. Cell*, **9**, 341–351.

42.Gonzales, F. A., Zanchin, N. I., Luz, J. S. and Oliveira, C. C. (2005). Characterization of *Saccharomyces cerevisiae* Nop17p, a novel Nop58p-interacting protein that is involved in pre-rRNA processing. *J. Mol. Biol.*, **18**, 437-455.

43. De Marchis, M. L., Giorgi, A., Schinina, M. E., Bozzoni, I. and Fatica, A. (2005). Rrp15p, a novel component of pre-ribosomal particles required for 60S ribosome subunit maturation. *RNA*, **11**, 495-502.

44. Tremblay, A., Lamontagne, B., Catala, M., Yam, Y., Larose, S., Good, L. and Elela, S.A. (2002). A physical interaction between Gar1p and Rnt1p is required for the nuclear import of H/ACA small nucleolar RNA-associated proteins. *Mol. Cell. Biol.*, **22**, 4792-4802.

45. Gadal, O., Strauss, D., Petfalski, E., Gleizes, P. E., Gas, N., Tollervey, D. and Hurt, E. (2002). Rlp7p is associated with 60S preribosomes, restricted to the granular component of the nucleolus, and required for pre-rRNA processing. *J. Cell. Biol.*, **157**, 941-951.

46. Galani, K., Nissan, T. A., Petfalski, E., Tollervey, D. and Hurt, E. (2004). Rea1, a dynein-related nuclear AAA-ATPase, is involved in late rRNA processing and nuclear export of 60 S subunits. *J. Biol. Chem.*, **279**, 55411-55418.

47. Grimm, T., Hölzel, M., Rohrmoser, M., Harasim, T., Malamoussi, A., Gruber-Eber, A., Kremmer, E. and Eick, D. (2006). Dominant-negative Pes1 mutants inhibit ribosomal RNA processing and cell proliferation via incorporation into the PeBoW-complex. *Nucleic Acids Res.*, **34**, 3030-3043.

3.4. Capítulo 4

The human Nip7 protein interacts with the putative RNA methyl-transferase FTSJ3 and with SUMO-2

Patrícia P. Coltri, Tereza C. L. Silva and Nilson I. T. Zanchin

The human Nip7 protein interacts with the putative RNA methyl-transferase FTSJ3 and with SUMO-2

Patrícia P. Coltri, Tereza C. L. Silva and Nilson I. T. Zanchin*

Center for Structural Molecular Biology
Brazilian Synchrotron Light Laboratory, LNLS
Rua Giuseppe Maximo Scolfaro 10000
PO Box 6192, CEP13083-970, Campinas SP, Brazil

Running title: HsNip7 interacts with FTSJ3 and SUMO-2

*Corresponding author: Nilson I. T. Zanchin
Centro de Biologia Molecular Estrutural
Laboratório Nacional de Luz Síncrotron
Campinas - SP
Caixa Postal (PO Box) 6192 -CEP 13084-971
Tel. 55 19 3512 1113
Fax. 55 19 3512 1004
e-mail:zanchin@lnls.br

ABSTRACT

The protein Nip7 was first characterized in *Saccharomyces cerevisiae,* being required for proper 27S pre-rRNA processing and 60S ribosome subunit biogenesis. Nip7 displays conserved two-domain architecture with the C-terminal region corresponding to the PUA domain which mediates interactions with polyuridine. In yeast, Nip7p interacts with the exosome subunit Rrp43p and with several nucleolar proteins, including Nop8p. HsNip7 and Nop132, which are the human orthologues of Nip7p and Nop8p also interact, consistently with the conservation of the ribosome biogenesis machinery in eukaryotes. In addition, we have recently found that a GST fusion of the Shwachman-Bodian-Diamond syndrome associated protein (SBDS) can pull-down HsNip7 from mammalian cells extracts, showing that both HsNip7 and SBDS function in close association. However, there is no information available on the set of proteins that interact with Nip7 in human cells. In this work, we have identified FTSJ3 and SUMO-2 (small ubiquitin-like modifier 2) as novel HsNip7 interacting partners. FTSJ3 is an uncharacterized orthologue of the yeast rRNA methyltransferase Spb1p, which is an RNA methyl-transferase responsible Gm_{2922} methylation in the 25S rRNA. SUMO-2 is involved in post-translational covalent modification of a wide range of substrates, and the human and yeast orthologues should play similar function in modification of pre-ribosomal subunits and several 60S-acting factors. The protein interaction analyses indicate that the human and yeast Nip7p counterparts interact directly with different sets of proteins during ribosome biogenesis.

INTRODUCTION

Saccharomyces cerevisiae has been widely used as a model system to study eukaryotic ribosome biogenesis and the studies in this system have provided information on the major pre-rRNA processing intermediates, on the transacting factors that function in pre-rRNA cleavage and covalent modification, on the interaction of the transacting factors and, on the composition of the pre-ribosomal particles (Grandi *et al.*, 2002; Fromont-Racine *et al.*, 2003; Peng *et al.*, 2003). In fact, mammalian pre-rRNA processing is highly similar to the yeast pathway (Figure 1). However, mutations in a number of crucial genes associated to genetic syndromes have brought attention to this process in human cells. Five human genetic syndromes have been associated to mutations in genes encoding proteins involved in ribosome biogenesis or in structural components of the ribosome (Liu & Ellis, 2006). These include the Shwachman-Bodian-Diamond Syndrome (SDS), an autosomal recessive disease characterized by pleiotropic phenotypes including pancreatic insufficiency, hematological dysfunctions and skeletal abnormalities. This syndrome has been associated to mutations in the *SBDS* gene that encodes a ubiquitously expressed nucleolar protein (Boocock *et al.*, 2003; Austin *et al.*, 2005) and its genetic depletion leads to defective 60S subunit biogenesis (Ganapathi *et al.*, 2007). Approximately 25% of Diamond Blackfan Anemia (DBA) patients show mutations in the gene *RPS19*, encoding the small ribosome subunit protein 19 (Draptchinskaia *et al.*, 1999). Cartilage-hair hypoplasia (CHH) has been linked to mutation in the RNA component of the RNase MRP that, among many functions in mitochondrial tRNA processing (Ridanpaa *et al.*, 2001), is responsible for endonucleolytic cleavage of ITS1 and its efficiency affects 5.8S rRNA maturation and 60S subunit biogenesis (Thiel *et al.*, 2005). The Treacher Collins associated

nuclear phosphoprotein treacle interacts with RNA polymerase I and Nop56, a protein subunit of the box C/D snoRNP, and has a role in rRNA methylation (Valdez *et al.*, 2004; Gonzales *et al.*, 2005). Dyskeratosis congenita has been associated to mutations in the X-linked *DKC1* gene (Heiss *et al.*, 1998), which encodes the pseudouridine synthase dyskerin, responsible for uridine isomerization in ribosomal RNA (Lafontaine *et al.*, 1998). Cells knock down for dyskerin show a ribosome deficiency that affects translation of mRNAs containing internal ribosomal entry sites (IRES) (Ruggero *et al.*, 2003; Yoon *et al.*, 2006). However, dyskerin along with the other protein subunits of the box H/ACA snoRNP, has also been described as a component of the telomerase reverse transcriptase complex (TERT) (Mitchell *et al.*, 1999), indicating that dyskerin may function both in pre-rRNA processing and telomere maintenance (Vulliamy *et al.*, 2001).

Previous interaction studies have indicated that both yeast and human Nip7 and SBDS orthologues are part of a single complex (Hesling *et al.*, 2007; Luz *et al.*, 2007). The functions of Nip7p and Sdo1p, the yeast orthologue of SBDS, are best characterized in the yeast model system, where Nip7p is required for accurate processing of the 27S pre-rRNA (Zanchin *et al.*, 1997) and Sdo1p has been shown to function in 60S ribosomal subunit translational activation and Tif6p recycling (Menne *et al.*, 2007). Studies with SBDS knock down cells indicated that SBDS is not required for general pre-rRNA processing in human HEK293 cells, although in these cells several genes showed altered expression at the transcriptional level and altered mRNA associated to polysomes (Hesling *et al.*, 2007). Highly conserved Nip7p orthologues are found in all eukaryotes and Archaea. In addition, the interaction between the yeast proteins Nip7p-Nop8p is conserved by their human orthologues (Sekiguchi *et al.*, 2004). In *S. cerevisiae*, Nip7p interacts with several proteins involved in 60S biogenesis, including the nucleolar proteins Nop53p and Nop8p, both

involved in processing of 27S precursor (Zanchin & Goldfarb, 1999; Granato *et al.*, 2005). Nip7p also interacts with H/ACA box core proteins (Coltri *et al.*, unpublished results) and Rrp43p, a component of the exosome complex (Zanchin & Goldfarb, 1999). Affinity purification analysis revealed novel interactions for *S. cerevisiae* Nip7p, including proteins associated to 60S-late processing steps, such as Nop7p, Nug1p, Npa1p, Rix1p and Rix7p (Baßler *et al.*, 2001; Gavin *et al.*, 2006).

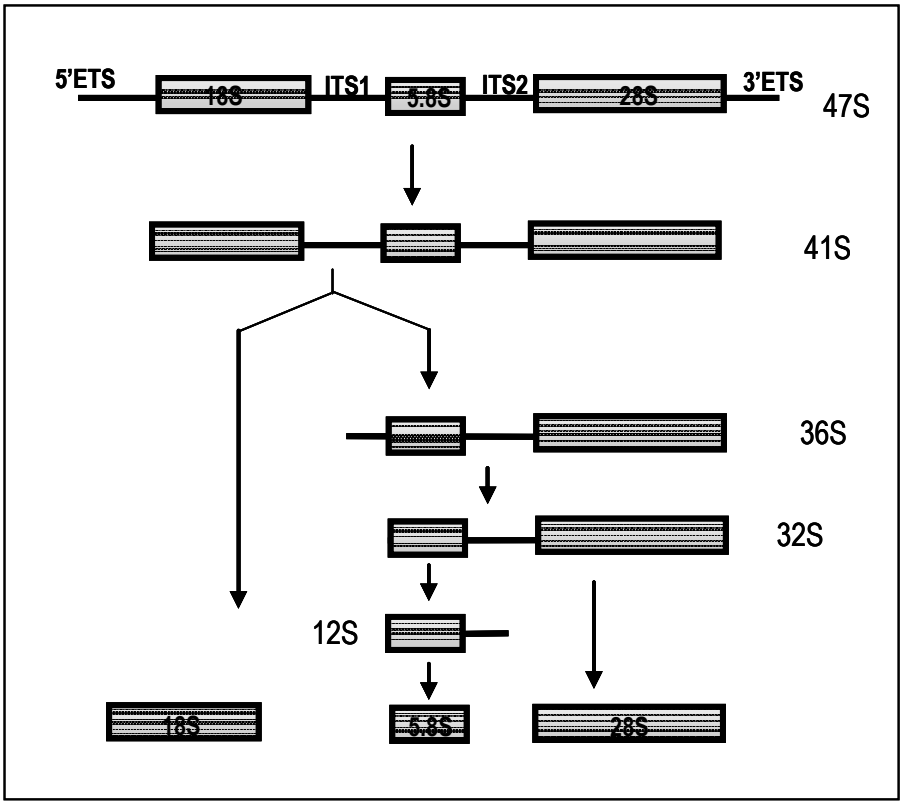

Figure 1. Schematic representation of the mammalian rRNA-processing pathway. Mammalian rRNA is transcribed as a single 47S precursor which is processed by successive cleavages, similarly to the yeast processing pathway. The mammalian 47S precursor is rapidly cleaved at the 5'ETS and at the 3'ETS to give rise to 41S pre-rRNA, which is rapidly processed to the 18S rRNA and a 36S precursor RNA that contains the sequences of the 5.8S and 28S rRNAs. Further processing in the 36S precursor generates the 32S precursor, processed to the 28S rRNA and a 12S pre-rRNA. The 12S precursor is further processed to form the 5.8S rRNA.

Since there is no functional information on the human Nip7 orthologue, we searched for new interactions of HsNip7 using the yeast two-hybrid system. Two novel interactions were confirmed by GST-pull down assays, with the human putative rRNA methyltransferase FTSJ3 and with the small ubiquitin-like modifier SUMO-2. The yeast orthologue of FTSJ3, Spb1p, has already been characterized, being required for methylation of Gm_{2922} in 27S pre-rRNA (Lapeyre & Purushothaman, 2004). Deficiency of Spb1p leads to accumulation of unprocessed 27S pre-rRNA and to deficient 60S subunit biosynthesis. Yeast orthologues of SUMO-2 have been found in affinity purified pre-60S complexes. In *S. cerevisiae*, pre-ribosomal subunits 40S and 60S as well as several 60S-acting factors are extensively sumoylated (Panse *et al.*, 2006). It is possible that human SUMO-2 plays an equivalent function in ribosome biogenesis of human cells. We also showed HsNip7 interacts preferentially with polyuridine sequences *in vitro*, similar to yeast and archaeal Nip7 counterparts. The results obtained in this work indicate that human and yeast Nip7 orthologues interact with different sets of proteins during pre-rRNA processing and 60S subunit biogenesis.

MATERIAL AND METHODS

1. Plasmids, strains and media

Plasmids used in this study are listed in Table 1 and cloning procedures are briefly summarized below. Plasmid pET28-Nip7 was described previously (Coltri *et al.*, 2007). The HsNip7 540 bp coding sequence was isolated from pTL1-HsNip7 (Hesling *et al.*, 2007) using the EcoRI/SalI restriction sites and inserted into the pET28a and pEGFPC2 plasmids, generating pET28-HsNip7 and pEGFP-HsNip7, respectively. The polylinker of pmRFP was modified to adjust the reading frame to that of the *FTSJ3* and *SUMO-2* cDNAs isolated in the yeast two-hybrid screen. pmRFP was modified by inserting a polylinker into the HindIII/SalI restriction sites, generating pmRFPL plasmid. The *FTSJ3* coding sequence was isolated from pACT-FTSJ3 using the EcoRI/XhoI restriction sites and inserted into pGEX-5X2 (GE Healthcare), generating plasmid pGEX-FTSJ3. Subsequently, the *FTSJ3* cDNA was isolated from pGEX-FTSJ3 and inserted into pmRFPL using the EcoRI/NotI restriction sites, generating pmRFPL-FTSJ3. The *SUMO-2* coding sequence was isolated from pACT-SUMO2 using the EcoRI/XhoI restriction sites and inserted into pGEX-5X2 generating plasmid pGEX-SUMO2. pmRFPL-SUMO2 was generated by transferring the EcoRI/BglII fragment from pACT-SUMO2 to pmRFPL. *Escherichia coli* strains DH5α and BL21(DE3) were maintained in LB medium containing 50 $mg.ml^{-1}$ of the required antibiotic used in transformant selection and manipulated according to standard techniques (Sambrook *et al.*, 1989). Growth and handling of *S. cerevisiae* strains were performed as previously described (Ausubel *et al.*, 1998).

Table 1. Plasmids used in this study

Plasmid	Relevant features	Reference
pTL1-HsNIP7	*lexADBD::HsNIP7 TRP1 2 µm*	Hesling *et al.*, 2007
pTL1- NIP7	*lexADBD::NIP7 TRP1 2 µm*	This study
pACT-NOP8	*GAL4AD::NOP8 LEU2 2 µm*	Zanchin & Goldfarb, 1999
pACT-FTSJ3	*GAL4AD::FTSJ3 LEU2 2 µm*	This study
pACT-SUMO2	*GAL4AD::SUMO-2 LEU2 2 µm*	This study
pET28-HsNIP7	*His::HsNIP7, Kan^R*	This study
pET28-NIP7	*His::NIP7, Kan^R*	Coltri *et al.*, 2007
pGEX-FTSJ3	*GST:: FTSJ3, Amp^R*	This study
pGEX-SUMO2	*GST:: SUMO-2, Amp^R*	This study
pEGFP-HsNIP7	*EGFP::HsNIP7 Kan^R*	This study
pmRFPL-FTSJ3	*mRFP::FTSJ3 Kan^R*	This study
pmRFPL-SUMO2	*mRFP::SUMO-2 Kan^R*	This study

2. Yeast two-hybrid assays

The host strain L40 (*MAT*a *his3*D*200,trp1-901,leu2-3,311,ade2,lys2801am URA3*::(*lexAop*)$_8$-*lacZ LYS2*::(*lexAop*)$_4$-*HIS3*; Hollenberg *et al.*, 1995) used in the two-hybrid analyses contains both yeast *HIS3* and *E. coli lac*Z genes as reporters for two-hybrid interaction integrated into the genome. An L40 derivative strain bearing plasmid pTL1-HsNip7, encoding a DNA-binding (DBD, *lexA*) fusion protein was transformed with a human fetal brain cDNA library constructed in the pACT2 vector (Clontech HL4028AH) using a PEG/lithium acetate mediated protocol (Matchmaker Yeast Protocol Handbook). Transformants showing positive interaction were selected on YNB plates supplemented with adenine and 6 mM 3-AT (3-amino-triazol; Sigma). The β-galactosidase activity assay was performed by growing cells directly on nitrocellulose membranes on YNB plates for 2 days at 30°C. Cells were lyzed by soaking membranes in a liquid nitrogen bath and the β-galactosidase activity was tested using 100 mg.ml^{-1} X-gal in buffer Z (60 mM Na_2HPO_4; 40 mM NaH_2PO_4; 10 mM KCl; 1 mM $MgSO_4$) at 28-30°C, as previously described (Ausubel *et al.*, 1998).

3. Electrophoretic mobility shift assays (EMSA)

EMSA was performed using recombinant proteins. Expression and purification of *S. cerevisiae* Nip7p was performed as described previously (Coltri *et al.*, 2007). Expression of HsNip7 was performed in *E. coli* BL21(DE3) cells incubated in LB medium containing kanamycin (50 $\mu g.ml^{-1}$) at 25°C. At an OD_{600} of ~0.8, the culture was induced by adding 0.5 mM IPTG and incubating at 25°C for further 4h. Cells were harvested by centrifugation, suspended in buffer containing 50 mM sodium phosphate pH 7.2, 100 mM NaCl, 10% glycerol and 0.5 mM phenylmethylsulfonyl fluoride (PMSF) and treated with lysozyme (50 $\mu g.ml^{-1}$) for 30 min on ice. Subsequently, the cells were disrupted by sonication and the histidine-tagged HsNip7 purified by metal-chelating affinity chromatography on Ni-NTA columns (Qiagen), using a 20-200 mM imidazole gradient for elution. HsNip7 was further purified by chromatography on a heparin-sepharose column (GE Healthcare) using the same buffer as above for binding and a 50 mM to 1 M KCl gradient for elution. For EMSA, 20 pmol of the RNA oligoribonucleotides poly-$G_{(25)}$, poly-$A_{(20)}$ and poly-$U_{(20)}$ were [^{32}P]-labeled using 1U T4 PNK (Fermentas) and 20µCi [γ^{32}P]-ATP. 0.4 pmol of each [^{32}P]-labeled oligoribonucleotide were incubated with 100 pmol of HsNip7 in buffer A (20 mM Tris-Cl pH 8.0, 5 mM magnesium acetate, 150 mM potassium acetate, 0.2% v/v Triton X-100, 1 mM DTT, 1 mM PMSF) for 30 min at 37°C. Recombinant *S. cerevisiae* Nip7p bound to [^{32}P]-poly-$U_{(20)}$ was used as a control for the experiment. Complexes were resolved on 8% polyacrylamide gels using TBE buffer pH 8.0 for electrophoresis and visualized on a Phosphorimager.

4. Protein interaction assays

GST pull-down assays using recombinant proteins were performed by co-expressing fusion proteins in *E. coli* BL21(DE3) incubated at 25°C and induced with 0.5 mM IPTG for 4h, followed by purification using glutathione-sepharose beads (GE Healthcare). Cell extracts were prepared in PBS buffer pH 7.5 (140 mM NaCl, 2.7 mM KCl, 10 mM Na_2HPO_4, 1.8 mM KH_2PO_4), containing 1 mM DTT, 1 mM PMSF, 0.5% v/v Nonidet-40 and 5% v/v glycerol, followed by incubation with glutathione-sepharose beads (GE Healthcare) for 1h at 4°C. After washing with PBS buffer containing 1 mM DTT and 1 mM PMSF, the beads were suspended in 100 µl of SDS-PAGE sample buffer (Sambrook *et al.*, 1989). Immunoblot analysis was performed according to standard techniques (Sambrook *et al.*, 1989). Membranes were probed with mouse antibodies directed against the poly-histidine tag (GE Healthcare) and against GST. Subsequently, the membranes were incubated with alkaline phosphatase-conjugated immunoglobulin G (Sigma) and visualized by using 5-bromo-4-chloro-3-indolylphosphate (BCIP) and nitroblue tetrazolium (NBT) as previously described (Sambrook *et al.*, 1989).

5. Cell culture methods

HEK293 cells (ATCC number CRL-1573) were maintained in MEM (Minimum Essential Alfa Medium, Gibco-BRL) supplemented with 10% fetal bovine serum, 100 $U.ml^{-1}$ penicillin and 100 $\mu g.ml^{-1}$ streptomycin. The cells were cultured at 37°C in a humidified atmosphere with 5% CO_2. Transient transfections were performed with Lipofectamine 2000 (Invitrogen), according to procedures described by the manufacturer, and the cells were analyzed 48-72h post-transfection. Briefly, 30 µg lipofectamine was added to a suspension of 4 µg DNA in MEM without serum and antibiotic in a final volume

of 200 µl. After a 30-minute incubation at room temperature, 600 µl of MEM were added to the mixture and the reactions were gently added to the well containing the cells. The cells were incubated for 5 h and the medium was supplied with 10% serum. For fluorescence microscopy analysis, cells were fixed with 4% paraformaldehyde for 20 min, permeabilized with 0.25% Triton X-100 in PBS for 10 min and mounted in medium containing 5 $\mu g.ml^{-1}$ DAPI. The subcellular localization of EGFP- and mRFP- fusion proteins was monitored by fluorescence. Images were obtained with a Nikon Eclipse E600 microscope and, digital images were processed using the Cool-SNAPPro digital system (Media Cybernetics).

RESULTS

1. Identification of HsNip7 interaction with FTSJ3 and SUMO-2

Taking into account the structural conservation observed among the yeast and human Nip7 orthologues, we asked whether the human Nip7 protein, HsNip7, interacts with the same set of proteins as yeast Nip7p. To address this question, we performed an extensive yeast two-hybrid analysis using the fusion lexA-HsNip7 as bait to screen a human fetal brain cDNA library (Clontech HL4028AH). 121 positive clones were isolated from over 3 x 10^6 yeast transformants. Ten of the positive clones corresponded to the human orthologue of yeast Spb1p, FTSJ3, and ten clones to the small ubiquitin-like modifier 2 (SUMO-2). The FTSJ3 clones comprised different cDNAs lengths, including the full-length sequence as well as truncated cDNAs starting at amino acids 291, 373 and 433 (Figure 2A). This finding shows that the interaction with HsNip7 takes place via the C-terminal region comprising residues 433 to 847 of FTSJ3 (Figure 2C). In the case of SUMO-2, most cDNAs isolated comprised the sequence starting at amino acid 3 and one cDNA starting at amino acid 33 (Figure 2B). The HsNip7-FTSJ3 and HsNip7-SUMO-2 interactions were verified by retransforming pTL1-HsNip7 with either pACT-FTSJ3 or pACT-SUMO-2 into the yeast strain L40 and assaying for reporter gene activation on YNB plates containing adenine and 6 and 10 mM 3-AT (Figure 2C). As a negative control, pTL1-HsNip7 was transformed with pACT2. The interaction of yeast Nip7p and Nop8p proteins was used as a positive control of this assay (Zanchin & Goldfarb, 1999).

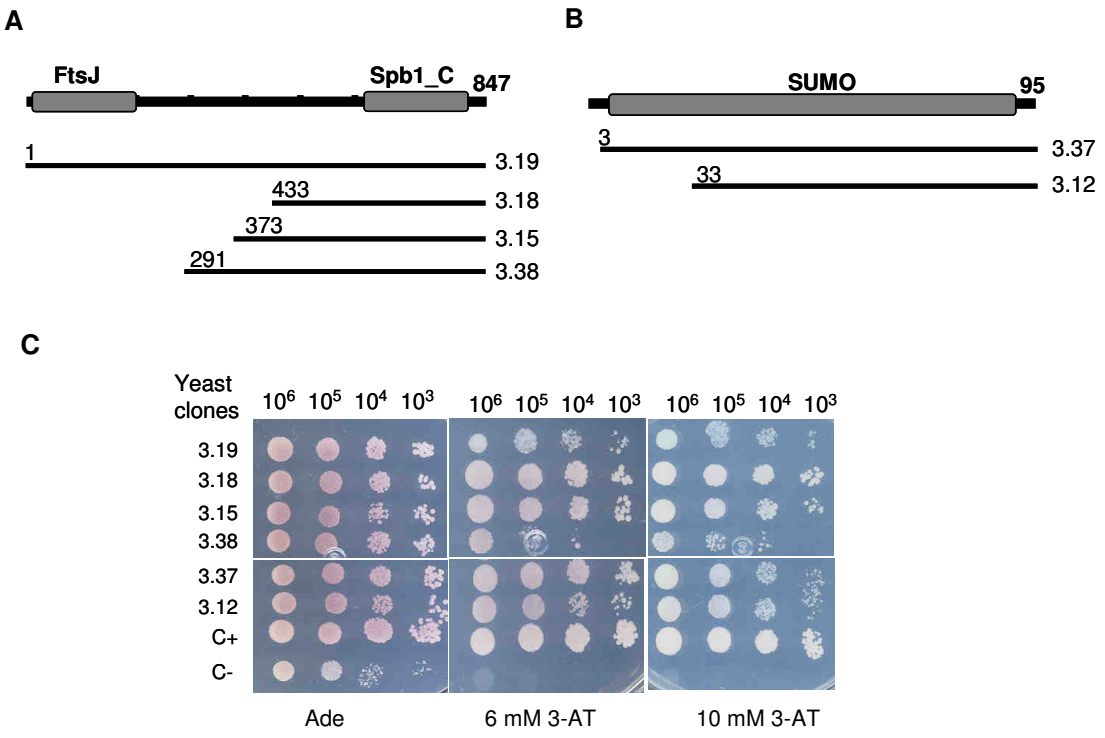

Figure 2. Yeast two-hybrid analysis of HsNip7 interacting proteins. Schematic representation of the positive cDNA clones of FTSJ3 (**A**) and SUMO-2 (**B**). The length of each cDNA isolated is represented by bars under the scheme of primary sequence of the protein and the first amino acid of each cDNA is indicated by the number on the left. The conserved domains are shown in grey boxes. On the right the yeast clones isolated in the two-hybrid screens are indicated. (**C**) Test for activation of reporter gene *HIS3*. HsNip7 fused to the DNA binding domain of *lexA* was used for assays with activation domain fusions of FTSJ3 and SUMO-2 proteins. Yeast strains isolated in the two-hybrid screening are indicated on the left. Assays were performed by using YNB plates containing adenine and 6 or 10 mM 3-AT using cell dilutions from 10^6 to 10^3. *LexA*-HsNip7 and the activation domain alone was used as negative control (C-) in the assays, Nip7p-Nop8p was used as a positive control (C+).

The direct interaction between HsNip7 with FTSJ3 and SUMO-2 was tested using GST-pull down assays with recombinant proteins. For this purpose, GST-FTSJ3 and GST-SUMO2 were co-expressed in *E. coli* with histidine-tagged HsNip7. The extracts were incubated with glutathione-sepharose beads and following extensive washing, the bound fractions were analyzed by immunoblot using antibodies raised against GST and the poly-histidine tag. A parallel negative control was carried out using GST co-expressed with His-HsNip7. As expected, His-HsNip7 was found associated to GST-FTSJ3 and GST-SUMO-2 but not with GST alone (Figure 3). Although the recombinant GST-FTSJ3 and GST-SUMO-2 fusion proteins are highly unstable (Figure 3), this assay was conclusive in showing the direct interaction between the proteins tested.

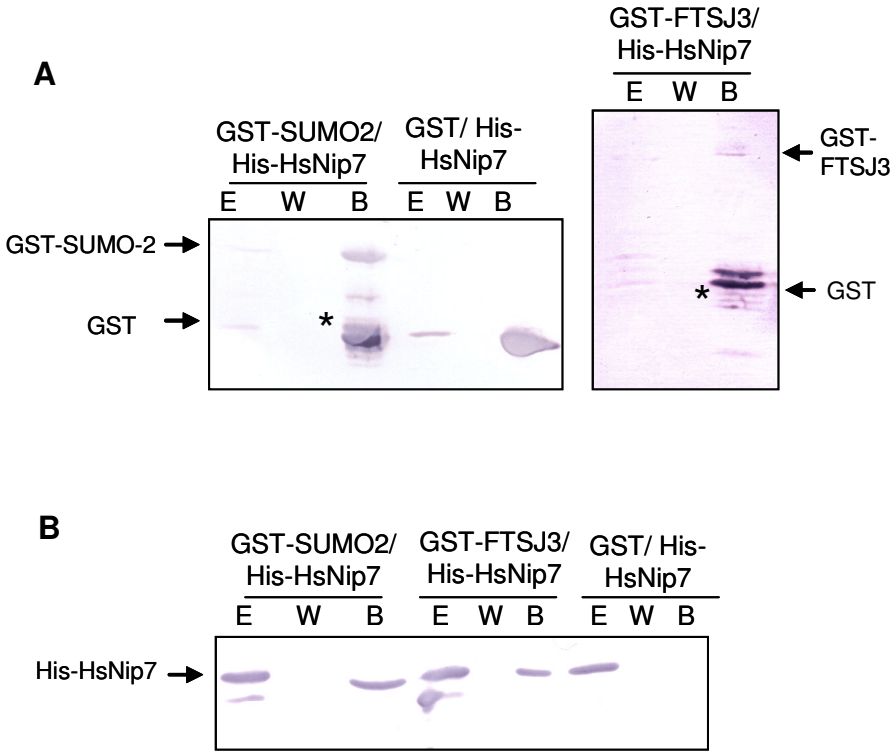

Figure 3. GST-pull down assays using recombinant proteins. GST-tagged proteins were co-expressed with His-HsNip7 in *E. coli* and isolated by binding to glutathione-sepharose beads as described on the Material and Methods section. (**A**) GST-tagged proteins were probed with an antibody for GST. (**B**) Bound His-HsNip7 was probed by using an antibody raised against poly-histidine. The full-length proteins are indicated by arrows. E, whole cell extract, W, last wash, B, bound fraction, (*) indicates the degradation products of GST-tagged proteins.

2. Analysis of FTSJ3 and SUMO-2 subcellular localization

Sekiguchi and co-workers (2004) reported the human Nip7 nucleolar colocalization with Nop132, the orthologue human of yeast Nop8p. For the purpose of determining FTSJ3 and SUMO-2 subcellular localization, a set of mammalian plasmids expressing EGFP- or mRFP-tagged proteins were constructed. A plasmid encoding EGFP-HsNip7 was transiently co-transfected with plasmids expressing either mRFP-FTSJ3 or mRFP-SUMO2 in HEK293 cells. As controls, HEK293 cells were co-transfected with plasmids expressing EGFP and either mRFP-FTSJ3 or mRFP-SUMO2. The plasmid encoding EGFP-HsNip7 was also co-transfected with a plasmid expressing mRFP. The results obtained in this experiment confirmed the nucleolar localization for HsNip7 (Figure 4), as previously reported (Sekiguchi *et al.*, 2004). Moreover, mRFP-FTSJ3 was also observed in the nucleolar region, showing superposition with HsNip7 (Figure 4A). This result suggests both proteins interact *in vivo*, possibly as part of a complex. The mRFP-SUMO2 fusion was observed mainly in the nuclear region (Figure 4B), consistently to previous reports for mammalian SUMO proteins, which are predominately localized to PML nuclear bodies (Su & Li, 2002; Gill, 2004).

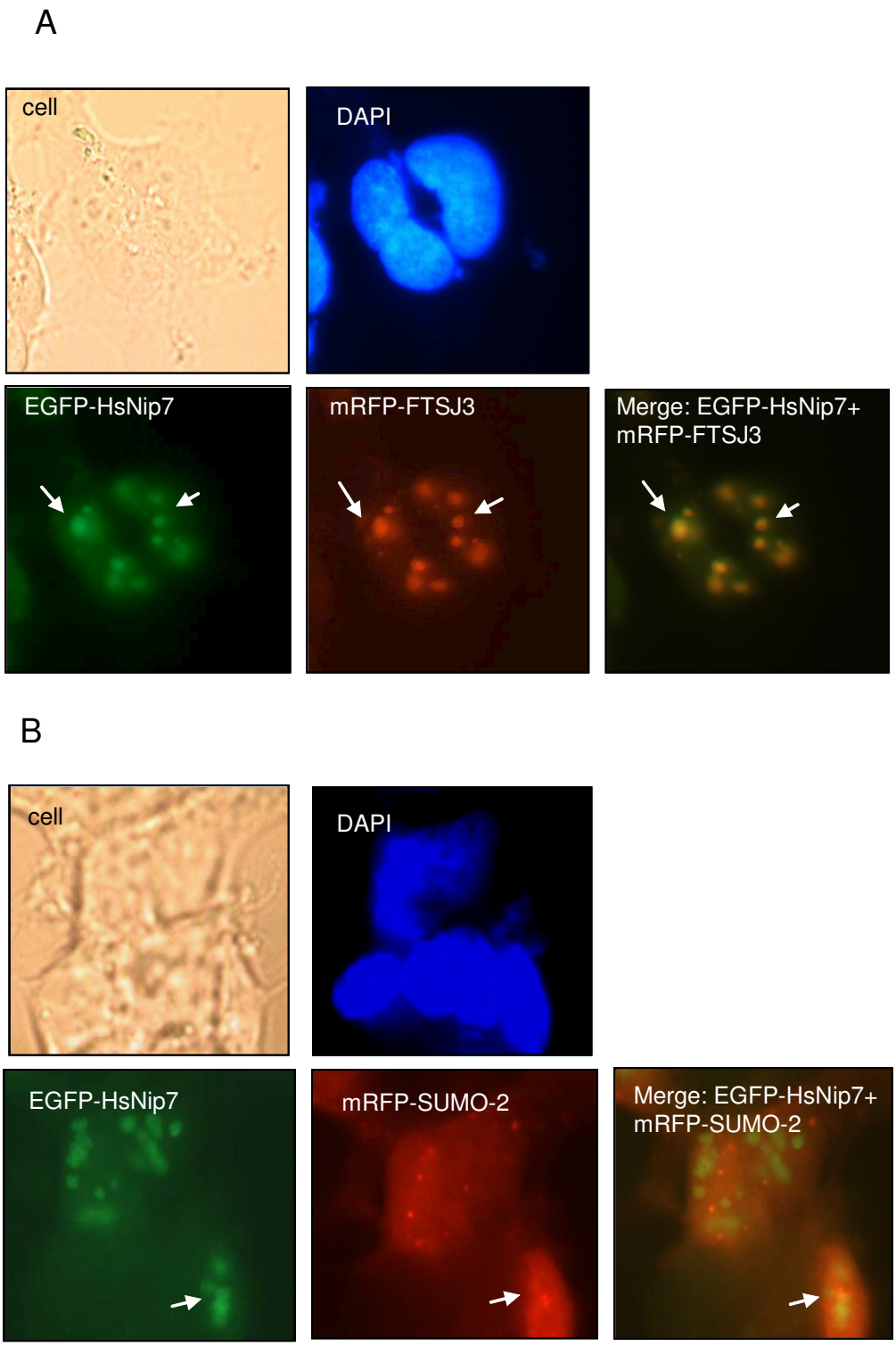

Figure 4. Subcellular localization of EGFP-HsNip7 and mRFP-FTSJ3 or mRFP-SUMO-2 visualized by fluorescence microscopy. HEK293 cells were transiently transfected with constructs encoding the fusion proteins EGFP-HsNip7 and mRFP with either FTSJ3 or SUMO-2 and analyzed 48-72h post transfection. The nuclei were counterstained in blue with DAPI. (**A**) Nucleolar colocalization of EGFP-HsNip7 and mRFP-FTSJ3; the arrows indicate the overlapping nucleolar distribution of both proteins. (**B**) While EGFP-HsNip7 is nucleolar, mRFP-SUMO-2 is localized to the nucleus.

3. Interaction of HsNip7 with RNA *in vitro*

In order to determine whether HsNip7 shows higher affinity to a particular RNA sequence, we performed electrophoretic mobility shift assays under native conditions using recombinant HsNip7 and homo-oligoribonucleotides. As expected, these assays confirmed that HsNip7 binds to polyuridine sequences (Figure 5) similarly to the *S. cerevisiae* and *P. abyssi* Nip7 orthologues (Coltri *et al.*, 2007). The EMSA of HsNip7 also shows a band in the well region that may be due to unspecific binding or protein aggregation.

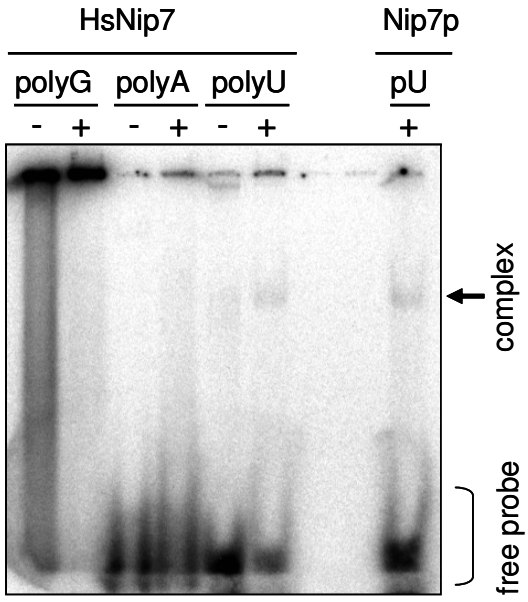

Figure 5. Analysis of the interaction of HsNip7 with oligoribonucleotides. The panel shows protein-RNA complexes resolved by electrophoretic mobility shift assay on native polyacrylamide gel and visualized by autoradiography as described in the Material and Methods section. One pmol of [^{32}P]-labeled poly-$G_{(25)}$, poly-$A_{(20)}$ and poly-$U_{(20)}$ was incubated with 100 pmol of the recombinant HsNip7.pU indicates the positive control in the assay containing [^{32}P]-labeled poly-$U_{(25)}$ and *S. cerevisiae* Nip7p. The arrow indicates the shifted bands corresponding to the complexes formed by HsNip7 and yeast Nip7p with poly-U.

DISCUSSION

Previous studies showed yeast Nip7p is an essential protein involved in 60S ribosome biogenesis. Nip7p depletion leads to accumulation of 27SB precursors, and primer extension assays showed this could be due to failure on ITS2 processing steps (Zanchin *et al.*, 1997). Eukaryotic Nip7 proteins show high structural conservation, indicating they may share similar functional features. In fact, electrophoretic mobility shift assays performed in this work showed HsNip7 binds polyuridine sequences *in vitro*. This preference was also observed in the *S. cerevisiae* and *P. abyssi* Nip7 orthologues, possibly indicating these proteins interact with similar RNAs *in vivo* (Coltri *et al.*, 2007). In order to investigate the interactions of the Nip7 human orthologue with other proteins we performed a yeast two-hybrid screening using a human fetal brain cDNA library (Clontech). Sekiguchi and co-workers (2004) reported HsNip7 interaction and nucleolar co-localization with Nop132, the orthologue of yeast Nop8p. Nop8p is an essential nucleolar protein involved in 27S precursor processing (Zanchin & Goldfarb, 1999). Recently, Hesling and co-workers (2007) showed HsNip7 could be pulled down from HEK293 cell extracts by GST-tagged Shwachman-Bodian-Diamond syndrome associated protein. These results suggest these proteins are in the same complex consistently with a role for HsNip7 in 60S ribosome biogenesis.

The analyses performed in this work identified the interaction of HsNip7 with FTSJ3 and SUMO-2. HsNip7 interacts directly with FTSJ3, whose yeast counterpart Spb1p is involved in 60S biogenesis. Amino acid sequence analysis revealed that FTSJ3 is formed by of two well-defined domains. The N-terminal FtsJ domain is characteristic of large subunit rRNA methyltransferases and was described for the *E. coli* methyltransferase RrmJ

and for *S. cerevisiae* Spb1p. The C-terminal domain has been termed Spb1_C domain, after the yeast Spb1p protein, and has been found in a number of 60S-biogenesis proteins. The presence of this domain is a strong indication that the protein participates on 60S subunit biogenesis (Pintard *et al.*, 2000). *E. coli* RrmJ has been identified as the site-specific methyltransferase for position U_{2552} in 23S rRNA (Bügl *et al.*, 2000; Caldas *et al.*, 2000). There are three yeast proteins with similarity to RrmJ: Trm7p, Mrm2p and Spb1p. While Trm7p and Mrm2p methylate specific residues in tRNA and in the 21S mitochondrial rRNA (Pintard *et al.*, 2002 a,b), Spb1p is required for methylation of the conserved Gm_{2922} in yeast 25S rRNA, an important site for translation activity. Different from regular snoRNA-guided modifications, this specific methylation occurs in 27S and not in 35S rRNA precursors (Lapeyre & Puroshothaman, 2004). Consistently with its late association to pre-60S complexes, yeast Spb1p deficiency affects directly the maturation of 25S and 5.8S rRNAs and leads to accumulation of 27SB pre-rRNAs (Kressler *et al.*, 1999; Pintard *et al.*, 2000), similar to the phenotype observed for *S. cerevisiae* Nip7p depletion (Zanchin *et al.*, 1997). Despite its interaction with C/D box core proteins Nop1p and Nop5/58p, and site-specific methylation activity, global rRNA methylation is not affected under Spb1p depletion (Kressler *et al.*, 1999; Lafontaine & Tollervey, 2000). The interaction of FTSJ3 and HsNip7, along with their nucleolar colocalization in HEK293 cells, strongly suggests their association during 60S biogenesis. Future studies should investigate their participation on rRNA processing steps using HsNip7 and FTSJ3 knock-down cells. Although yeast Nip7 has not shown interaction with C/D box core proteins, it would also be important to verify HsNip7 association to this complex.

The HsNip7 interaction with SUMO-2 is intriguing. Small ubiquitin-like modifiers (SUMO) proteins are structurally related to ubiquitin and responsible for post-translational

modification in a wide range of substrates. Mammalian cells possess four SUMO proteins and only SUMO-1 is best characterized. SUMO-2 and SUMO-3 are very similar and show 95% amino-acid identity and SUMO-4 is mainly found in kidney (Gill, 2004). The post-translational covalent modification performed by SUMO proteins (sumoylation) can regulate protein function, affecting protein-protein interaction, transcription activation and subcellular localization (Gill, 2004; Vertegaal *et al.*, 2006). Sumoylation may also regulate the affinity for RNA-binding, as in the cases of SART1 and hnRNPM, known to have RNA-binding and processing activities, which are extensively modified by SUMO-2 (Vertegaal *et al.*, 2004). Interestingly, the putative sites of sumoylation in hnRNP proteins overlap with the sites for RNA-binding (Li *et al.*, 2004). Zinc-finger proteins known to bind RNA and DNA are also regularly sumoylated, suggesting a role for this modification on transcription regulation (Gill, 2004; Li *et al.*, 2004). Furthermore sumoylation of hnRNP suggests that SUMO proteins might regulate the RNA metabolism, from transcription to translation.

Recently, Panse and co-workers (2006) showed that *S. cerevisiae* pre-ribosomal subunits 40S and 60S as well as several pre-60S transacting factors are sumoylated. Among these factors, there are some proteins belonging to the Nip7p-containing complexes, as for example, Nop7p, Nug1p and Rix7p (Baßler *et al.*, 2001; Gavin *et al.*, 2006). In this case, sumoylation seems to function as a surveillance mechanism, in which correctly processed subunits are modified and subsequently transported to the cytoplasm. Covalent modification by SUMO mainly occurs in sites comprising a hydrophobic residue (h) followed by a lysine hKXXE (Li *et al.*, 2004). In fact, an analysis using the SUMOplot software (Xue *et al.*, 2006) showed several high-score sites for HsNip7 sumoylation. It would be interesting to investigate whether HsNip7 is sumoylated *in vivo* and if this

modification affects 60S ribosome subunit export to cytoplasm, similarly to the observed in *S. cerevisiae* (Panse *et al.*, 2006).

In conclusion, we showed HsNip7 interacts preferentially with polyuridine sequences, similarly to yeast and archaeal counterparts. We also identified two novel interacting partners for HsNip7. GST-pull down assays and subcellular localization experiments strongly suggest HsNip7 and FTSJ3 are interacting during rRNA processing in the nucleolar region. Interaction with SUMO-2 suggests 60S biogenesis factors are involved in a control mechanism of correctly processed subunit export in humans.

ACKNOWLEDGEMENTS

The authors are grateful to Thiago V. Seraphim for assistance, Zildene G. Correa for DNA sequencing and Dr. Jörg Kobarg for providing GST anti-serum. This work was supported by FAPESP grants (CEPID/CBME 98/14138-2, SMolBNet 00/10266-8 and 06/02083-7). PPC is recipient of FAPESP PhD fellowships (03/06299-6).

REFERENCES

Austin, K. M., Leary, R. J. and Shimamura, A. (2005) The Shwachman–Diamond SBDS protein localizes to the nucleolus. *Blood*, 106, 1253–1258.

Ausubel, F.M., Brent, R., Kingston, R., Moore, D. D., Seidman, J. G., Smith, J. A., and Struha, K. (1998) Current Protocols in Molecular Biology. John Wiley and Sons, New York, NY.

Baßler, J., Grandi, P., Gadal, O., Leßmann, T., Petfalski, E., Tollervey, D., Lechner, J. and Hurt, E. (2001) Identification of a 60S preribosomal particle that is closely linked to nuclear export. *Mol. Cell*, 8, 517-529.

Boocock, G. R., Morrison, J. A., Popovic, M., Richards, N., Ellis, L., Durie, P. R. and Rommens, J. M. (2003) Mutations in SBDS are associated with Shwachman–Diamond syndrome. *Nat. Genet.*, 33, 97–101.

Bügl, H., Fauman, E.B., Staker, B.L., Zheng, F., Kushner, S.R., Saper, M.A., Bardwell, J.C. and Jakob, U. (2000) RNA methylation under heat shock control. *Mol. Cell*, 6, 349-360.

Caldas, T., Binet, E., Bouloc, P. and Richarme, G. (2000) Translational defects of *Escherichia coli* mutants deficient in the Um(2552) 23S ribosomal RNA methyltransferase RrmJ/FtsJ. *Biochem. Biophys. Res. Commun.*, 271, 714-718.

Coltri, P.P., Guimarães, B.G., Granato, D.C., Luz, J., Teixeira, E., Oliveira, C.C. and Zanchin, N.I.T. Structural insights into the interaction of the Nip7 PUA domain with polyuridine RNA. *Biochemistry*, 46, 14177-14187.

Draptchinskaia, N., Gustavsson, P., Andersson, B., Pettersson, M., Willig, T. N., Dianzani, I., Ball, S., Tchernia, G., Klar, J., Matsson, H., Tentler, D., Mohandas, N., Carlsson, B. and Dahl, N. (1999) The gene encoding ribosomal protein S19 is mutated in Diamond–Blackfan anaemia. *Nat. Genet.*, 21, 169–175.

Fromont-Racine, M., Senger, B., Saveanu, C. and Fasiolo, F. (2003) Ribosome assembly in eukaryotes. *Gene*, 313, 17-42.

Ganapathi, K. A., Austin, K. M., Lee, C. S., Dias, A., Malsch, M. M., Reed, R. and Shimamura, A. (2007) The human Shwachman-Diamond syndrome protein, SBDS, associates with ribosomal RNA. *Blood*, 110, 1458-1465.

Gavin, A.C., Aloy, P., Grandi, P., Krause, R., Boesche, M., Marzioch, M., Rau, C., Jensen, L.J., Bastuck, S., Dümpelfeld, B., Edelmann, A., Heurtier, M.A., Hoffman, V., Hoefert, C., Klein, K., Hudak, M., Michon, A.M., Schelder, M., Schirle, M., Remor, M., Rudi, T., Hooper, S., Bauer, A., Bouwmeester, T., Casari, G., Drewes, G., Neubauer, G., Rick, J.M., Kuster, B., Bork, P., Russell, R.B. and Superti-Furga, G. (2006) Proteome survey reveals modularity of the yeast cell machinery. *Nature*, 440, 631-636.

Gill, G. (2004) SUMO and ubiquitin in the nucleus: different functions, similar mechanisms? *Genes & Dev.*, 18, 2046-2059.

Gonzales, B., Henning, D., So, R. B., Dixon, J., Dixon, M. J. and Valdez, B. C. (2005) The Treacher Collins syndrome (TCOF1) gene product is involved in pre-rRNA methylation. *Hum. Mol. Genet.*, 14, 2035–2043.

Granato, D.C., Gonzales, F.A., Luz, J.S., Cassiola, F., Machado-Santelli, G.M. and Oliveira, C.C. (2005) Nop53p, an essential nucleolar protein that interacts with Nop17p and Nip7p, is required for pre-rRNA processing in *Saccharomyces cerevisiae*. *FEBS J*., 272, 4450-4463.

Grandi, P., Rybin, V., Bassler, J., Petfalski, E., Strauss, D., Marzioch, M. *et al.* (2002) 90S pre-ribosomes include the 35S pre-rRNA, the U3 snoRNP, and 40S subunit processing factors but predominantly lack 60S synthesis factors. *Mol. Cell*, 10, 105-115.

Heiss, N. S., Knight, S. W., Vulliamy, T. J., Klauck, S. M., Wiemann, S., Mason, P. J., Poustka, A. and Dokal, I. (1998) X-linked dyskeratosis congenital is caused by mutations in a highly conserved gene with putative nucleolar functions. *Nat. Genet.*, 19, 32–38.

Hesling, C., Oliveira, C. C., Castilho, B. A., and Zanchin, N. I. T. (2007) The Shwachman-Bodian-Diamond syndrome associated protein interacts with HsNip7 and its down-regulation affects gene expression at the transcriptional and translational levels. *Exp. Cell Res*., 313, 4180-4195.

Hollenberg, S. M., Sternglanz, R., Cheng, P. F. and Weintraub, H. (1995) Identification of a new family of tissue-specific basic helix-loop-helix proteins with a two-hybrid system. *Mol. Cell. Biol.*, 15, 3813-3822.

Kressler, D., Rojo, M., Linder, P. and Cruz, J. (1999) Spb1p is a putative methyltransferase required for 60S ribosomal subunit biogenesis in *Saccharomyces cerevisiae*. *Nucleic Acids Res.*, 27:4598- 4608.

Lafontaine, D.L., Bousquet-Antonelli, C., Henry, Y., Caizergues-Ferrer, M. and Tollervey, D. (1998) The box H+ACA snoRNAs carry Cbf5p, the putative rRNA pseudouridine synthase. *Genes Dev*.,15, 527-537.

Lafontaine, D. L. and Tollervey, D. (2000) Synthesis and assembly of the box C+D small nucleolar RNPs. *Mol. Cell. Biol.*, 20, 2650-2659.

Lapeyre, B. and Purushothaman, S.K. (2004) Spb1p-directed formation of Gm2922 in the ribosome catalytic center occurs at a late processing stage. *Mol. Cell*, 16, 663-669.

Li, T., Evdokimov, E., Shen, R.F., Chao, C.C., Tekle, E., Wang, T., Stadtman, E.R., Yang, D.C. and Chock, P.B. (2004) Sumoylation of heterogeneous nuclear ribonucleoproteins,

zinc finger proteins, and nuclear pore complex proteins: a proteomic analysis. *Proc. Natl. Acad. Sci. U.S.A*, 101, 8551-8556.

Liu, J.M. and Ellis, S.R. (2006) Ribosomes and marrow failure: coincidental association or molecular paradigm? *Blood*, 107, 4583-4588.

Luz, J. S., Georg, R. C. and Oliveira, C. C. (2007) Sdo1p, the yeast ortholog of Shwachman-Bodian-Diamond syndrome protein binds RNA and interacts with nuclear rRNA processing factors. *Submetido para publicação.*

Menne, T.F., Goyenechea, B., Sánchez-Puig, N., Wong, C.C., Tonkin, L.M., Ancliff, P.J., Brost, R.L., Costanzo, M., Boone, C. and Warren, A.J. (2007) The Shwachman-Bodian-Diamond syndrome protein mediates translational activation of ribosomes in yeast. *Nat. Genet*., 39, 486-495.

Mitchell, J. R., Wood, E. and Collins, K. (1999) A telomerase component is defective in the human disease dyskeratosis congenital. *Nature*, 402, 551–555.

Panse, V.G., Kressler, D., Pauli, A., Petfalski, E., Gnadig, M., Tollervey, D. and Hurt, E. (2006) Formation and nuclear export of preribosomes are functionally linked to the small-ubiquitin-related modifier pathway. *Traffic*, 7, 1311-1321.

Peng, W. T., Robinson, M. D., Mnaimneh, S., Krogan, N. J., Cagney, G., Morris, Q. *et al.* (2003) A panoramic view of yeast noncoding RNA processing. *Cell*, 113, 919-933.

Pintard, L., Lecointe, F., Bujnicki, J.M., Bonnerot, C., Grosjean, H. and Lapeyre, B. (2002a) Trm7p catalyses the formation of two 2'-O-methylriboses in yeast tRNA anticodon loop. *EMBO J.*, 21, 1811-1820.

Pintard, L., Bujnicki, J.M., Lapeyre, B. and Bonnerot, C. (2002b) MRM2 encodes a novel yeast mitochondrial 21S rRNA methyltransferase. *EMBO J.*, 21, 1139-1147.

Pintard, L., Kressler, D. and Lapeyre, B. (2000) Spb1p is a yeast nucleolar protein associated with Nop1p and Nop58p that is able to bind S-adenosyl-L-methionine *in vitro*. *Mol. Cell. Biol.*, 20, 1370-1381.

Ridanpaa, M., van Eenennaam, H., Pelin, K., Chadwick, R., Johnson, C., Yuan, B., vanVenrooij, W., Pruijn, G., Salmela, R., Rockas, S., Makitie, O., Kaitila, I. and de la Chapelle, A. (2001) Mutations in the RNA component of RNase MRP cause a pleiotropic human disease, cartilage-hair hypoplasia. *Cell*, 104, 195–203.

Ruggero, D., Grisendi, S., Piazza, F., Rego, E., Mari, F., Rao, P. H., Cordon-Cardo, C. and Pandolfi, P. P. (2003) Dyskeratosis congenita and cancer in mice deficient in ribosomal RNA modification. *Science*, 299, 259–262.

Sambrook, J., Fritsch, E. J., and Maniatis, T. (1989) Molecular cloning, a laboratory manual 2nd ed., Cold Spring Harbor Laboratory Press, Cold Spring Harbor, NY.

Sekiguchi, T., Todaka, Y., Wang, Y., Hirose, E., Nakashima, N., and Nishimoto, T. (2004) A novel human nucleolar protein, Nop132, binds to the G proteins, RRAG A/C/D, *J. Biol. Chem*., 279, 8343-8350.

Su, H. L. and Li, S.S. (2002) Molecular features of human ubiquitin-like SUMO genes and their encoded proteins. *Gene*, 296, 65-73.

Thiel, C. T., Horn, D., Zabel, B., Ekici, A. B., Salinas, K., Gebhart, E., Ruschendorf, F., Sticht, H., Spranger, J., Muller, D., Zweier, C., Schmitt, M. E., Reis, A. and Rauch, A. (2005) Severely incapacitating mutations in patients with extreme short stature identify RNA-processing endoribonuclease RMRP as an essential cell growth regulator. *Am. J. Hum. Genet*., 77, 795–806.

Valdez, B. C., Henning, D., So, R. B., Dixon, J. and Dixon, M. J. (2004) The Treacher Collins syndrome (TCOF1) gene product is involved in ribosomal DNA gene transcription by interacting with upstream binding factor. *Proc. Natl. Acad. Sci. U. S. A.*, 101, 10709–10714.

Vertegaal, A.C., Andersen, J.S., Ogg, S.C., Hay, R.T., Mann, M. and Lamond, A.I. (2006) Distinct and overlapping sets of SUMO-1 and SUMO-2 target proteins revealed by quantitative proteomics. *Mol Cell. Proteomics*, 5, 2298-2310.

Vertegaal, A.C., Ogg, S.C., Jaffray, E., Rodriguez, M.S., Hay, R.T., Andersen, J.S., Mann, M. and Lamond, A.I. (2004) A proteomic study of SUMO-2 target proteins, *J. Biol. Chem*., 279, 33791-33798.

Vulliamy, T. J., Knight, S. W., Mason, P. J. and Dokal, I. (2001) Very short telomeres in the peripheral blood of patients with X-linked and autosomal dyskeratosis congenital. *Blood Cells Mol. Diseases*, 27, 353–357.

Xue, Y., Zhou, F., Fu, C., Xu, Y. and Yao, X. (2006) SUMOsp: a web server for sumoylation site prediction. *Nucleic Acids Res*., 34, W254-257.

Yoon, A., Peng, G., Brandenburg, Y., Zollo, O., Xu, W., Rego, E. and Ruggero, D. (2006) Impaired Control of IRES-Mediated Translation in X-Linked Dyskeratosis Congenita. *Science*, 312, 902-906.

Zanchin, N.I.T., and Goldfarb, D. S. (1999) Nip7p interacts with Nop8p, an essential nucleolar protein required for 60S ribosome biogenesis, and the exosome subunit Rrp43p, *Mol. Cell. Biol. 19*, 1518-1525.

Zanchin, N. I. T., Roberts, P., DeSilva, A., Sherman, F., and Goldfarb, D. S. (1997) *Saccharomyces cerevisiae* Nip7p is required for efficient 60S ribosome subunit biogenesis, *Mol. Cell. Biol. 17*, 5001-5015.

4. DISCUSSÃO

4.1. Interação de Nip7p com RNA

A hipótese inicial de trabalho considerava que Nip7p interagiria com alguma sequência do pré-rRNA. No entanto, os primeiros ensaios de EMSA utilizando sequências do pré-rRNA transcritas *in vitro* não foram conclusivos. Não foi possível visualizar a formação dos complexos já que grande parte da proteína ficava retida no "poço" de aplicação da amostra. Isto se deve provavelmente ao alto ponto isoelétrico de Nip7p, em torno de 9,28. Ao utilizar tampão TBE pH 8,0 (Sambrook *et al.*, 1989) no ensaio de ligação, Nip7p teria carga positiva, dificultando sua migração na eletroforese. Assim, os ensaios de interação com sequências do pré-rRNA foram realizados utilizando *UV-crosslinking* seguido de tratamento com RNase, utilizando tampão CAPS pH 11 na eletroforese. Para verificar se Nip7p apresentava maior afinidade na ligação a alguma sequência do pré-rRNA, foram realizados ensaios de competição utilizando as sequências do rRNA 5,8S (180 nucleotídeos), dos espaçadores ITS2 e 5'ETS (220 e 550 nucleotídeos, respectivamente) e de um RNA derivado do plasmídio pBlueScript (pBS; 65 nucleotídeos) transcritas *in vitro*. 20 pmol da proteína foram incubados com 1 pmol dos RNAs marcados radioativamente [^{32}P]-5,8S ou [^{32}P]-ITS2. Às reações foram adicionadas quantidades crescentes (de 5 a 20 pmol) dos RNAs 5,8S, ITS2, 5'ETS e pBS não marcados. Nestes ensaios, o competidor ITS2 apresentou eficiência levemente superior aos competidores 5'ETS e 5,8S para ligar Nip7p. De fato, a quantificação dos resultados mostrou que a intensidade relativa das bandas, comparadas às amostras sem competidor, diminuiu na presença de quantidades crescentes do RNA ITS2.

Os resultados obtidos nos ensaios de interação com o pré-RNA são coerentes com a hipótese de que a ausência de Nip7p afeta o processamento da região ITS2, levando ao acúmulo de precursor 27S (Zanchin *et al.*, 1997). Embora seja preciso considerar que a afinidade pelas sequências do pré-rRNA possa ser baixa, já que a análise foi realizada com *UV-crosslinking*, os resultados indicam uma maior preferência de Nip7p pela sequência do espaçador ITS2. Além disso, Nip7p interage com as proteínas nucleolares Nop8p e

Nop53p, que possuem domínios de interação com RNA e podem se ligar ao pré-rRNA, o que poderia estabilizar a ligação de Nip7p ao ITS2 *in vivo* (Granato *et al.*, 2005).

As análises funcionais aliadas à presença do domínio PUA indicavam interação direta de Nip7p com RNA. Para investigar essa possível interação, foram realizados ensaios utilizando proteínas recombinantes e sequências de homopolímeros de RNA (poli-$A_{(25)}$, poli-$U_{(25)}$, poli-$C_{(25)}$ e poli-$G_{(18)}$) marcados radioativamente. Os resultados revelaram a marcante preferência de Nip7p pela ligação ao poli-$U_{(25)}$. É interessante que PaNip7 e HsNip7 também apresentaram essa preferência, indicando que estas proteínas podem interagir com RNAs similares na célula. A interação específica com poli-uridina pode indicar a interação de Nip7p com snRNAs ou snoRNAs, pequenos RNAs com alta concentração de uridinas em suas seqüências. Os snRNAs participam das reações de processamento e edição do mRNA, enquanto que os snoRNAs atuam principalmente na síntese de ribossomos e modificação do rRNA (Venema & Tollervey, 1999; Dragon *et al.*, 2002; Valadkhan, 2005). A mesma preferência por poli-uridina foi identificada na proteína Rrp5p, que possui repetições do domínio S1 de ligação ao RNA na região N-terminal. Ensaios de interação *in vitro* e de deleção de sequências do pré-rRNA demonstraram a ligação de Rrp5p ao espaçador ITS1, que apresenta alta concentração de uridinas na sua sequência. A partir da interação com o ITS1, Rrp5p seria capaz de promover o correto processamento do precursor $27SA_2$ (Venema & Tollervey, 1996; de Boer *et al.*, 2006). De forma similar, a preferência de Nip7p por poli-uridina pode explicar a maior afinidade pelo espaçador ITS2, que possui regiões com alta concentração de uridinas em sua sequência.

4.2. Mecanismo de interação da Nip7 com RNA

O domínio PUA foi relacionado à interação e modificação do RNA em diferentes proteínas (Aravind & Koonin, 1999; Pérez-Arelano *et al.*, 2007). PUA é um domínio encontrado em cerca de 600 proteínas de diferentes famílias, incluindo pseudo-uridina sintases da família TruB, transglicosilases, uma metil-transferase de *E. coli* (YebU), a glutamato 5-kinase de *E. coli* (G5K) e o oncogene MCT-1 (Aravind & Koonin, 1999; Ishitani *et al.*, 2002; Hallberg *et al.*, 2006; Reinert *et al.*, 2006; Marco-Marín *et al.*, 2007). A pseudo-uridina sintase Cbf5p possui o domínio PUA (Charpentier *et al.*, 2005), e dados

de reconstituição do complexo *H/ACA box* de Archaea sugerem que o PUA tem importância na ligação ao RNA (Manival *et al.*, 2006; Rashid *et al.*, 2006). Embora não apresente alta similaridade na sequência primária, a estrutura tri-dimensional do domínio é bastante conservada (Pérez-Arelano *et al.*, 2007).

O mecanismo de interação do domínio PUA com RNA é baseado na análise de estruturas cristalográficas das proteínas Cbf5p, TruB e ArcTGT em complexo com RNA (Pan *et al.*, 2003; Ishitani *et al.*, 2003; Li & Ye, 2006). Estas estruturas indicam que a interação com RNA ocorre através de um *loop* de glicina, que conecta a primeira α-hélice e segunda folha-β do domínio, sendo mediada por resíduos da folha-β6, adjacentes na estrutura tri-dimensional. Nas diferentes proteínas, a interação ocorre por diferentes contatos entre o domínio PUA e o RNA, já que os resíduos envolvidos não são conservados (Pérez-Arelano *et al.*, 2007). No caso das pseudo-uridina sintases Cbf5 de *P. furisosus* e TruB de *E. coli*, a interação ocorre através da formação de pontes de hidrogênio entre os resíduos da α-hélice 1 e folha-β2 e as bases do RNA (Pan *et al.*, 2003; Li & Ye, 2006). A estrutura do complexo da proteína archaeosina transglicosilase de *P. horikoshii* (ArcTGT) com tRNA revelou que a interação é eletrostática, e ocorre por meio da afinidade dos grupos fosfato do RNA por resíduos de lisina e arginina localizados na folha-β6. A sobreposição desta estrutura com a do domínio PUA de PaNip7 mostrou que os resíduos da folha-β6 são conservados (R151, R152, K155 e K158) e formam uma superfície básica nesta região, capaz de mediar a interação da proteína com RNA. Este alinhamento com a estrutura de ArcTGT indica, ainda, que a interação de PaNip7 com RNA envolve principalmente a α-hélice 1 e a folha-β6 do domínio PUA (equivalentes a α-hélice 5 e a folha-β12 na estrutura completa de PaNip7; Fig. 2, Cap. 2). A comparação estrutural com HsNip7 e o modelo gerado por homologia para Nip7p mostrou que as proteínas eucarióticas não possuem esses resíduos conservados. Esta região é ocupada por uma glicina e três resíduos com cadeia lateral hidrofóbica. De fato, a distribuição de cargas do domínio PUA da Nip7p de eucariotos é bastante diferente daquela encontrada na PaNip7. O domínio PUA da proteína PaNip7 possui uma superfície mais carregada ao passo que, nas proteínas eucarióticas, observa-se uma superfície hidrofóbica (Fig. 3 e Tab. 3, Cap. 2). Estas análises indicam que, possivelmente, a interação com RNA na PaNip7 e na Nip7 de eucariotos é mediada por resíduos diferentes.

Conforme análise das estruturas de complexos com proteínas que possuem o domínio PUA, o contato com o RNA ocorre através da região da α-hélice 1 e folha-β2 e de resíduos da folha-β6 (Pérez-Arelano *et al.*, 2007). Para verificar a hipótese do envolvimento de resíduos desta região de PaNip7 e de Nip7p no contato com RNA, foram realizados ensaios utilizando proteínas com mutações sítio-dirigidas. Foram utilizados dois duplo-mutantes de PaNip7 (PaNip7$^{R151A/R152A}$ e PaNip7$^{K155A/K158A}$), além de um duplo-mutante de Nip7p (Nip7$^{I161A/F164A}$). Estas proteínas foram testadas para interação direta com RNA poli-$U_{(25)}$. Com relação a PaNip7, os resíduos de lisina e arginina interferem diretamente na ligação ao RNA, já que ambas as proteínas mutantes perdem a capacidade de ligar ao RNA poli-$U_{(25)}$. No caso da proteína Nip7p, os resultados dos ensaios indicam que a mutação diminui muito a afinidade ao RNA poli-$U_{(25)}$, embora esta não seja completamente perdida. A quantificação dos resultados mostrou que a interação de Nip7$^{I161A/F164A}$ com RNA diminui cerca de 60% em comparação com a interação realizada pela proteína selvagem. Estes resultados confirmaram o envolvimento dos resíduos da folha-β6 R151, R152, K155 e K158 na PaNip7, e I161 e F164 nas proteínas de eucariotos, na ligação ao RNA.

4.3. Nip7p faz parte de um grande complexo de proteínas

A maior parte dos processos celulares depende da interação entre proteínas. O método do duplo-híbrido de leveduras (Fields & Song, 1989) é bastante utilizado para analisar interações em larga-escala e também para testar interações específicas. Com relação ao estudo de proteínas de *S. cerevisiae*, este método não permite distinguir a interação entre proteínas que formam complexos ou proteínas que interagem diretamente entre si, porém os resultados são bastante relevantes. A confirmação das interações pode ser realizada por ensaios *in vitro*, utilizando proteínas recombinantes isoladamente, por imunoprecipitação ou co-purificação (Uetz *et al.*, 2000; Ito *et al.*, 2001; Steltz *et al.*, 2005; Rual *et al.*, 2005; Krogan *et al.*, 2006).

Neste trabalho foi realizada uma extensa análise das interações da proteína Nip7p de *S. cerevisiae*. Os experimentos de *pull down* a partir de células de *S. cerevisiae* revelaram que Nip7p interage com as quatro proteínas do complexo *H/ACA box*, envolvido na pseudo-uridinilação do rRNA. Além disso, estes ensaios demonstraram a interação de Nip7p com a

proteína Rrp15p. Esta proteína nucleolar de 28 kDa co-precipita os pré-rRNAs 27S, 7S e 5S (De Marchis *et al.*, 2005). Os efeitos observados na sua ausência aliados às suas interações sugerem o envolvimento de Rrp15p na síntese da subunidade ribossomal 60S. Na ausência de Rrp15p ocorre clivagem prematura no sítio C_2 (localizado no ITS2), levando a degradação do pré-rRNA $27SA_2$. Estes defeitos levam a uma drástica redução na formação dos rRNAs maduros 25S e 5,8S, causando diminuição na quantidade de subunidades 60S (De Marchis *et al.*, 2005), similar ao que ocorre na ausência de Nip7p (Zanchin *et al.*, 1997). Estas evidências indicam que ambas as proteínas podem atuar no mesmo complexo na formação da subunidade 60S.

A confirmação da interação direta de Nip7p com as proteínas nucleolares Nop8p e Nop53p foi realizada a partir de ensaios *in vitro* utilizando proteínas recombinantes. A ausência de Nop8p provoca defeitos semelhantes aos encontrados em cepas deficientes em Nip7p, ocorrendo redução no nível de subunidades 60S. O estudo realizado com mutantes condicionais mostrou que enquanto a ausência de Nip7p leva ao processamento retardado do precursor 27SB, a deficiência em Nop8p leva a rápida degradação deste precursor (Zanchin & Goldfarb, 1999a). A Nop53p co-precipita os precursores 27S e 7S e interfere diretamente no seu processamento (Granato *et al.*, 2005; Sydorsky *et al.*, 2005; Thomsom & Tollervey, 2005). Ensaios *in vitro* demonstraram sua ligação ao rRNA 5,8S (Granato *et al.*, 2005). Análises de *primer extension* revelaram que, na ausência de Nop53p, as clivagens nos sítios C_1 e C_2 são muito afetadas, reduzindo a síntese dos rRNAs 25S e 5,8S e levando a diminuição nas subunidades 60S, similar ao observado na ausência de Nip7p (Granato *et al.*, 2005).

Além disso, Nip7p interage com a proteína Rrp43p, uma componente do exossomo (Zanchin & Goldfarb, 1999b). O exossomo atua diretamente no processamento da extremidade 3' do precursor 7S, gerando o rRNA 5,8S maduro (Mitchell *et al.*, 1997; Oliveira *et al.*, 2002). Ensaios *in vitro* com as proteínas ortólogas de Archaea revelaram que esta interação é conservada e pode representar uma relação direta de Nip7p com o exossomo ao longo da evolução. Em Archaea, a PaNip7 inibe a atividade do exossomo, bloqueando a ligação e a degradação do RNA pelo complexo. Em parte, esta atividade está relacionada à interação com PaRrp42, ortóloga de Rrp43p em *P. abyssi* (J.S. Luz e C.C. Oliveira, comunicação pessoal). Em *S. cerevisiae* isso poderia ocorrer a partir da interação

de Nip7p com o exossomo através de Rrp43p. Ao interagir com o pré-RNA, Nip7p impediria a atividade contínua do exossomo na região 3' do pré-7S, promovendo a maturação correta do rRNA 5,8S (Oliveira *et al.*, 2002).

Em conjunto, os resultados deste trabalho confirmaram a participação de Nip7p em um grande complexo na formação da subunidade ribossomal 60S (Tabela 4.1 e Figura 4.1). É intrigante o fato de Nip7p interagir com várias proteínas, conforme observado nos ensaios de duplo-híbrido e co-purificação. No entanto, parte das interações pode ocorrer maneira indireta em *S. cerevisiae*, provavelmente no complexo de proteínas responsáveis pela maturação da subunidade ribossomal 60S (Baβler *et al.*, 2001; Grandi *et al.*, 2002; Horsey *et al.*, 2004). É muito provável que o núcleo principal de interação de Nip7p seja com as proteínas Nop8p e Nop53p, que também atuam no processamento do precursor 27S (Zanchin & Goldfarb, 1999a; Granato *et al.*, 2005). Considerando que Nip7p e Nop53p podem interagir com os precursores, é possível, ainda, que as interações sejam mediadas pelo rRNA *in vivo*.

Tabela 4.1. Proteínas que interagem com Nip7p em *S. cerevisiae*.

Proteína	Função	Referência
Nop8p	Atua no processamento do precursor 27S, possui domínio RRM de interação com RNA.	Zanchin & Goldfarb, 1999a
Nop53p	Atua no processamento do precursor 27S e mutantes condicionais apresentam acúmulo do precursor 7S. Interage com RNA 5,8S *in vitro*.	Granato *et al.*, 2005; Sydorsky *et al.*, 2005; Thomson & Tollervey, 2005
Nop10p	Componente do complexo snoRNP *H/ACA box*, interage diretamente com Cbf5p.	Henras *et al.*, 2001; Manival *et al.*, 2006
Nhp2p	Componente do complexo snoRNP *H/ACA box*. Possui domínio que pode mediar a interação com snoRNAs.	Henras *et al.*, 2001
Cbf5p	Pseudo-uridina sintase do complexo snoRNP *H/ACA box*. Atua também na síntese de subunidades 60S.	Lafontaine *et al.*, 1998; Henras *et al.*, 2004
Gar1p	Parte do complexo snoRNP *H/ACA box*, possui domínio que pode mediar interação com o pré-rRNA. Atua também nas clivagens em A_1 e A_2.	Henras *et al.*, 1998; Torchet *et al.*, 2005
Rrp43p	Componente do exossomo. Interage com Rrp46 no anel PH. A ausência desta proteína prejudica as clivagens iniciais em A_0, A_1 e A_2.	Zanchin & Goldfarb, 1999b; Oliveira *et al.*, 2002
Rrp15p	Atua no processamento do precursor 27S, interferindo diretamente na síntese de rRNAs 25S e 5,8S. Mutantes condicionais apresentam clivagens prematuras no sítio C_2. Co-purifica com Rrp1p em análises de complexos.	Horsey *et al.*, 2004; De Marchis *et al.*, 2005
Sdo1p	Atua na reciclagem do fator nucleolar Tif6p, envolvido com a exportação da subunidade 60S ao citoplasma e com a iniciação da tradução. Células deficientes em Sdo1p acumulam precursores 35S e 27S.	Menne *et al.*, 2007; Luz *et al.*, 2007

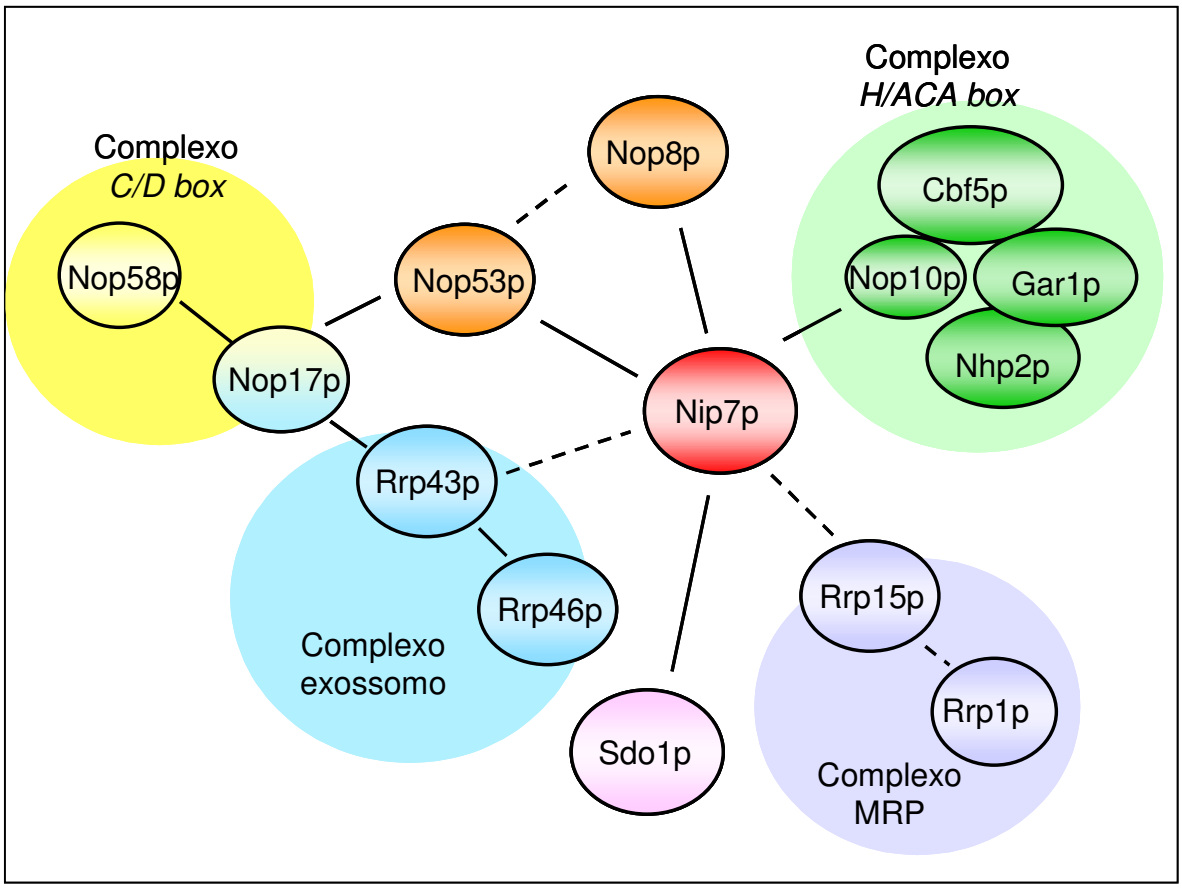

Figura 4.1. Esquema das interações da proteína Nip7p em *S. cerevisiae*. Os dados obtidos neste trabalho mostraram a interação direta de Nip7p com as proteínas Nop8p, Nop53p e Nop10p. Em conjunto com os dados da literatura, estes resultados indicam a interação de Nip7p com diferentes complexos (ver Tabela 4.1). As linhas inteiras indicam interações diretas confirmadas, e as linhas tracejadas representam interações indiretas ou obtidas em experimentos de duplo-híbrido em *S. cerevisiae*.

4.4. Análise do processamento de rRNA em células deficientes em Nip7p

Os resultados dos ensaios de duplo-híbrido confirmados por experimentos de *pull down* mostraram que a Nip7p interage com proteínas do complexo *H/ACA box*. Mais especificamente, essas interações são mediadas pelo domínio PUA da Nip7p. Tendo em vista que este domínio está presente em outras proteínas que atuam na modificação do rRNA, como a Cbf5p (Charpentier *et al.*, 2005, Hamma *et al.*, 2005), foram realizados experimentos de *primer extension* para verificar se Nip7p está envolvida na pseudo-uridinilação do rRNA em *S. cerevisiae*. Os resultados mostraram que, apesar da interação

com os componentes do complexo, a ausência de Nip7p não interfere diretamente na pseudo-uridinilação. Os pequenos defeitos observados nos sítios de pseudo-uridinilação podem ser secundários, já que a falta de Nip7p compromete todo processamento do rRNA. De forma alternativa, Nip7p pode interagir com os componentes do complexo *H/ACA box* durante o processamento do rRNA. É importante lembrar que alguns efeitos secundários são observados na ausência de Nip7p, como a falha nas clivagens iniciais do precursor 35S, etapas em que a proteína Gar1p atua (Zanchin *et al.*, 1997; Henras *et al.*, 1998). Assim como a Nip7p, a pseudo-uridina sintase Cbf5p e sua ortóloga em mamíferos, dyskerina, também atuam no processamento de precursores da subunidade 60S (Zanchin *et al.*, 1997; Cadwell *et al.*, 1997; Mochizuki *et al.*, 2004).

Considerando que o principal defeito observado na ausência de Nip7p é a falha no processamento do precursor 27S, foram realizadas análises de *primer extension* com o objetivo de verificar a clivagem dos precursores de rRNA. De forma geral, as reações de clivagem do rRNA são comprometidas na ausência de Nip7p. As análises para verificar a extremidade 5' do rRNA 18S revelaram, nas cepas condicionais, a presença de bandas extras de tamanho menor do que o esperado, indicando que o rRNA está sendo degradado (Fig. 4A, Cap. 3). Os defeitos mais drásticos foram observados nas reações com oligos da região do espaçador ITS2. A extensão com o oligo P4 revelou uma banda principal correspondente ao sítio C_2, e várias outras bandas de peso molecular maior, a cerca de 100 nucleotídeos de distância do sítio C_2 (Fig. 4C, Cap. 3). Estes resultados indicam que a clivagem neste sítio não ocorre corretamente, o que pode explicar o acúmulo dos precursores 27SB observado em cepas deficientes de Nip7p (Zanchin *et al.*, 1997). É possível que isso aconteça através de alguma proteína com a qual Nip7p interage, já que endonuclease responsável pela clivagem do sítio C_2, na região espaçadora ITS2, ainda é desconhecida.

Defeitos semelhantes no processamento do ITS2 foram observados em cepas condicionais das proteínas Rea1p e Rlp7p (Gadal *et al.*, 2002; Galani *et al.*, 2004). Fatores associados que atuam nas etapas finais da maturação da subunidade 60S, como Nmd3p, Gsp1p, Rrp12p e as GTPases Nog1p e Nug2p, também interferem nesse processamento (Baβler *et al.*, 2001; Grandi *et al.*, 2002; Horsey *et al.*, 2004). Krogan e colaboradores (2004) identificaram um grupo de três proteínas envolvidas no processamento da região

ITS2, denominado complexo IPI. O estudo com a cepa condicional de uma destas proteínas, codificada pela ORF Yhr085w, revela a redução na quantidade de rRNA 25S maduros e acúmulo de precursor 27S (Wu *et al.*, 2002). De acordo com análises de *northern blot*, na ausência de qualquer uma das três proteínas deste complexo é observado o acúmulo dos precursores 27S e 7S de forma que todas interferem na formação da subunidade 60S (Krogan *et al.*, 2004). Entretanto, não foi observada interação de Nip7p com nenhuma destas proteínas.

Embora Nip7p, Nop53p e Rrp43p influenciem diretamente o processamento do ITS2 (Granato *et al.*, 2005), não possuem atividade catalítica conhecida. A Rrp43p é componente do complexo exossomo, e por isso uma atividade endonucleolítica estaria descartada. Ensaios *in vitro* mostraram que Nop53p interage com o rRNA 5,8S (Granato *et al.*, 2005). Nop8p possui o domínio RRM, típico de interação com RNA (Birney *et al.*, 1993; Zanchin & Goldfarb, 1999a). Desta forma, futuros trabalhos poderiam investigar a interação de Nip7p com possíveis endonucleases para confirmar sua participação no processamento da região ITS2.

4.5. Interação da Nip7 humana com outras proteínas

Considerando o papel da Nip7p de *S. cerevisiae* no processamento de rRNA, na participação no complexo pré-ribossomal 60S e a conservação estrutural entre as ortólogas, seria relevante investigar se HsNip7 desempenha papel semelhante em humanos. Com este objetivo, foi realizada uma análise de duplo-híbrido utilizando HsNip7 como isca. Neste ensaio, duas interações de HsNip7 foram confirmadas, com a proteína FTSJ3 e com SUMO-2. Através das sequências de cDNA dos clones isolados foi possível mapear a interação com FTSJ3, que deve ocorrer na região C-terminal da proteína. Ensaios *in vitro* confirmaram a interação direta de HsNip7 com as proteínas FTSJ3 e SUMO-2.

FTSJ3 é uma proteína não caracterizada que possui o domínio FtsJ na região N-terminal, descrito inicialmente para rRNA metil-transferases de procariotos. Além disso, FTSJ3 apresenta similaridade de sequência às proteínas RrmJ de *E. coli* e Spb1p de levedura. Em *E. coli*, a metil-transferase RrmJ é responsável pela metilação do U_{2552} no rRNA 23S. RrmJ possui três ortólogos em *S. cerevisiae*, as proteínas Trm7p, Mrm2p e

Spb1p. Trm7p é responsável pela metilação 2'OH no tRNA (Pintard et al, 2002a) e Mrm2p realiza a metilação no sítio Um_{2791} do rRNA 21S mitocondrial (Pintard *et al.*, 2002b). Spb1p é a proteína que realiza a metilação do sítio conservado Gm_{2922} no rRNA 25S em *S. cerevisiae* (Kressler *et al.*, 1999; Pintard *et al.*, 2000; Lapeyre & Puroshothaman, 2004). Este sítio faz parte do centro catalítico do ribossomo, de forma que a modificação é importante para a tradução. Diferente das modificações guiadas por snoRNAs, que ocorrem no precursor 35S, a metilação em Gm_{2922} ocorre no precursor 27S, logo após a associação de Spb1p ao complexo pré-60S (Lapeyre & Puroshothaman, 2004). Mutantes condicionais de Spb1p apresentaram acúmulo do precursor 27S e diminuição dos rRNAs maduros 5,8S e 25S. Esses defeitos levam a um desequilíbrio na razão de subunidades ribossomais 40S/60S, e ao aparecimento de polissomos *halfmers*, muito similar ao observado na ausência de Nip7p (Zanchin *et al.*, 1997; Pintard *et al.*, 2000). Embora esteja diretamente associada a proteínas do complexo *C/D box* em *S. cerevisiae*, Spb1p não atua na metilação global do pré-rRNA (Kressler *et al.*, 1999; Pintard *et al.*, 2000). A colocalização nucleolar de FTSJ3 e HsNip7 em célula HEK293 aliada ao papel que suas respectivas ortólogas possuem em *S. cerevisiae*, indica que estas proteínas podem atuar no processamento de rRNA e biogênese da subunidade 60S também em células humanas.

A proteína SUMO-2 (*small ubiquitin-related modifier* 2) está envolvida em um tipo específico de modificação pós-traducional denominada *sumoylation*, muito similar a ubiquitinação (Wilson & Rangasamy, 2001; Gill, 2004). Em vertebrados, são encontradas as proteínas SUMO-1 a 4, no entanto a ortóloga Smt3p de *S. cerevisiae* pode ser complementada apenas por SUMO-1 (Hannich *et al.*, 2005; Itahana *et al.*, 2006). Em mamíferos, as modificações exercidas pelas SUMO tem papel importante na localização subcelular e no tráfego nucleocitoplasmático (Wilson & Rangasamy, 2001). Proteínas envolvidas no metabolismo de mRNA, *splicing* e exportação nuclear, como as hnRNPs, além de proteínas oncogênicas como p53, c-Jun e IK-B, sofrem modificação pelas SUMO (Wilson & Rangasamy, 2001; Vassileva & Matunis, 2004). Além das partículas pré-ribossomais 40S e 60S, diversos fatores relacionados ao processamento de pré-rRNA, principalmente envolvidos com a maturação da subunidade 60S, são modificados pelas SUMO antes da exportação para o citoplasma (Panse *et al.*, 2006). Entre os fatores modificados em *S. cerevisiae* estão proteínas associadas a Nip7p, como Nop7p, Nug1p e

Rix7p (Gavin *et al.*, 2006), além de outros relacionados à subunidade 40S. Além de tornar as partículas aptas à exportação nuclear, a modificação exercida pelas SUMO parece ser importante para regular as interações entre os fatores que atuam no pré-rRNA em *S. cerevisiae* (Panse *et al.*, 2006). A interação direta entre HsNip7 e SUMO-2 indica que este processo pode ser conservado em humanos. Através da interação com HsNip7, SUMO-2 estaria ligada a partícula pré-ribossomal 60S, e poderia modificar proteínas relacionadas à exportação desta subunidade.

A afinidade ao RNA também parece ser modulada pela modificação covalente exercida pela SUMO-2. SART1 e hnRNPM, duas proteínas que atuam no processamento do RNA, são modificadas nos mesmos sítios utilizados na ligação ao RNA (Li *et al.*, 2004; Vertegaal *et al.*, 2004). Proteínas com domínios *zinc-finger*, que atuam na transcrição, também são alvos constantes da modificação pelas SUMO, sugerindo que esta modificação possa ter um papel na regulação da transcrição (Li *et al.*, 2004). Em trabalhos futuros, seria importante verificar se HsNip7 ou proteínas associadas que estão no pré-60S sofrem modificação pela SUMO-2 e se essa modificação interfere na exportação da subunidade 60S para o citoplasma.

4.6. Referências Bibliográficas

Aravind, L. and Koonin, E. (1999) Novel predicted RNA-binding Domains Associated with the Translation Machinery. *J. Mol. Evol.*, 48, 291-302.

Baßler, J., Grandi, P., Gadal, O., Leßmann, T., Petfalski, E., Tollervey, D., Lechner, J. and Hurt, E. (2001) Identification of a 60S preribosomal particle that is closely linked to nuclear export. *Mol. Cell*, 8, 517-529.

Birney E., Kumar, S. and Krainer, A.R. (1993) Analysis of the RNA-recognition motif and RS and RGG domains: conservation in metazoan pre-mRNA splicing factors. *Nucleic Acids Res.*, 21, 5803-5816.

Cadwell, C., Yoon, H.J., Zebarjadian, Y. and Carbon, J. (1997) The yeast nucleolar protein Cbf5p is involved in rRNA biosynthesis and interacts genetically with the RNA polymerase I transcription factor RRN3. *Mol. Cell. Biol.*, 17, 6175-6183.

Charpentier, B., Muller, S. and Branlant, C. (2005) Reconstitution of archaeal H/ACA small ribonucleoprotein complexes active in pseudouridylation. *Nucleic Acids Res.*, 33, 3133-3144.

de Boer, P., Vos, H.R., Faber, A.W., Vos, J.C., and Raué, H.A. (2006) Rrp5p, a trans-acting factor in yeast ribosome biogenesis, is an RNA-binding protein with a pronounced preference for U-rich sequences, *RNA*, 12, 263-271.

De Marchis, M.L., Giorgi, A., Schinina, M.E., Bozzoni, I. And Fatica, A. (2005) Rrp15p, a novel component of pre-ribosomal particles required for 60S ribosome subunit maturation. *RNA*, 11, 495-502.

Dragon, F., Gallagher, J.E., Compagnone-Post, P.A., Mitchell, B.M., Porwancher, K.A., Wehner, K.A., Wormsley, S., Settlage, R.E., Shabanowitz, J., Osheim, Y., Beyer, A.L., Hunt, D.F. and Baserga, S.J. (2002) A large nucleolar U3 ribonucleoprotein required for 18S ribosomal RNA biogenesis. *Nature*, 417, 967-970.

Fields, S. and Song, O. (1989) A novel genetic system to detect protein-protein interactions. *Nature*, 340, 245-246.

Gadal, O., Strauss, D., Petfalski, E., Gleizes, P. E., Gas, N., Tollervey, D. and Hurt, E. (2002) Rlp7p is associated with 60S preribosomes, restricted to the granular component of the nucleolus, and required for pre-rRNA processing. *J. Cell. Biol.*, 157, 941-951.

Galani, K., Nissan, T. A., Petfalski, E., Tollervey, D. and Hurt, E. (2004) Rea1, a dynein-related nuclear AAA-ATPase, is involved in late rRNA processing and nuclear export of 60 S subunits. *J. Biol. Chem.*, 279, 55411-55418.

Gavin, A.C., Aloy, P., Grandi, P., Krause, R., Boesche, M., Marzioch, M., Rau, C., Jensen, L.J., Bastuck, S., Dümpelfeld, B., Edelmann, A., Heurtier, M.A., Hoffman, V., Hoefert, C., Klein, K., Hudak, M., Michon, A.M., Schelder, M., Schirle, M., Remor, M., Rudi, T., Hooper, S., Bauer, A., Bouwmeester, T., Casari, G., Drewes, G., Neubauer, G., Rick, J.M., Kuster, B., Bork, P., Russell, R.B. and Superti-Furga, G. (2006) Proteome survey reveals modularity of the yeast cell machinery. *Nature*, 440, 631-636.

Gill, G. (2004) SUMO and ubiquitin in the nucleus: different functions, similar mechanisms? *Genes & Dev.*, 18, 2046-2059.

Granato, D.C., Gonzales, F.A., Luz, J.S., Cassiola, F., Machado-Santelli, G.M. and Oliveira, C.C. (2005) Nop53p, an essential nucleolar protein that interacts with Nop17p and Nip7p, is required for pre-rRNA processing in *Saccharomyces cerevisiae*. *FEBS J*., 272, 4450-4463.

Grandi, P., Rybin, V., Bassler, J., Petfalski, E., Strauss, D., Marzioch, M., Schäfer, T., Kuster, B., Tschochner, H., Tollervey, D., Gavin, A.C. and Hurt, E. (2002) 90S pre-ribosomes include the 35S pre-rRNA, the U3 snoRNP, and 40S subunit processing factors but predominantly lack 60S synthesis factors. *Mol. Cell*, 10, 105-115.

Hallberg, B.M., Ericsson, U.B., Johnson, K.A., Andersen, N.M., Douthwaite, S., Nordlund, P., Beuscher, A.E. 4th and Erlandsen, H. (2006) The structure of the RNA m5C methyltransferase YebU from *Escherichia coli* reveals a C-terminal RNA-recruiting PUA domain. *J. Mol. Biol*., 360, 774-787.

Hamma, T., Reichow, S.L., Varani, G. and Ferre-D'Amare, A.R. (2005) The Cbf5-Nop10 complex is a molecular bracket that organizes box H/ACA RNPs. *Nat. Struct. Mol. Biol.*, 12, 1101-1107.

Hannich, J.T., Lewis, A., Kroetz, M.B., Li, S.J., Heide, H., Emili, A. and Hochstrasser, M. (2005) Defining the SUMO-modified proteome by multiple approaches in *Saccharomyces cerevisiae*. *J. Biol. Chem.*, 280, 4102-4110.

Henras, A., Henry, Y., Bousquet-Antonelli, C., Noaillac-Depeyre, J., Gélugne, J.P. and Caizergues-Ferrer, M. (1998) Nhp2p and Nop10p are essential for the function of H/ACA snoRNPs. *EMBO J.*, 17, 7078-7090.

Henras, A., Capeyrou, R., Henry, Y. and Caizergues-Ferrer, M. (2004) Cbf5p, the putative pseudouridine synthase of H/ACA-type snoRNPs, can form a complex with Gar1p and Nop10p in absence of Nhp2p and box H/ACA snoRNAs. *RNA*, 10, 1704-1712.

Henras, A., Dez, C., Noaillac-Depeyre, J., Henry, Y. and Caizergues-Ferrer, M. (2001) Accumulation of H/ACA snoRNPs depends on the integrity of the conserved central domain of the RNA-binding protein Nhp2p. *Nucleic Acids Res*., 29, 2733-2746

Horsey, E.W., Jakovljevic, J., Miles, T.D., Harnpicharnchai, P. and Woolford, Jr, J.L. (2004) Role of the yeast Rrp1p protein in the dynamics of pre-ribosome maturation. *RNA*, 10, 813-827.

Ishitani, R., Nureki, O., Fukai, S., Kijimoto, T., Nameki, N., Watanabe, M., Kondo, H., Sekine, M., Okada, N., Nishimura, S. and Yokoyama, S. (2002) Crystal Structure of Archaeosine tRNA-guanine Transglycosylase. *J. Mol. Biol.,* 318, 665-677.

Ishitani, R., Nureki, O., Nameki, N., Okada, N., Nishimura, S. and Yokoyama, S. (2003) Alternative tertiary structure of tRNA for recognition by a posttranscriptional modification enzyme. *Cell*, 113, 383-394.

Itahana, Y., Yeh, E.T. and Zhang, Y. (2006) Nucleocytoplasmic shuttling modulates activity and ubiquitination-dependent turnover of SUMO-specific protease 2. *Mol. Cell. Biol.*, 26, 4675-4689.

Ito,T., Chiba, T. Ozawa, R., Yoshida, M., Hattori, M. and Sakaki, Y. (2001) A comprehensive two-hybrid analysis to explore the yeast protein interactome. *Proc. Natl. Acad. Sci. USA*, 98, 4569-4574.

Kressler, D., Rojo, M., Linder, P. and de la Cruz, J. (1999) Spb1p is a putative methyltransferase required for 60S ribosomal subunit biogenesis in *Saccharomyces cerevisiae*. *Nucleic Acids Res.*, 27,4598- 4608.

Krogan, N.J., Peng, W.T., Cagney, G., Robinson, M.D., Haw, R., Zhong, G., Guo, X., Zhang, X., Canadien, V., Richards, D.P., Beattie, B.K., Lalev, A., Zhang, W., Davierwala, A.P., Mnaimneh, S., Starostine, A., Tikuisis, A.P., Grigull, J., Datta, N., Bray, J.E., Hughes, T.R., Emili, A. and Greenblatt, J.F. (2004) High-definition macromolecular composition of yeast RNA-processing complexes. *Mol. Cell*, 13, 225-239.

Krogan, N.J., Cagney, G., Yu, H., Zhong, G., Guo, X., Ignatchenko, A., Li, J., Pu, S., Datta, N., Tikuisis, A.P., Punna, T., Peregrín-Alvarez, J.M., Shales, M., Zhang, X., Davey, M., Robinson, M.D., Paccanaro, A., Bray, J.E., Sheung, A., Beattie, B., Richards, D.P., Canadien, V., Lalev, A., Mena, F., Wong, P., Starostine, A., Canete, M.M., Vlasblom, J., Wu, S., Orsi, C., Collins, S.R., Chandran, S., Haw, R., Rilstone, J.J., Gandi, K., Thompson, N.J., Musso, G., St Onge, P., Ghanny, S., Lam, M.H., Butland, G., Altaf-Ul, A.M., Kanaya, S., Shilatifard, A., O'Shea, E., Weissman, J.S., Ingles, C.J., Hughes, T.R., Parkinson, J., Gerstein, M., Wodak, S.J., Emili, A. and Greenblatt, J.F. (2006) Global landscape of protein complexes in the yeast *Saccharomyces cerevisiae*. *Nature*, 440, 637-643.

Lafontaine, D.L., Bousquet-Antonelli, C., Henry, Y., Caizergues-Ferrer, M. and Tollervey, D. (1998) The box H+ACA snoRNAs carry Cbf5p, the putative rRNA pseudouridine synthase. *Genes Dev*., 15, 527-537.

Lapeyre, B. and Purushothaman, S.K. (2004) Spb1p-directed formation of Gm2922 in the ribosome catalytic center occurs at a late processing stage. *Mol. Cell*, 16, 663-669.

Li, L., and Ye, K. (2006) Crystal structure of an *H/ACA box* ribonucleoprotein particle, *Nature*, 443, 302-307.

Li, T., Evdokimov, E., Shen, R.F., Chao, C.C., Tekle, E., Wang, T., Stadtman, E.R., Yang, D.C. and Chock, P.B. (2004) Sumoylation of heterogeneous nuclear ribonucleoproteins, zinc finger proteins, and nuclear pore complex proteins: a proteomic analysis. *Proc. Natl. Acad. Sci. USA*, 101, 8551-8556.

Luz, J. S., Georg, R. C. and Oliveira, C. C. (2007) Sdo1p, the yeast ortholog of Shwachman-Bodian-Diamond syndrome protein binds RNA and interacts with nuclear rRNA processing factors. *Submetido para publicação.*

Manival, X., Charron, C., Fourmann, J.B., Godard, F., Charpentier, B. and Branlant, C. (2006) Crystal structure determination and site-directed mutagenesis of the *Pyrococcus abyssi* aCBF5-aNOP10 complex reveal crucial roles of the C-terminal domains of both proteins in H/ACA sRNP activity. *Nucleic Acids Res.*, 34, 826-839.

Marco-Marín, C., Gil-Ortiz, F., Pérez-Arellano, I., Cervera, J., Fita, I., and Rubio, V. (2007) A novel two-domain architecture within the amino acid kinase enzyme family revealed by the crystal structure of *Escherichia coli* glutamate 5-kinase, *J. Mol. Biol.,* 367, 1431-1446.

Menne, T.F., Goyenechea, B., Sánchez-Puig, N., Wong, C.C., Tonkin, L.M., Ancliff, P.J., Brost, R.L., Costanzo, M., Boone, C. and Warren, A.J. (2007) The Shwachman-Bodian-Diamond syndrome protein mediates translational activation of ribosomes in yeast. *Nat. Genet*., 39, 486-495.

Mitchell, P., Petfalski, E., Shevchenko, A., Mann, M. and Tollervey, D. (1997) The exosome: A conserved eukaryotic RNA processing complex containing multiple 3'→5' exoribonucleases. *Cell*, 91, 457-466.

Mochizuki, Y., He, J., Kulkarni, S., Bessler, M. and Mason, P.J. (2004) Mouse dyskerin mutations affect accumulation of telomerase RNA and small nucleolar RNA, telomerase activity, and ribosomal RNA processing. *Proc. Natl. Acad. Sci. USA*, 101, 10756-10761.

Oliveira, C.C., Gonzales, F.A. and Zanchin, N.I.T. (2002) Temperature-sensitive mutants of the exosome subunit Rrp43p show a deficiency in mRNA degradation and no longer interact with the exosome. *Nucleic Acids Res.*, 30, 4186-4198.

Pan, H., Agarwalla, S., Moustakas, D.T., Finer-Moore, J. and Stroud, R. M. (2003) Structure of tRNA pseudouridine synthase TruB and its RNA complex: RNA recognition through a combination of rigid docking and induced fit. *Proc. Natl. Acad. Sci USA*, 100, 12648-12653.

Panse, V.G., Kressler, D., Pauli, A., Petfalski, E., Gnadig, M., Tollervey, D. and Hurt, E. (2006) Formation and nuclear export of preribosomes are functionally linked to the small-ubiquitin-related modifier pathway. *Traffic*, 7, 1311-1321.

Pérez-Arellano, I., Gallego, J., and Cervera, J. (2007) The PUA domain - a structural and functional overview, *FEBS J.*, 274, 4972-4984.

Pintard, L., Lecointe, F., Bujnicki, J.M., Bonnerot, C., Grosjean, H. and Lapeyre, B. (2002a) Trm7p catalyses the formation of two 2'-O-methylriboses in yeast tRNA anticodon loop. *EMBO J.*, 21, 1811-1820.

Pintard, L., Bujnicki, J.M., Lapeyre, B. and Bonnerot, C. (2002b) MRM2 encodes a novel yeast mitochondrial 21S rRNA methyltransferase. *EMBO J.*, 21, 1139-1147.

Pintard, L., Kressler, D. and Lapeyre, B. (2000) Spb1p is a yeast nucleolar protein associated with Nop1p and Nop58p that is able to bind S-adenosyl-L-methionine *in vitro*. *Mol. Cell. Biol.*, 20,1370-1381.

Rashid, R.; Liang, B., Baker, D.L., Youssef, O.A., He,Y., Phipps, K., Terns, R.M., Terns, M.P. and Li, H. (2006) Crystal structure of a Cbf5-Nop10-Gar1 complex and implications in RNA-guided pseudouridylation and dyskeratosis congenita. *Mol. Cell*, 21,249-260.

Reinert, L.S., Shi, B., Nandi, S., Mazan-Mamczarz, K., Vitolo, M., Bachman, K.E., He, H., and Gartenhaus, R.B. (2006) MCT-1 protein interacts with the cap complex and modulates messenger RNA translational profiles. *Cancer Res.*, 66, 8994- 9001.

Rual, J.F., Venkatesan, K., Hao, T., Hirozane-Kishikawa, T., Dricot, A., Li, N., Berriz, G.F., Gibbons, F.D., Dreze, M., Ayivi-Guedehoussou, N., Klitgord, N., Simon, C., Boxem, M., Milstein, S., Rosenberg, J., Goldberg, D.S., Zhang, L.V., Wong, S.L., Franklin, G., Li, S., Albala, J.S., Lim, J., Fraughton, C., Llamosas, E., Cevik, S., Bex, C., Lamesch, P., Sikorski, R.S., Vandenhaute, J., Zoghbi, H.Y., Smolyar, A., Bosak, S., Sequerra, R., Doucette-Stamm, L., Cusick, M.E., Hill, D.E., Roth, F.P., Vidal, M. (2005) Towards a proteome-scale map of the human protein-protein interaction network. *Nature*, 437, 1173-1178.

Sambrook, J., Fritsch, E.F. and Maniatis, T. (1989) Molecular cloning, a laboratory manual. (2nd ed.) Cold Spring Harbor Laboratory Press. Cold Spring Harbor, N.Y., U.S.A.

Steltz, U., Worm, U., Lalowski, M., Haenig,C., Brembeck, F.H., Goehler, H., Stroedicke, M., Zenker, M., Schoenherr, A., Koeppen, S., Timm, J., Mintzlaff, S., Abraham, C., Bock, N., Kietzman, S., Goedde, A., Toksöz, E., Droege, A., Krobitsch, S., Korn, B., Birchmeier, W., Lehrach, H. and Wanker, E. (2005) A Human protein-protein interaction network: A resource for annotating the proteome. *Cell*, 122, 957-968.

Sydorskyy, Y., Dilworth, D.J., Halloran, B., Yi, E.C., Makhnevych, T., Wozniak, R.W. and Aitchison, J.D. (2005) Nop53p is a novel nucleolar 60S ribosomal subunit biogenesis protein. *Biochem. J.*, 388, 819-826.

Thomsom, E. and Tollervey, D. (2005) Nop53p is required for late 60S ribosome subunit maturation and nuclear export in yeast. *RNA*, 11, 1215-1224.

Torchet, C., Badis, G., Devaux, F., Costanzo, G., Werner, M. and Jacquier, A. (2005) The complete set of H/ACA snoRNAs that guide rRNA pseudouridylations in *Saccharomyces cerevisiae*. *RNA*, 11, 928-938.

Uetz, P., Giot, L., Cagney, G., Mansfield, T.A., Judson, R.S., Knight, J.R., Lockshon, D., Narayan, V., Srinivasan, M., Pochart, P., Qureshi-Emili, A., Li, Y., Godwin, B., Conover, D., Kalbfleisch, T., Vijayadamodar, G., Yang, M., Johnston, M., Fields, S. and Rothberg, J.M. (2000) A comprehensive analysis of protein-protein interactions in *Saccharomyces cerevisiae*. *Nature*, 403, 623-627.

Valadkhan, S. (2005) snRNAs as the catalysts of pre-mRNA splicing. *Curr. Opin. Chem. Biol.*, 9, 603-608.

Vassileva, M.T. and Matunis, M.J. (2004) SUMO modification of heterogeneous nuclear ribonucleoproteins. *Mol. Cell. Biol.*, 24, 3623-3632.

Venema, J. and Tollervey, D. (1999) Ribosome synthesis in *Saccharomyces cerevisiae*. *Annu. Rev. Genet.*, 33, 261-311.

Venema, J. and Tollervey, D (1996) RRP5 is required for formation of both 18S and 5.8S rRNA in yeast. *EMBO J.*, 15, 5701-5714.

Vertegaal, A.C., Ogg, S.C., Jaffray, E., Rodriguez, M.S., Hay, R.T., Andersen, J.S., Mann, M. and Lamond, A.I. (2004) A proteomic study of SUMO-2 target proteins, *J. Biol. Chem.*, 279, 33791-33798.

Wilson, V. G. and Rangasamy, D. (2001) Intracellular targeting of proteins by sumoylation. *Exp. Cell Res.*, 271, 57-65.

Wu, L.F., Hughes, T.R., Davierwala, A.P., Robinson, M.D., Stoughton, R., and Altschuler, S.J. (2002) Large-scale prediction of *Saccharomyces cerevisiae* gene function using overlapping transcriptional clusters. *Nat. Genet.*, 31, 255–265.

Zanchin, N.I.T. and Goldfarb, D.S. (1999a) Nip7p interacts with Nop8p, an essential nucleolar protein required for 60S ribosome biogenesis, and the exosome subunit Rrp43p. *Mol. Cell. Biol.*, 19, 1518-1525.

Zanchin, N.I.T. and Goldfarb, D.S. (1999b) The exosome subunit Rrp43p is required for the efficient maturation of 5.8S, 18S and 25S rRNA. *Nucleic Acids Res.*, 27, 1283-1288.

Zanchin, N.I.T., Roberts, P., DeSilva, A., Sherman, F. and Goldfarb, D.S. (1997) *Saccharomyces cerevisiae* Nip7p is required for efficient 60S ribosome subunit biogenesis. *Mol. Cell. Biol*, 17, 5001-5015.

5. CONCLUSÕES

As conclusões deste trabalho estão apontadas abaixo.

5.1. A PaNip7 e a Nip7 de eucariotos (de *S. cerevisiae* e humana) tem preferência pela ligação a poli-uridina. Embora os resíduos envolvidos não sejam conservados, a interação ocorre através da mesma região do domínio PUA, envolvendo o *loop* da α-hélice 1 e folha-β2 e resíduos da folha-β6. Resíduos básicos na PaNip7 (R151, R152, K155 e K158) e resíduos hidrofóbicos na Nip7 de eucariotos (I161 e F164) são responsáveis pela interação.

5.2. A Nip7p interage com um grande número de proteínas no ensaio de duplo-híbrido. Ensaios *in vitro* mostraram a interação direta de Nip7p com as proteínas Nop8p, Nop53p e Nop10p.

5.3. Apesar de interagir com todas as componentes do complexo *H/ACA box* no ensaio de duplo-híbrido, a deficiência em Nip7p não afeta significativamente a pseudo-uridinilação do rRNA em *S. cerevisiae*.

5.4. O processamento da região ITS2 é seriamente comprometido na ausência de Nip7p. Além disso, Nip7p possui maior afinidade pela ligação ao rRNA da região ITS2, o que está de acordo com a função de Nip7p no processamento da ITS2.

5.5. O duplo-híbrido com a proteína humana, HsNip7, revelou as interações com as proteínas FTSJ3 e SUMO-2. Além disso, HsNip7 e FTSJ3 co-localizaram na região nucleolar de células HEK293.

DECLARAÇÃO

Declaro para os devidos fins que o conteúdo de minha tese de doutorado intitulada "Estudo funcional e estrutural de Nip7p, uma proteína conservada envolvida na síntese de ribossomos":

( ) não se enquadra no Artigo 1º, § 3º da Informação CCPG 002/06, referente a bioética e biossegurança.

(X) está inserido no Projeto CIBio (Protocolo n°NITZ 04.01), intitulado "Caracterização estrutural da proteína Nip7p de *Saccharomyces cerevisiae* e de suas homólogas de *Homo sapiens* e *Pyrococcus abyssi* e análise do seu papel no metabolismo de RNA"

( ) tem autorização da Comissão de Ética em Experimentação Animal (Protocolo n°_____).

( ) tem autorização do Comitê de Ética para Pesquisa com Seres Humanos (?) (Protocolo n°_____).

Patricia Colli
Aluno

Nilson J. C. Zanchin
Orientador

Para uso da Comissão ou Comitê pertinente:

( ) Deferido ( ) Indeferido

Helena C. Oliveira

Nome: Profa. Dra. HELENA COUTINHO F. DE OLIVEIRA
Função: Presidente
Comissão Interna de Biossegurança
CIBio/IB - UNICAMP